Construction of Minimal Gauge Invariant Subsets of Feynman Diagrams with Loops in Gauge Theories

Vom Fachbereich Physik
der Technischen Universität Darmstadt

zur Erlangung des Grades
eines Doktors der Naturwissenschaften
(Dr. rer. nat)

genehmigte Dissertation von
Dipl.-Phys. David Ondreka
aus Hanau

Referent: Prof. Dr. P. Manakos
Korreferent: Prof. Dr. J. Wambach

Tag der Einreichung: 12. 4. 2005
Tag der Prüfung: 6. 6. 2005

Darmstadt 2005
D17

Zusammenfassung

Diese Arbeit beschäftigt sich mit Feynmandiagrammen mit Schleifen in renormierbaren Eichtheorien mit oder ohne spontane Symmetriebrechung. Es wird gezeigt, dass die Menge der Feynmandiagramme, die zur Entwicklung einer zusammenhängenden Green'schen Funktion in einer bestimmten Schleifenordnung beitragen, mit Hilfe von graphischen Manipulationen an Feynmandiagrammen, sogenannten Eichflipps, in minimal eichinvariante Untermengen zerlegt werden kann. Zu diesem Zweck werden die Slavnov-Taylor-Identitäten für die Entwicklung der Green'schen Funktionen in Schleifenordnung so zerlegt, dass sie für Untermengen der Menge aller Feynmandiagramme definiert werden können. Es wird dann mit diagrammatischen Methoden bewiesen, dass die mittels Eichflipps konstruierten Untermengen tatsächlich minimal eichinvariante Untermengen sind. Anschließend werden die Eichflipps benutzt, um die minimal eichinvarianten Untermengen von Feynmandiagrammen mit Schleifen im Standardmodell zu klassifizieren. Es wird ein ausführliches Beispiel diskutiert und mit Resultaten verglichen, die mit Hilfe eines für die vorliegende Arbeit entwickelten Computerprogramms erhalten wurden.

Abstract

In this work, we consider Feynman diagrams with loops in renormalizable gauge theories with and without spontaneous symmetry breaking. We demonstrate that the set of Feynman diagrams with a fixed number of loops, contributing to the expansion of a connected Green's function in a fixed order of perturbation theory, can be partitioned into minimal gauge invariant subsets by means of a set of graphical manipulations of Feynman diagrams, called gauge flips. To this end, we decompose the Slavnov-Taylor identities for the expansion of the Green's function in such a way that these identities can be defined for subsets of the set of all Feynman diagrams. We then prove, using diagrammatical methods, that the subsets constructed by means of gauge flips really constitute minimal gauge invariant subsets. Thereafter, we employ gauge flips in a classification of the minimal gauge invariant subsets of Feynman diagrams with loops in the Standard Model. We discuss in detail an explicit example, comparing it to the results of a computer program which has been developed in the context of the present work.

Contents

—1—
Introduction

Over the past decades, the Standard Model has provided us with a remarkably accurate description of all experiments within the reach of currently available experiments. To challenge the Standard Model, we have to either perform experiments at higher energy scales, or else look for deviations from Standard Model predictions in high precision measurements.

In the former case, the processes observed at future high energy colliders (LHC, TESLA) will involve increasingly complicated final states. In particular, at LHC, calculations for processes with eight or more particles in the final state will have to be performed. In the latter case, increasingly accurate predictions from theory will be required to compare with the experimental results. This will necessitate routine calculations of higher order corrections in the Standard Model.

Despite the indisputable successes of the Standard Model, calculations of processes with many particles in the final state as well as calculations of a full set of higher order corrections are still inherently difficult. In particular, until now there is no tool available for doing fully automated calculations of full one-loop or two-loop corrections to Standard Model processes.

The reason for this situation is twofold. On the one hand, even at one-loop, the calculation of the contributions of higher tensor n-point functions is extraordinarily difficult, numerically or analytically, through the presence of many different masses and the intricate structure of many particle phase space. On the other hand, the number of Feynman diagrams increases dramatically (roughly, the growth is factorial) with the number of loops and the number of particles in the final state.

If we aim at a fully automated calculation of higher order corrections in the Standard Model, progress has to be made in both respects. In this work, we will not be concerned with the problem of actually calculating higher order diagrams. Rather, we shall focus on the question whether it is possible to reduce the number of Feynman diagrams necessary to obtain sensible partial results.

One way to avoid the factorial growth of individual contributions to the amplitude is to dispense completely with the definition of the amplitude in terms of Feynman diagrams. In QCD calculations, a possible approach is to express the amplitude in terms of subamplitudes corresponding to color $SU(3)$ invariants.[1] The contributions of a single invariant will in general be given by a sum of fewer terms than the complete amplitude. However, such an approach is not possible in a gauge theory with spontaneous symmetry breaking, since it makes use of the linear realization of the color $SU(3)$ symmetry.

A second approach, particularly suited to calculations in spontaneously broken gauge theories, is motivated by the observation that in a typical set of Feynman diagrams there are always subsets of diagrams that have large parts in common. If one can find a systematic way to exploit this feature, the complexity of the problem can be considerably reduced. Indeed, an algorithm for matrix element generation based on this approach has been developed [2], which reduces the combinatorial complexity from a factorial of the number of external particles to an exponential. A related earlier algorithm satisfying these requirements is [3]. However, at present these algorithms are limited to the lowest order of perturbation theory.

For the calculation of higher order corrections, we still need the contribution of the full set of Feynman diagrams to compute the complete amplitude. However, a major problem in gauge theories like the Standard Model is that the numerical contribution of an individual diagram to the amplitude may be considerably larger, under certain conditions even by several orders of magnitude, than the sum of all diagrams. This can lead to serious numerical problems. In gauge theories, it is therefore desirable to partition the set of all Feynman diagrams into subsets, such that all the large cancellations dictated by gauge invariance would occur separately within each subset.

In fact, few Standard Model calculations of complete higher order corrections to scattering processes with four or more particles in the final state exist. In most cases, approximations based on estimation and evaluation of the numerically most important corrections are used. In general then, only a subset of the full higher order corrections is taken into account. Doing this naively may lead to incorrect results due to violation of gauge invariance. In particular, gauge invariance in principle dictates the selection of other diagrams once a certain subset of the complete set of diagrams has been selected, so as to render the resulting expressions gauge invariant.

Of course, by consistently working in a particular gauge, it is actually possible to do calculations with a subset of Feynman diagrams which is not gauge invariant by itself, if the contributions of the omitted diagrams are negligible in the chosen gauge. However, in order to make sure that the omitted diagrams can safely be disregarded, one still has to determine the full set of diagrams that would lead to a gauge invariant final result.

It is then natural to ask whether in a gauge theory, spontaneously broken or not, the set of Feynman diagrams contributing to a given process can be divided into subsets that lead to gauge invariant expressions by themselves. In this work, we derive and implement an algorithm for the construction of minimal gauge invariant subsets of Feynman diagrams with loops in general gauge theories. The algorithm is based on a set of graphical manipulations of Feynman diagrams, called *gauge flips*, originally invented for the construction of minimal gauge invariant subsets of tree diagrams.[4]

Gauge flips are defined as the transformations in four-point subdiagrams with external gauge boson lines.[1] As a specific example, consider the transfor-

[1] In spontaneously broken gauge theories, there are also gauge flips of five-point subdiagrams. For simplicity, we ignore these in the present chapter.

mations among the following sets of subdiagrams in the Standard Model:[2]

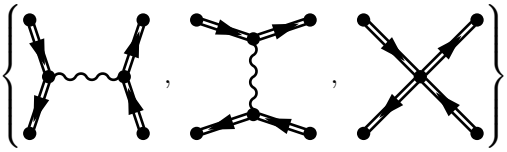

(1.1)

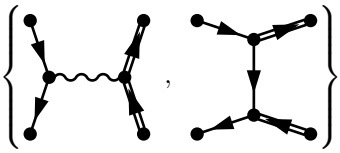

(1.2)

Here, wavy lines represent the neutral bosons, i. e. Z^0 and photon, while arrowed double lines denote the charged W bosons.

Although gauge flips have been invented for tree level diagrams, they can be readily extended to diagrams with loops. As an example, consider the following diagram contributing to the process $e^+e^- \to u\bar{u}d\bar{d}$ at the one-loop level:

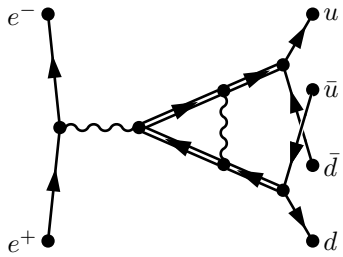

(1.3)

If we choose to flip the subdiagram defined by the four W-lines connected by the neutral gauge boson line, we can apply the gauge flips in (1.1) to obtain:

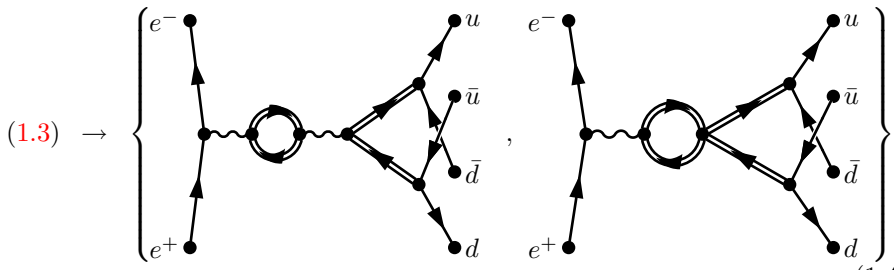

(1.4)

Observe that the flip has decreased the number of vertices in the loop.

We can also increase the number of vertices in the loop. To this end, in (1.3) consider the subdiagram defined by the electron line. This subdiagram can be

[2]The complete set of Standard Model gauge flips is discussed in chapter 6.

flipped using (1.2):

(1.3) →

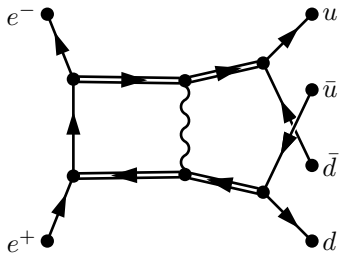

(1.5)

By repeatedly applying similar gauge flips to the resulting diagram, we can increase the number of vertices in the loop further, producing diagrams with five or six vertices in the loop:

(1.5) →

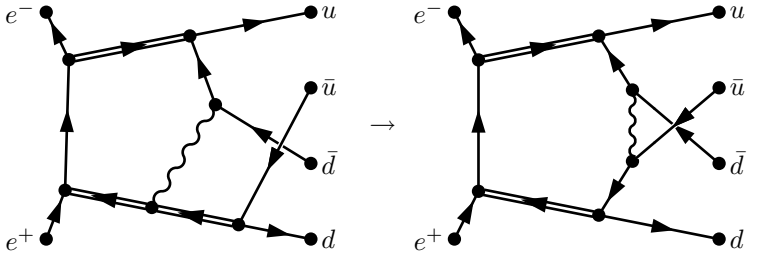

(1.6)

Thus, gauge flips can be used to transform diagrams contributing to $e^+e^- \to u\bar{u}d\bar{d}$ into each other. However, this may or may not be true for the complete set of diagrams contributing to this process, called the *forest*. In general, the gauge flips induce a partition of the forest into disjoint subsets called *groves*.

For tree level processes, the connection between gauge flips and gauge invariance is made by a theorem, stating that *the groves of a tree level forest are precisely the minimal gauge invariant subsets of the corresponding connected Green's function.*[4][5]

Using this theorem, one can set out to classify the groves of tree level Standard Model processes. One finds [6] that, for purely fermionic external states with fermions in the dublet representation of $SU(2)$, the finest possible partitioning of the forest corresponds to a classification according to the flavors in the external state, if a charged boson line is present in the diagrams. On the other hand, for diagrams without a charged boson line, the groves constitute, in general, a finer partitioning.

In this work, we extend the stated theorem to the case of diagrams with loops in general gauge theories. Subsequently, we use the method of gauge flips to classify the forest of n-loop corrections to general Standard Model processes. We find that, for diagrams containing charged boson lines, the finest possible partitioning is characterized by the flavors of fermions in the external state and the number of fermion loops. On the other hand, the diagrams without charged boson lines generally show a richer structure of groves than in the tree level case.

1.1 Overview

The remainder of this work is organized as follows. We intend to prove that the groves obtained by gauge flips correspond to the minimal gauge invariant subsets of Feynman diagrams corresponding to the expansion of a connected Green's function at n-loop order in a general gauge theory. To this end, we have to verify that the relevant *Slavnov-Taylor-Identities* (STIs) for the Green's functions of the gauge theory are satisfied. In order to put these STIs in a context and to introduce the necessary notation, we briefly review the derivation of STIs for Green's functions in a general gauge theory in the next chapter. There, we also introduce a graphical notation for the expansion of STIs in perturbation theory. This requires additional Feynman rules compared to the usual Feynman rules of a gauge theory.

Our proof of the STIs will be performed by using the STIs for tree level vertices inside diagrams with loops. Therefore, we derive the relevant tree level STIs in chapter 3. We demonstrate the use of vertex STIs in the proof of STIs for connected Green's functions at tree level, providing the connection to gauge flips. Also, we develop further tools that will help to simplify the complicated combinatorics of gauge cancellations at the n-loop order.

Chapter 4 is then devoted to the actual proof that groves are the minimal gauge invariant subsets of n-loop forests. We begin by studying the gauge cancellations in one-loop diagrams, then extend our arguments to the n-loop case. We demonstrate that all cancellations occur within the groves of the forest.

In chapter 5, we introduce the concept of flips for diagrams with loops independent from the connection with gauge invariance.

In chapter 6, the decomposition of Standard Model forests using gauge flips is discussed in detail. We obtain a very general classification of Standard Model forests. As an application, we elaborate on the structure of the one-loop forest for $e^+e^- \to u\bar{u}d\bar{d}$, which we have employed for demonstration purposes above. For this example, we present the results we have obtained by means of our computer program implementing the algorithm for the construction of groves using gauge flips. We conclude the main part with a summary.

In the appendix, we collect the Feynman rules for the expansion of STIs, the tree level STIs used in chapters 3 and 4, and a brief description of our program for grove construction.

—2—
Identities in Gauge Theories

In this chapter we are going to introduce the Slavnov-Taylor identities (STIs) of connected and 1PI Green's functions in gauge theories. It is these identities that we shall use later to demonstrate how the expansion of a connected Green's function in perturbation theory can be decomposed into separately gauge invariant pieces.

The STIs follow directly from the BRST invariance of the quantized gauge theory. Therefore, we begin our discussion by briefly sketching the derivation of BRST invariance. We then demonstrate how BRST invariance can be used to derive STIs for the generating functionals of the Green's functions of the theory. From these identities the STIs for individual Green's functions follow easily. We adopt a notation for the graphical representation of STIs, introducing Feynman rules to write out the perturbative expansions of STIs.

2.1 From Classical Lagrangian to BRST Invariance

We consider a gauge theory with a gauge group $\mathcal{G}$, which in general may be the direct product of compact simple groups and abelian $U(1)$ factors. However, for ease of notation we shall denote the set of generators of $\mathcal{G}$ by a single symbol t^a. These generators satisfy the commutation relations

$$\left[t^a, t^b\right] = \mathrm{i} f^{abc} t^c \ , \tag{2.1}$$

with f^{abc} the structure constants of the Lie algebra of $\mathcal{G}$, which we may assume to be completely antisymmetric. If $\mathcal{G}$ is not simple, then f^{abc} vanishes unless all indices belong to a single simple factor of $\mathcal{G}$.

The gauge bosons W_μ^a are coupled to a set of fermions Ψ and a set of scalars Φ. Both Ψ and Φ transform under some—in general reducible—representation of $\mathcal{G}$. Without loss of generality the scalars can be chosen real, in which case the representation matrices X^a are real and antisymmetric:

$$\left[X^a, X^b\right] = f^{abc} X^c \tag{2.2}$$

In particular, an infinitesimal gauge transformation, parametrized by a space-time dependent parameter ω^a, takes the form

$$\Psi \to \Psi + \mathrm{i}\omega^a t^a \Psi \tag{2.3}$$

$$\Phi \to \Phi - \omega^a X^a \Phi \ . \tag{2.4}$$

Fermions and scalars are coupled to the gauge bosons through the (gauge) covariant derivatives. For simplicity, we introduce only vector couplings for the fermions. Thus, the covariant derivatives are given, respectively, by

$$D_\mu \Psi = \partial_\mu \Psi - \mathrm{i} g W_\mu^a t^a \Psi \tag{2.5}$$

$$D_\mu \Phi = \partial_\mu \Phi + g W_\mu^a X^a \Phi \ . \tag{2.6}$$

Note that, for a non-simple gauge group $\mathcal{G}$, instead of the product gW^a we would have one such term for each factor of $\mathcal{G}$:

$$g W^a \to \sum_r g_r W^{a_r} \tag{2.7}$$

This interpretation will be implied in the following.

For the covariant derivatives of Ψ and Φ to transform like Ψ and Φ, respectively, under infinitesimal local gauge transformations, the gauge bosons must transform according to

$$W_\mu^a \to W_\mu^a + \frac{1}{g} \partial_\mu \omega^a - f^{abc} \omega^b W_\mu^c \ . \tag{2.8}$$

It follows that the field strenght tensor $F_{\mu\nu}^a$ of the gauge bosons, defined by the commutator of covariant derivatives

$$[D_\mu, D_\nu] \equiv -\mathrm{i} g F_{\mu\nu}^a t^a \ , \tag{2.9}$$

transforms homogeneously under local gauge transformations:

$$F_{\mu\nu}^a \to F_{\mu\nu}^a + \omega^c f^{cab} F_{\mu\nu}^b \tag{2.10}$$

From the classical fields W_μ^a, Ψ and Φ we can construct the classical Lagrangian $\mathcal{L}_{\mathrm{cl}}$ of the gauge theory, invariant under Lorentz transformations as well as the local gauge transformations (2.3), (2.4) and (2.8), and containing only renormalizable interactions:

$$\mathcal{L}_{\mathrm{cl}} = -\frac{1}{4} F_{\mu\nu}^a F^{a\mu\nu} + \bar{\Psi} \left(\mathrm{i} \not{D} - m \right) \Psi + \frac{1}{2} \left(D_\mu \Phi \right) \left(D^\mu \Phi \right) - V(\Phi) \tag{2.11}$$

Here, the scalar potential $V(\Phi)$ is a polynomial in the fields Φ of degree at most four, which is invariant under gauge transformations.[1]

As it stands, the classical Lagrangian (2.11) is not suitable for quantization in the canonical or path integral formulation. In the former case, the obstacle is the occurrence of first class constraints (in Dirac's terminology [7]), in the latter case the path integral is ill defined because the weight factor $\exp\left(\mathrm{i} S_{\mathrm{cl}}\right)$ is constant along orbits of the local gauge transformation due to the local gauge invariance of the classical action S_{cl}.

If a Lorentz covariant quantization is desired, the standard way to obtain an effective Lagrangian suitable for quantization is the Faddeev-Popov procedure [8]. In effect, it amounts to the addition of a gauge fixing Lagrangian $\mathcal{L}_{\mathrm{gf}}$ as well as a ghost Lagrangian $\mathcal{L}_{\mathrm{gh}}$ to $\mathcal{L}_{\mathrm{cl}}$:

$$\mathcal{L}_{\mathrm{gf}} = -\frac{1}{2\xi^a} \left(G^a[\varphi] \right)^2 \tag{2.12}$$

[1] Note that we have omitted Yukawa couplings of scalars to fermions. In principle, these could be incorporated, but in order to do so we would have to make further assumptions about the representations t^a and X^a.

$$\mathcal{L}_{\text{gh}} = -\bar{c}^a \frac{\delta G_a[\varphi_\omega]}{\delta \omega^b} c^b \tag{2.13}$$

The gauge fixing functional $G^a[\varphi]$ depends on the gauge fields W_μ^a and Φ, here denoted collectively by φ. φ_ω denotes the gauge transformed fields. For the formalism to be consistent, G^a must not be invariant under local gauge transformations. The gauge parameters ξ^a are arbitrary positive real numbers. c^a and $\bar{c}^a$ are the Faddeev-Popov ghost fields, two multiplets of real, anticommuting scalar fields in the adjoint representation.

Given the infinitesimal form of the local gauge transformations (2.8) and (2.4), the functional derivative of the gauge fixing functional G^a can be expressed as

$$\frac{\delta G^a[\varphi_\omega]}{\delta \omega^b} = \frac{\delta G^a}{\delta \varphi} \frac{\delta \varphi_\omega}{\delta \omega^b} = \frac{\delta G^a}{\delta W_\mu^b} \left(\partial_\mu - g f^{abc} W_\mu^c\right) - \frac{\delta G^a}{\delta \Phi_j} \left(X^a \Phi\right)_j \quad . \tag{2.14}$$

In unbroken gauge theories, the gauge fixing function is usually chosen independent of the scalar fields. The situation is different in spontaneously broken gauge theories. Here, the gauge fixing function is usually chosen to depend on both the gauge fields and the scalar fields, at least if the Lagrangian is used to derive Feynman rules for doing actual calculations in perturbation theory. We will come back to this point later when we discuss gauge theories with spontaneous symmetry breaking in a little more detail in a separate section.

Adding $\mathcal{L}_{\text{gf}}$ and $\mathcal{L}_{\text{gh}}$ to the classical Lagrangian, we get an effective Lagrangian suitable for quantization *via* the path integral approach:

$$\begin{aligned}\mathcal{L} &= \mathcal{L}_{\text{cl}} + \mathcal{L}_{\text{gf}} + \mathcal{L}_{\text{gh}} \\ &= -\frac{1}{4} F_{\mu\nu}^a F^{a\mu\nu} + \bar{\Psi} \left(\mathrm{i}\not{D} - m\right) \Psi + \frac{1}{2} \left(D_\mu \Phi\right) \left(D^\mu \Phi\right) - V(\Phi) \\ &\quad - \frac{1}{2\xi^a} \left(G^a[\varphi]\right)^2 - \bar{c}^a \frac{\delta G_a[\varphi_\omega]}{\delta \omega^b} c^b \end{aligned} \tag{2.15}$$

Remarkably, this Lagrangian, though no longer invariant under local gauge transformations, is invariant under a set of global nonlinear transformations of the fields, called BRST transformations.[9][10] Under these transformations, a general field φ (now including fermion fields) undergoes the change

$$\varphi \to \varphi + \delta\varphi \quad , \tag{2.16}$$

where $\delta\varphi$ is written as

$$\delta\varphi = \lambda s\varphi \quad , \tag{2.17}$$

with λ an infinitesimal Grassmann number. Explicitely, the BRST transformations are given by

$$sW_\mu^a = \partial_\mu c^a - g f^{abc} c^b W_\mu^c \tag{2.18a}$$

$$s\Phi = -g c^a X^a \Phi \tag{2.18b}$$

$$s\Psi = \mathrm{i} g c^a t^a \Psi \tag{2.18c}$$

$$s\bar{\Psi} = -\mathrm{i} g c^a \bar{\Psi} t^a \tag{2.18d}$$

$$sc^a = -\frac{1}{2} g f^{abc} c^b c^c \tag{2.18e}$$

$$s\bar{c}^a = -\frac{1}{\xi^a} G^a \tag{2.18f}$$

For the fields W_μ^a, Ψ and Φ, present in the classical Lagrangian, the BRST transformation is just a local gauge transformation parametrized by the ghost field c^a (or, rather, by the commuting quantity λc^a). Therefore, the invariance of the classical Lagrangian under BRST transformations is evident. The invariance of the gauge fixing and ghost terms can be shown using the Jacobi identity for the structure constants f^{abc}.

Although the effective Lagrangian (2.15) in connection with the BRST invariance is sufficient for a consistent covariant quantization of the gauge theory *via* the path integral approach, the BRST invariance can best be exploited by recasting (2.15) into a slightly different form through the introduction of the Nakanishi-Lautrup auxiliary field B^a.[11][12] To this end, instead of the gauge fixing Lagrangian (2.12) one chooses the Lagrangian

$$\mathcal{L}_{\rm NL} = \frac{\xi^a}{2} B^a B^a + B^a G^a \ . \tag{2.19}$$

The equation of motion for B^a following from this Lagrangian is

$$0 = \xi^a B^a + G^a \ . \tag{2.20}$$

Thus, B^a has no independent dynamics. (This justifies the term "auxiliary" field.) Solving for B^a and inserting back into (2.19), we get back to the original gauge fixing Lagrangian (2.12). Also, through this equation of motion, the BRST transformations (2.18f) and (2.21) are equivalent.

The advantage of choosing $\mathcal{L}_{\rm NL}$ instead of $\mathcal{L}_{\rm gf}$ is that the BRST transformation s is now nilpotent also off-shell, provided we modify the BRST transformation properties according to

$$s\bar{c}^a = B^a \tag{2.21}$$

$$sB^a = 0 \ . \tag{2.22}$$

The BRST invariance of the modified Lagrangian

$$\mathcal{L}' = \mathcal{L}_{\rm cl} + \mathcal{L}_{\rm NL} + \mathcal{L}_{\rm gh} \tag{2.23}$$

follows easily from the nilpotency of the BRST operator s and the observation that the gauge fixing plus ghost Lagrangian can be written as a BRST variation:

$$\mathcal{L}_{\rm NL} + \mathcal{L}_{\rm gh} = s\left(\bar{c}_a\left(\frac{\xi_a}{2} B_a + G_a\right)\right) \tag{2.24}$$

Thus, since, as argued above, the classical Lagrangian is BRST invariant, so is the complete Lagrangian $\mathcal{L}'$.

2.2 Quantum BRST Transformations and Slavnov-Taylor Identities

So far, we have discussed the BRST invariance of the effective gauge theory Lagrangian $\mathcal{L}$ in (2.15) (or, equivalently, the modified Lagrangian $\mathcal{L}'$ in (2.23)) in a purely classical setting.

We must now ask whether the BRST invariance of the classical Lagrangian survives the quantization procedure. This question is nontrivial because the

BRST transformations are nonlinear in the fields and therefore require renormalization. Fortunately, the quantized gauge theory is still invariant under renormalized BRST transformations.

In the operator formulation, i. e. canonical quantization, this means that, provided the theory is free of anomalies, there exists a renormalized BRST operator Q, which generates the BRST transformation on the state vector space of the theory, such that

$$[\mathrm{i}\lambda Q, \varphi] = \lambda s\varphi \ , \tag{2.25}$$

where φ is a generic (renormalized) field operator, and λ a Grassmann valued parameter.[13][14]

In the path integral formulation, the statement means that the identities obtained by naively applying the classical BRST transformations are valid in the renormalized theory.

The importance of the BRST operator Q for a consistent Lorentz covariant quantization can hardly be overemphasized. In particular, Q can be used to construct a physically satisfactory Hilbert Space with a positive definite metric, in which the S-matrix for physical external states can be shown to be unitary and gauge invariant. In fact, the classification of the asymptotic state vector space into physical and unphysical states depends crucially on the existence of the BRST operator Q. Namely, unphysical states are states $|\beta\rangle$ for which $Q|\beta\rangle \neq 0$, while physical external states $|\mathrm{phys}\rangle$ must satisfy $Q|\mathrm{phys}\rangle = 0$. In addition, there are states states $|\alpha\rangle$ of the form $|\alpha\rangle = Q|\beta\rangle$, which satisfy $Q|\alpha\rangle$ automatically due to the nilpotency of Q. These states are called BRST-exact. A BRST-exact state is physically equivalent to the null vector. That is, $|\mathrm{phys}\rangle + |\alpha\rangle$ and $|\mathrm{phys}\rangle$ describe the same physical state.

The BRST transformations of the asymptotic states can be derived from the BRST transformations of the asymptotic field operators, using the LSZ formalism. Asymptotically, only terms linear in field operators contribute to the BRST transformations. We split the BRST transformation $s\varphi$ of a generic field into a term linear and quadratic in fields, respectively, according to

$$s\varphi = \varrho_\varphi[c] + c^a \Delta^a \varphi \ . \tag{2.26}$$

Here, $\varrho_\varphi[c]$ may contain derivatives, while Δ^a is just a complex valued matrix. As an example, consider the BRST transformation law (2.18a) of the gauge boson, where we have $\varrho^a_W[c] = \partial c^a$ and $\Delta^a_{bc} W^c = -g f^{bac} W^c$.

Equivalently, (2.26) is a split into inhomogeneous and homogeneous pieces, respectively. Using this decomposition, the asymptotic field operator corresponding to φ generates an unphysical state precisely if $\varrho_\varphi[c]$ is nonzero. The BRST-exact states then are generated by the asymptotic field operators corresponding to $\varrho_\varphi[c]$.

Given the existence of renormalized BRST transformations, we can derive the Slavnov-Taylor identities for Green's functions of the gauge theory. To this end, we consider the generating functional for the full Green's functions of the theory. Due to the necessity to renormalize the nonlinear BRST transformations, we are forced to introduce not only sources J_ℓ for the generic field φ_ℓ, but also sources K_ℓ for the BRST transforms $s\varphi_\ell$. Furthermore, if we do not consider Green's functions with B^a fields, we can use the Lagrangian $\mathcal{L}$ and omit the field B^a everywhere, using (2.18f) as the BRST transformation of the antighost field. We assume that the gauge fixing functional G^a is linear in the

fields. Therefore, we need not introduce a source term for the BRST transform of the antighost. Under these assumptions, the generating functional $Z[J,K]$ of Green's functions with insertions of BRST transformed field operators is then given explicitely, in path integral formulation, by

$$Z[J,K] = \int \mathcal{D}[\varphi] \exp\left\{ \mathrm{i} \left(S + \sum_{\varphi} J_\varphi \cdot \varphi + \sum_{\varphi \neq \bar{c}^a} K_\varphi \cdot s\varphi \right) \right\} \quad . \tag{2.27}$$

In this equation, a dot denotes space time integration. $S = \int d^4x \mathcal{L}$ is the action corresponding to the effective Lagrangian $\mathcal{L}$. The sums extend over all fields in $\mathcal{L}$, except that the antighost field can be omitted in the second sum, because of the linearity of G^a.

Using the invariance of the path integral measure and the action S under BRST transformations, we obtain the *Slavnov-Taylor identities* (STIs) for the generating functional Z:[15][16]

$$0 = \left\{ \sum_{\varphi \neq \bar{c}^a} (-1)^\varphi J_\varphi \cdot \frac{\delta}{\delta K_\varphi} + \frac{1}{\xi^a} G^a \left[\frac{\delta}{\delta J} \right] J_{\bar{c}^a} \right\} Z[J,K] \tag{2.28}$$

Here, $(-1)^\varphi$ is $+1$ or -1 for bosonic or fermionic fields, respectively.

Defining the generating functional $Z_c[J,K]$ of connected Green's functions (with insertions of BRST transformed field operators) by

$$Z[J,K] = \exp\left(\mathrm{i} Z_c[J,K]\right) \quad , \tag{2.29}$$

it is easy to see that Z_c satisfies an identical STI:

$$0 = \left\{ \sum_{\varphi \neq \bar{c}^a} (-1)^\varphi J_\varphi \cdot \frac{\delta}{\delta K_\varphi} + \frac{1}{\xi^a} G^a \left[\frac{\delta}{\delta J} \right] J_{\bar{c}^a} \right\} Z_c[J,K] \tag{2.30}$$

Connected Green's functions are obtained from Z_c by taking functional derivatives[2] of Z_c w.r.t. the sources J_φ, putting all sources J and K to zero afterwards. Therefore, the STI (2.30) for Z_c implies STIs for individual connected Green's functions.

Now in order to obtain a nonzero Green's function after setting sources to zero, functional derivatives w.r.t. fermionic sources, i. e. the sources J_Ψ, $J_{\bar{\Psi}}$, J_{c^a}, and $J_{\bar{c}^a}$, must come in pairs. That is, there must be as many derivatives w.r.t. $J_{\bar{\Psi}}$ and $J_{\bar{c}^a}$ as there are derivatives w.r.t. J_Ψ and J_{c^a}, respectively. However, the functional differentiation operator acting on Z_c in (2.30) has ghost number one. Therefore, in order to obtain a nonzero STI for an individual connected Green's function, we have to take an additional functional derivative w.r.t. the source of the antighost $J_{\bar{c}^a}$.

In this work, we will be exclusively concerned with the STIs for connected Green's functions with a single insertion of the gauge fixing functional G^a. Therefore, we shall use the term "STI" exclusively in this sense in this work, unless explicitely stated otherwise. In particular, these STIs ensure that a single

[2] We take all functional derivatives with respect to anticommuting quantities as *left* derivatives.

insertion of the unphysical linear combination of fields corresponding to G^a does not contribute in matrix elements on the mass shell.

Now consider the functional derivative of (2.30) w.r.t. the source $J_{\bar{c}^b}$. Taking care of fermion signs, we get

$$0 = \left\{ \sum_{\varphi \neq \bar{c}^a} J_\varphi \frac{\delta}{\delta J_{\bar{c}^b}} \frac{\delta}{\delta K_\varphi} - \frac{1}{\xi^b} G^b \left[\frac{\delta}{\delta J} \right] + \frac{1}{\xi^a} G^a \left[\frac{\delta}{\delta J} \right] J_{\bar{c}^a} \frac{\delta}{\delta J_{\bar{c}^b}} \right\} Z_c[J,K] \ . \tag{2.31}$$

Evidently, further functional derivatives w.r.t. $J_{\bar{c}^a}$ will produce further terms with a single insertion of G^a, but no Green's function with more than one insertion of G^a can be produced. Therefore, all STIs for connected Green's functions with a single insertion of the gauge fixing functional G^a are exhausted by taking arbitrary functional derivatives of (2.30) w.r.t. sources J_φ.[3]

In order to determine the explicit form of an STI for a connected Green's function, it is actually easier to work in the canonical formalism. Remember that in the canonical formalism we have the BRST operator Q which is nilpotent, hermitean, and annihilates the ground state $|0\rangle$. Therefore, if ϕ_ℓ are generic fields of the theory, we immediately have[4]

$$0 = \left\langle \left[\mathrm{i}\lambda Q, \varphi_1 \dots \varphi_n \right] \right\rangle^c \ , \tag{2.32}$$

where here and in the following, the superscript c indicates a connected Green's function. Evaluating the commutator with the help of (2.25), we get

$$0 = \sum_\ell \left\langle \varphi_1 \dots (\lambda s \varphi_\ell) \dots \varphi_n \right\rangle^c \ . \tag{2.33}$$

Using the decomposition (2.26) of $s\varphi$, this can be rewritten

$$0 = \sum_\ell (-1)^{\sigma_\ell} \Big(\left\langle \varphi_1 \dots \varrho_{\varphi_\ell} \dots \varphi_n \right\rangle^c + \left\langle \varphi_1 \dots (c^a \Delta^a \varphi_\ell) \dots \varphi_n \right\rangle^c \Big) \ . \tag{2.34}$$

The sign factor counts the number of anticommuting field operators preceding the ℓth field.

We can get rid of the sign factor for the second term by moving the ghost c^a in the homogeneous parts to the left. The same can be done for all inhomogeneous pieces in the BRST transformation of *bosonic* fields, because ϱ is fermionic for these. On the other hand, the only fermionic field variables with a nonzero ϱ are the antighost fields $\bar{c}^a$. It is convenient to write

$$\varrho_{\bar{c}^a} = -\frac{1}{\xi^a} G^a \equiv B^a \ , \tag{2.35}$$

using B^a as an abbreviation.[5] If we write antighost fields first in connected Green's functions, the generic STI takes the form, with φ_ℓ now denoting any field *except* antighosts and a caret indicating omission,

[3] Remember that, if there is no derivative w.r.t. J_φ, or if derivatives w.r.t. fermion sources don't come in pairs, the resulting identity is just the trivial statement $0 = 0$.

[4] In this and subsequent equations, we suppress the spacetime arguments of the field operators in Green's functions. The correct argument should always be clear from the indices.

[5] Note that we have defined the generating functionals Z and Z_c with the action $S = \int d^4x \mathcal{L}$, in which B^a does not appear.

$$0 = \sum_{k=1}^{m} (-1)^{k+1} \left\langle \bar{c}^{a_1} \dots B^{a_k} \dots \bar{c}^{a_m} \varphi_1 \dots \varphi_n \right\rangle^c$$
$$+ \sum_{\ell} \Big(\left\langle \varrho_{\varphi_\ell} \bar{c}^{a_1} \dots \bar{c}^{a_m} \varphi_1 \dots \hat{\varphi}_\ell \dots \varphi_n \right\rangle^c + \left\langle c^b \bar{c}^{a_1} \dots \bar{c}^{a_m} \varphi_1 \dots (\Delta^b \varphi_\ell) \dots \varphi_n \right\rangle^c \Big) \tag{2.36}$$

The signs in the first sum are essential. However, if this sum has more than one term, we have an STI for a Green's function with external ghost lines.[6] Since ghosts are unphysical degrees of freedom, such Green's functions are less frequently needed, although in unbroken gauge theories, like QCD, ghost amplitudes may be usefully employed in evaluating gluon polarization sums. In spontaneously broken gauge theories, like the SM, amplitudes for ghost production are rarely needed.

In this work—with a single exception, that can easily be treated explicitely—we will not need STIs for Green's functions with external ghost lines. Therefore, we specialize now to the case of a single antighost field. The resulting STI for connected Green's functions is the central identity in this work:

$$0 = \left\langle B^a \varphi_1 \dots \varphi_n \right\rangle^c$$
$$+ \sum_{\ell} \Big(\left\langle \varrho_{\varphi_\ell} \bar{c}^a \varphi_1 \dots \hat{\varphi}_\ell \dots \varphi_n \right\rangle^c + \left\langle c^b \bar{c}^a \varphi_1 \dots (\Delta^b \varphi_\ell) \dots \varphi_n \right\rangle^c \Big) \tag{2.37}$$

We will later introduce a graphical notation to represent this STI. First, however, we discuss the STIs for the 1PI Green's functions of the theory. We denote by $\Gamma[\varphi, K]$ the generating functional for 1PI Green's functions with insertions of BRST transformed operators. $\Gamma[\varphi, K]$. Is obtained from Z_c by Legendre transformation w.r.t. the sources J_φ, but not K_φ:

$$\Gamma[\varphi, K] = Z_c[J, K] - \sum_{\varphi} J_\varphi \cdot \varphi \tag{2.38}$$

Here, the argument φ of Γ is defined as

$$\varphi = \langle \varphi \rangle^c_{J,K} = \frac{\delta Z_c}{\delta J_\varphi}[J, K] \ . \tag{2.39}$$

Note that we use the same symbol φ for the expectation value as well as for the field operator. The subscript on the connected Green's function indicates that the Green's function is to be evaluated in the presence of the external sources J and K. Thus, $\Gamma[\varphi, K]$ is the effective action in the presence of the external sources K.

We will generally denote functional derivatives of Γ w.r.t. φ or K by subscripts. Thus,

$$\frac{\delta \Gamma}{\delta \varphi} \equiv \Gamma_\varphi \tag{2.40}$$

$$\frac{\delta \Gamma}{\delta K_\varphi} \equiv \Gamma_{K_\varphi} \ . \tag{2.41}$$

[6] Of course, the insertions of BRST transformed operators may lead to Green's functions with external ghost fields in the STI. These external ghosts are unavoidable.

$\Gamma[\varphi, K]$ satisfies the fundamental relations

$$\Gamma_\varphi[\varphi, K] = -(-1)^\varphi J_\varphi \tag{2.42}$$

$$\frac{\delta\Gamma}{\delta K_\varphi}[\varphi, K] = \frac{\delta Z_c}{\delta K_\varphi}[J[\varphi], K] \ . \tag{2.43}$$

Using (2.42) and (2.43) and the chain rule for functional differentiation, (2.30) can be transformed into an identity for Γ:

$$0 = \sum_{\varphi \neq \bar{c}^a} \Gamma_\varphi \cdot \Gamma_{K_\varphi} - \frac{1}{\xi^a} G^a[\varphi] \Gamma_{\bar{c}^a} \tag{2.44}$$

This is the STI for the generating functional of 1PI Green's functions, also called *Lee identity*.[17][18] The Lee identity implies STIs for individual 1PI Green's functions. Eventually, we will introduce a graphical notation for these identies, too. Before we can do this, however, we must leave our general discussion and consider the explicit form of the STIs for connected and 1PI Green's functions in unbroken and broken gauge theories.

2.2.1 STI in Unbroken Gauge Theories

In unbroken gauge theories, the scalars Φ coupled to the gauge bosons must not have vacuum expectation values that would break the invariance under a generator X^a of the gauge group, i. e. the vacuum expectation value $\langle\Phi\rangle$ must satisfy

$$X^a \langle\Phi\rangle = 0 \ . \tag{2.45}$$

for all generators X^a, which implies $\langle\Phi\rangle = 0$ for all components of Φ that couple to at least one gauge boson. But this means that $s\Phi = 0$, which in turn is equivalent to the statement that all scalars are physical fields. In particular, there is no inhomogeneous term in the BRST transformation of the scalars. The same applies to the fermion fields Ψ and $\bar{\Psi}$.

Consequently, apart from the antighost field, the gauge field W_μ^a is the only field with an inhomogeneous term in the BRST transformation law. We choose the Lorentz covariant linear gauge fixing functional

$$G^a = \partial^\mu W_\mu^a \ . \tag{2.46}$$

Equivalently, we set

$$B^a = -\frac{1}{\xi^a} \partial^\mu W_\mu^a \ . \tag{2.47}$$

Of course, for doing actual calculations one would choose the ξ^a equal within a factor of the gauge group $\mathcal{G}$, since this makes the gauge fixing Lagrangian invariant under *global* gauge transformations. However, this is only a matter of convenience.

We can now write down the explicit form of the STI (2.37) in an unbroken gauge theory:

$$\begin{aligned} 0 = &-\frac{1}{\xi^a} \partial^\mu \left\langle W_\mu^a \varphi_1 \dots \varphi_n \right\rangle^c \\ &+ \sum_{\varphi_\ell = W_\mu^a} \partial_{\mu_\ell} \left\langle c^{a_\ell} \bar{c}^a \varphi_1 \dots \hat{\varphi}_\ell \dots \varphi_n \right\rangle^c + \sum_{\varphi_\ell \neq \bar{c}^a} \left\langle c^{a_\ell} \bar{c}^a \varphi_1 \dots (\Delta^{a_\ell} \varphi_\ell) \dots \varphi_n \right\rangle^c \end{aligned} \tag{2.48}$$

2.2.2 STI in Spontaneously Broken Gauge Theories

In a spontaneously broken gauge theory, the scalar potential V produces a nonzero vacuum expectation value (vev) $\langle\Phi\rangle \equiv \Phi_0$, which in general is invariant under a subgroup $\mathcal{H}$ of the full gauge group $\mathcal{G}$. We use greek indices to label the generators of broken symmetries and latin indices following q to label the generators of unbroken symmetries. Thus, broken and unbroken generators satisfy, respectively,

$$X^\alpha \Phi_0 \neq 0 \tag{2.49}$$

$$X^q \Phi_0 = 0 \tag{2.50}$$

$$. \tag{2.51}$$

According to Goldstone's theorem,[19][20] before the theory is coupled to the gauge bosons, there is a massless Goldstone boson corresponding to each broken generator X^α. Once the set of broken generators has been determined, we can always arrange Φ in such a way that its first components correspond precisely to the Goldstone bosons ϕ^α. This leads to the following decomposition of Φ:

$$\Phi = \begin{pmatrix} \phi \\ \eta \end{pmatrix} \tag{2.52}$$

Correspondingly, the generators X^a of $\mathcal{G}$ can be written as block matrices:

$$X^a = \begin{pmatrix} t^a & u^a \\ -(u^a)^T & T^a \end{pmatrix} \tag{2.53}$$

Φ_0 has no components in the directions of the Goldstone bosons:

$$\Phi_0 = \begin{pmatrix} 0 \\ v \end{pmatrix} \quad \text{with} \quad v = \langle\eta\rangle \tag{2.54}$$

To generate a useful perturbative expansion, the Lagrangian $\mathcal{L}$ has to be expanded about the vev Φ_0. To this end, the scalars η are reparametrized as

$$\eta = v + H \ . \tag{2.55}$$

We will not carry out the expansion of the Lagrangian, for the results are well known. Most importantly, the gauge bosons corresponding to broken generators aquire masses through the Higgs mechanism. For our further considerations, we will need an expression for the gauge boson masses in terms of the broken generators X^α and the vev v. First, observe that the broken generators T^α must satisfy

$$T^\alpha v = 0 \ , \tag{2.56}$$

because all nonzero vectors of this form point into the direction of Goldstone boson fields. Next, by choosing the basis in the space of Goldstone bosons accordingly, we can always arrange that

$$u^\alpha v \equiv \frac{1}{g} M_\alpha e^\alpha \ , \tag{2.57}$$

where e^α is a unit vector in the Goldstone boson subspace in the direction of $u^\alpha v$. With these conventions, the mass matrix M^2 for the gauge bosons is diagonal:

$$M^2_{\alpha\beta} = g^2 v^T \left(u^\alpha\right)^T u^\beta v = M^2_\alpha \delta_{\alpha\beta} \ . \tag{2.58}$$

On the other hand, from fact that the unbroken generators X^q form a subgroup, it can be shown that these generators are block diagonal, i. e. both ϕ and H transform linearly under the subgroup $\mathcal{H}$:

$$X^q \Phi = X^q \big(\Phi - \Phi_0\big) = \begin{pmatrix} t^q \phi \\ T^q H \end{pmatrix} \tag{2.59}$$

We are now ready to determine the BRST transformation properties of the scalar fields ϕ and H. The Lagrangian $\mathcal{L}$ is invariant under a BRST transformation of the original field Φ. Inserting the expansion (2.55), we obtain

$$s\phi^\alpha = -c^\alpha M_\alpha - g c^\beta \left((t^\beta \phi)^\alpha + (u^\beta H)^\alpha \right) - g c^q (t^q \phi)^\alpha \tag{2.60a}$$

$$sH = -g c^\alpha \Big(- (u^\alpha)^T \phi + T^\alpha H \Big) - g c^q T^q H \ . \tag{2.60b}$$

The inhomogeneous term in the BRST transformation law of ϕ indicates clearly that the Goldstone bosons, when coupled to gauge bosons, become unphysical degrees of freedom. Therefore, they are often referred to in the literature as *would-be Goldstone bosons* or *Goldstone ghosts*. In this work, we will use the term "Goldstone boson" exclusively for the unphysical scalar degrees of freedom of a spontaneously broken gauge theory. No confusion is possible, because we do not consider physical Goldstone bosons of a broken global symmetry.

On the other hand, the fields H, lacking an inhomogeneous term in their BRST transformation law, form a set of physical scalars, which we refer to as *Higgs bosons*.[7]

Like in the case of the unbroken gauge theory, the BRST transformation of the antighost is determined by the gauge fixing functional. For the massive gauge bosons corresponding to broken symmetries, we choose a general linear 't Hooft gauge fixing:[21]

$$G^\alpha = \partial^\mu W_\mu^\alpha - \xi^\alpha M_\alpha \phi^\alpha \equiv -\xi^\alpha B^\alpha \tag{2.61}$$

This choice is essentially uniquely determined by requiring, in addition to linearity in fields and Lorentz covariance, that the Lagrangian contain no bilinear mixing between Goldstone bosons and gauge bosons. Thus, the BRST transformation law of the antighost fields $\bar{c}^\alpha$ explicitely reads

$$s\bar{c}^\alpha = -\frac{1}{\xi^a} \partial^\mu W_\mu^\alpha + M_\alpha \phi^\alpha \ . \tag{2.62}$$

For the massless gauge bosons corresponding to unbroken symmetries, we choose the same gauge fixing (2.46) as in the case of unbroken gauge theories. Likewise, the BRST transformation properties of W_μ^a, c^a, Ψ and $\bar{\Psi}$ remain the same. Consequently, the explicit form of the STI (2.37), for an antighost $\bar{c}^\alpha$ corresponding to a broken generator, is given by

$$0 = -\frac{1}{\xi^\alpha} \partial^\mu \left\langle W_\mu^\alpha \varphi_1 \dots \varphi_n \right\rangle^c + M_\alpha \left\langle \phi^\alpha \varphi_1 \dots \varphi_n \right\rangle^c$$

[7] In general, only some of the components of η will aquire a nonzero vev. In other words, the vector v may contain many zeros. Those components of η with nonzero vevs are the real Higgs bosons, while the remaining components have nothing to do with symmetry breaking. It is, however, not uncommon to use the term "Higgs boson" for all components of H.

$$+\sum_{\varphi_\ell=W_\mu^a}\partial_{\mu_\ell}\left\langle c^{a_\ell}\bar{c}^\alpha\varphi_1\ldots\hat{\varphi}_\ell\ldots\varphi_n\right\rangle^c-\sum_{\varphi_\ell=\phi^\alpha}M_{\alpha_\ell}\left\langle c^{a_\ell}\bar{c}^\alpha\varphi_1\ldots\hat{\varphi}_\ell\ldots\varphi_n\right\rangle^c$$
$$+\sum_{\varphi_\ell\neq\bar{c}^a}\left\langle c^{a_\ell}\bar{c}^\alpha\varphi_1\ldots(\Delta^{a_\ell}\varphi_\ell)\ldots\varphi_n\right\rangle^c \quad . \tag{2.63}$$

Observe that, in contrast to the situation in unbroken gauge theories, this identity relates two different Green's functions for unphysical fields to the sums over Green's functions with BRST insertions.

The choice of the 't Hooft gauge fixing (2.61) has other profound effects: On one hand, it leads to the gauge parameter dependent masses $\sqrt{\xi^\alpha}M_\alpha$ for the scalar modes of a massive gauge boson W_μ^α as well as the associated Goldstone bosons and ghosts ϕ^α, c^α, and $\bar{c}^\alpha$, respectively. On the other hand, it introduces gauge parameter dependent ghost-scalar interactions. These effects are important when studying the gauge parameter dependence of Green's functions.

2.3 Graphical Representation of STIs

Having discussed in detail the explicit form of the STIs for connected Green's functions in unbroken and broken gauge theories, we are now going to discuss a graphical notation to represent these STIs, invented in [5]. We can treat unbroken and broken gauge theories on an equal footing, if we formally define $M_q=0$ and $\phi^q\equiv 0$ for unbroken generatros X^q. The details can always be filled in by going back to the explicit expressions derived in the foregoing section.

An even more compact notation is obtained if we treat gauge bosons and Goldstone bosons as components of a single five dimensional gauge field A_r^a:

$$A_r^a=\left(W_\mu^a,\phi^a\right) \tag{2.64}$$

Introduce a five dimensional derivative operator according to

$$\bar{\Theta}_r^a(x)=\left(-\frac{1}{\xi^a}\partial_\mu^x,M_a\right) \tag{2.65}$$
$$\Theta_r^a(x)=\left(\partial_\mu^x,-M_a\right) \quad . \tag{2.66}$$

Employing this notation, the insertion of B^a in a Green's function can be written

$$\left\langle B^a\varphi_1\ldots\varphi_n\right\rangle^c=\bar{\Theta}^{ar}\left\langle A_r^a\varphi_1\ldots\varphi_n\right\rangle^c \quad . \tag{2.67}$$

The inhomogeneous terms in the BRST transformation laws of gauge bosons and Goldstone bosons are given by

$$sA_r^a\big|_{\text{inhom}}=\Theta_r^a c^a \quad . \tag{2.68}$$

Then, the STI for connected Green's functions takes the unified form

$$0=\bar{\Theta}^{as}\left\langle A_s^a\varphi_1\ldots\varphi_n\right\rangle^c+\sum_{\varphi_\ell\neq\bar{c}^a}\left\langle c^{a_\ell}\bar{c}^a\varphi_1\ldots(\Delta^{a_\ell}\varphi_\ell)\ldots\varphi_n\right\rangle^c$$
$$+\sum_{\varphi_\ell=A_r^a}\Theta_r^{a_\ell}\left\langle c^{a_\ell}\bar{c}^a\varphi_1\ldots\hat{\varphi}_\ell\ldots\varphi_n\right\rangle^c \quad . \tag{2.69}$$

We will represent all fields but ghost and antighosts collectively as straight lines. Ghosts and antighosts, on the other hand,are drawn, as usual, in dotted style with arrows indicating ghost number flow. Thus, we have the following associations:

$$\left\{A^a_r, H, \Psi, \bar{\Psi}\right\} \quad \to \quad \text{———} \tag{2.70}$$

$$\left\{c^a, \bar{c}^a\right\} \quad \to \quad \bar{c} \cdots\blacktriangleright\cdots c \tag{2.71}$$

We will frequently need a special notation for gauge bosons and Goldstone bosons, which have inhomogeneous terms in their BRST transformation laws. To denote these fields exclusively, we use a wavy line:

$$A^a_r \quad \to \quad \sim\sim\sim \tag{2.72}$$

Next we have to represent the BRST transformed operators $s\varphi$. We will use separate notations for the homogeneous parts and the inhomogeneous parts. The homogeneous parts, present for all fields except antighosts, will be drawn as follows:

$$c^a \Delta^a \varphi \quad \to \tag{2.73}$$

The inhomogeneous parts in the transformation of gauge bosons and Goldstone bosons are denoted by

$$\Theta^a_r c^a \quad \to \tag{2.74}$$

Finally, the insertion of B^a will be represented by a double line:

$$B^a = \Theta^{ar} A^a_r \quad \to \tag{2.75}$$

Using these conventions, the STI (2.69) is represented graphically as

$$0 \;=\; + \sum_\ell \;+ \sum_\ell \;. \tag{2.76}$$

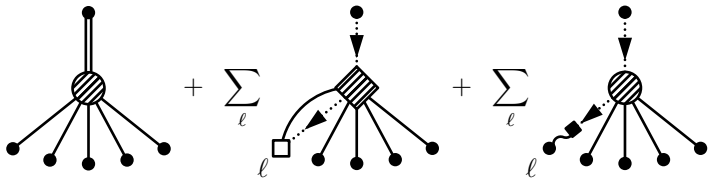

To complete our conventions for the graphical notation, we note that connected Green's functions will always be denoted by shaded blobs. Next, a dot at the end of an external line indicates that the corresponding line is not amputated. Since we will later deal with 1PI Green's functions and Green's functions with amputated external lines, these distinctions are essential. Finally, observe that we have deliberately chosen a diamond shaped blob for the connected Green's functions with insertions of $c^a \Delta^a \varphi$. This distinction is made because, in perturbation theory, most contributions to these Green's functions are contact terms. This means that, in momentum space, most contributions vanish when all external lines are multiplied by inverse propagators and external momenta are set to onshell values.

The case of the two-point function, i. e. the propagator, is special, because in this case it does not make sense to consider amputation. Therefore, we do *not* use a diamond shaped blob in the corresponding STI, which we state explicitely:

$$0 \;=\; + \;+ \tag{2.77}$$

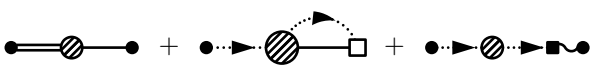

Having established a notation for the STIs of connected Green's functions, we turn to the Lee identities, i. e. the STIs for 1PI Green's functions. In this case, it proves useful to develop a notation for the Lee identity (2.44) of the generating functional Γ itself.

To begin with, Γ is depicted as a white blob:

$$\Gamma \;=\; \bigcirc \tag{2.78}$$

The derivatives of Γ w.r.t. a classical field are drawn as an external line indicating the respective field:

$$\Gamma_\varphi \;=\; \underset{\varphi}{\text{—}\bigcirc}\;. \tag{2.79}$$

The generalization to higher functional derivatives is obvious. Note that, in contrast to the case of connected Green's functions, external lines do *not* have a dot. This indicates an amputated line.

The derivatives of Γ w.r.t. the sources K_φ of the BRS transformed fields are 1PI vacuum expectation values of the BRS transformed operators $s\varphi$. Again, we split these into homogeneous and inhomogeneous parts. The homogeneous parts are depicted as

$$\Gamma_{K_\varphi} \;=\; \underset{\Delta\varphi}{\bigcirc\!\!-\!\!\square}\;. \tag{2.80}$$

For the inhomogeneous parts contributed by gauge bosons and Goldstone bosons, it is best to write them out analytically. This is easy, because the corresponding operators are linear in c^a. Hence, we have

$$\Gamma_{K_{A^a_r}}\Big|_{\text{inhom}} = \Theta^a_r c^a \;. \tag{2.81}$$

Likewise, the gauge fixing functional can be inserted analytically. The Lee identity (2.44) can then be depicted as

$$0 = (\Theta^a_r c^a)\cdot \overset{r}{\sim\!\bigcirc} \;+\; \sum_{\varphi\neq\bar{c}^a} \underset{\Delta\varphi}{\bigcirc\!\!-\!\!\square}\!\!-\!\!\underset{\varphi}{\bigcirc} \;+\; (\bar\Theta^{ar} A^a_r)\cdot \bigcirc\!\!\cdots\!\!\blacktriangleright\!\!\cdots \tag{2.82}$$

We would now like to use partial integration to let Θ and $\bar\Theta$ act onto the Green's functions instead of the fields.[8] Unfortunately, the fifth component of either Θ or $\bar\Theta$, being a mere number, cannot be partially integrated. To avoid the introduction of an extra symbol, we adopt the convention that, whenever Θ or $\bar\Theta$ act on an 1PI Green's function, the sign of the spacetime derivative has to be reversed. While this definition may seem confusing at first sight, it will appear quite natural and convenient, once we consider the perturbative expansion of STIs in momentum space.

It is now evident, that the first term of the Lee identity can be written as a functional differential operator:

$$\Theta^a_r \overset{r}{\sim\!\bigcirc} = \Theta^a_r \frac{\delta}{\delta A^a_r} \bigcirc \;\equiv\; \text{=}\bigcirc \tag{2.83}$$

We have chosen a double bar notation to represent this particular linear combination of 1PI Green's functions because, as we shall demonstrate shortly, it

[8] Remember in this context that the dots denote spacetime integration.

is closely related to the insertion of B^a in a connected Green's function. In a similar manner, we can represent the last term as

$$A^a_r \cdot \bar{\Theta}^{ar} \quad = \quad \cdot A^a_r \tag{2.84}$$

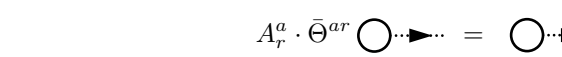

Notice the absence of a dot at the end of the line. This allows a distinction from the symbols used for connected Green's functions. The change in the order of factors has been performed to make more apparent, that the spacetime argument associated with the end of the ghost line is the same as that of A^a_r.

The Lee identity for the generating functional of 1PI Green's functions now takes the final form

$$0 \;=\; c^a \times \;+\; \sum_{\varphi \neq \bar{c}^a} \;+\; \cdot A^a_r \;. \tag{2.85}$$

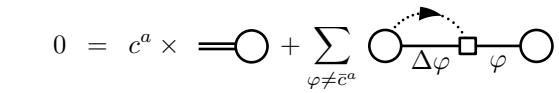

Some remarks concerning the interpretation of this identity are in order. Most importantly, this identity is still dependent on external sources. Therefore, despite appearances, ghost number is not violated in the displayed diagrams. A second consequence of the source dependence is that individual 1PI Green's functions in the identity are in general *not* proportional to momentum conserving delta functions in momentum space. Finally, since, in this work, we have no need for Green's functions with more than one insertion of a BRST transformed operator, we will implicitely assume that the sources K_φ are set to zero.

A further remark concerns the term involving the homogeneous parts of the BRST transformations. We emphasize that the φ-line in the homogeneous term is *not* a propagator. Rather, this term represents the multiplication (or, more precisely, convolution) of two 1PI Green's functions.

In spite of these cautionary remarks, the prescription for deriving STIs for individual 1PI Green's functions is actually simple: Take a suitable number of functional derivatives w.r.t. fields φ, remembering to apply the product rule for differentiation, and afterwards set sources to zero. In particular, to obtain a nonzero identity after setting sources to zero, at least one derivative w.r.t. a ghost field c^a must be taken.

To illustrate the rules, we derive a master identity for 1PI Green's funtions without external ghost lines. This is done by taking a functional derivative w.r.t. c^a and setting c^a and $\bar{c}^a$ to zero. The result is:

$$0 \;=\; \;+\; \sum_{\varphi \neq c^a, \bar{c}^a} \;+\; \cdot A^a_r \tag{2.86}$$

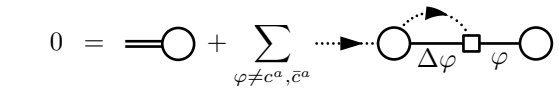

We will soon need the STI for the inverse propagators with at least one A^a_r-line, which we can readily get by taking a functional derivative w.r.t. A^a_r and setting all sources to zero:

$$0 \;=\; \;+\; \;+\; \tag{2.87}$$

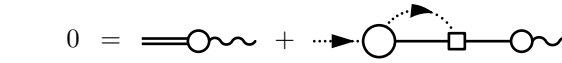

Here and in the following, the sum over fields should be implied. In momentum space, this is now really an identity among momentum conserving 1PI Green's functions, where the homogeneous term contains the product of two such Green's

functions. The sum is over all bosonic fields that do not carry a conserved quantum number.

Since the Lee identities are nonlinear identities, the product rule would make it rather cumbersome to depict an STI for an individual 1PI Green's function with several external lines, like we did for the STIs of connected Green's functions in (2.76). Therefore, we refrain from doing so in this general setting. We will have ample opportunity to demonstrate the explicit form of such STIs in the perturbative expansions.

2.4 STI for Ghost Green's Functions

Before discussing the perturbative expansion of the STIs, we derive an STI for a connected Green's function with external ghosts. We will need this STI later to determine the correct set of gauge flips for diagrams with ghost lines. These flips have not been determined in [5], because ghosts do not contribute at tree level.

We are interested in the STI for the following connected Green's function:

$$G_{12} \;=\; \langle W_1^\mu \bar{c}_2 c_3 \varphi_4 \rangle^c \quad , \tag{2.88}$$

where φ can be any field but ghost or antighost, and spacetime arguments have been indicated by subscripts.

The STI for G_{12} can most easily be derived in the canonical formalism, using the BRST charge Q:

$$\begin{aligned} 0 &= \langle \{ \mathrm{i}Q, \bar{c}_1 \bar{c}_2 c_3 \varphi_4 \} \rangle \\ &= \langle B_1 \bar{c}_2 c_3 \varphi_4 \rangle - \langle \bar{c}_1 B_2 c_3 \varphi_4 \rangle + \langle \bar{c}_1 \bar{c}_2 (sc)_3 \varphi_4 \rangle - \langle \bar{c}_1 \bar{c}_2 c_3 (s\varphi)_4 \rangle \quad . \end{aligned} \tag{2.89}$$

The graphical representation of this STI reads[9]

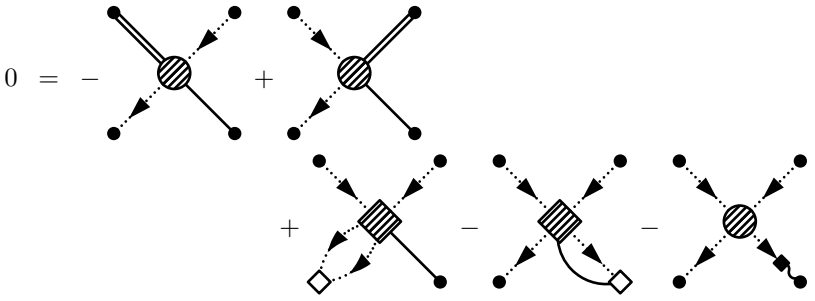

Observe that this STI is actually an identity relating the contractions of *two* Green's functions, G_{12}, as defined above, and $G_{21} = \langle \bar{c}_1 W_2^\mu c_3 \varphi_4 \rangle^c$. However, the contact terms in this STI do not show a similar decomposition.

[9] The sign change for the first two diagrams is caused by bringing the fields into canonical order, with fermions preceding antifermions. Had we not done this here, the sign would have crept in on expanding at tree level.

2.5 Perturbative Expansion

The STIs for connected Green's functions in (2.76) and (2.90) as well as the STIs for 1PI Green's functions derived from the Lee identity (2.85) must be evaluated in perturbation theory.

This can be done in the standard way, for instance, by using the Gell-Man-Low formula for expressing the Green's functions in the interaction picture, using Wick's theorem to evaluate contractions. The resulting expansion in the coupling constant can, as usual, be expressed through Feynman rules. In addition to the normal Feynman rules of the gauge theory, however, additional rules are necessary for the insertions of BRST transformed operators.

We have already introduced graphical notations for these operators in the last section. Now, however, we promote these drawings from mere mnemonic devices to representatives for analytical expressions. Consider, for instance, the homogeneous part in the BRST transformation rule of a gauge boson W^a_μ:

$$sW^a_\mu\big|_{\text{hom}} = c^b \Delta^b W^a_\mu = -g f^{abc} c^b W^c_\mu \tag{2.91}$$

The Feynman rule for this operator is just what remains when the field operators are taken away by contractions. Therefore, we have the rule

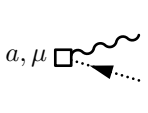

$$= \; -g f^{abc} \delta^\nu_\mu \; . \tag{2.92}$$

In a similar way, the Feynman rules for the homogeneous parts in the BRST transformation laws of the other fields can be obtained. They are listed in the appendix A.

The inhomogeneous parts in the BRST transformation laws of gauge bosons, Goldstone bosons and antighosts are all expressible by means of the operators Θ and $\bar{\Theta}$. These operators contain derivatives. Therefore, we have to be careful to obtain the correct momentum space Feynman rules. To this end, we define the Fourier transforms of Θ and $\bar{\Theta}$ by

$$\int d^4x \, \mathrm{e}^{\mathrm{i}px} \, \Theta^a_r(x) f(x) = \big(-\mathrm{i}p_\mu, -M_a\big) f(p) \equiv \Theta^a_r(p) f(p) \tag{2.93}$$

$$\int d^4x \, \mathrm{e}^{\mathrm{i}px} \, \bar{\Theta}^a_r(x) f(x) = \left(\frac{1}{\xi^a}\mathrm{i}p_\mu, M_a\right) f(p) \equiv \bar{\Theta}^a_r(p) f(p) \; . \tag{2.94}$$

The sign in the exponential function of the Fourier transformation corresponds to *outgoing* momenta. Thus, the momentum space Feynman rules for connected Green's functions are given by

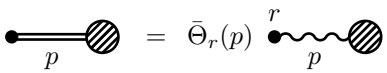

$$= \; \bar{\Theta}_r(p) \tag{2.95}$$

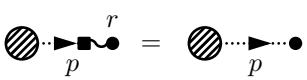

$$= \; \Theta_r(p) \; . \tag{2.96}$$

In both cases, the momentum p is to be interpreted as outgoing, i. e. p is directed from the blob to the end of the external line.

1PI Green's functions will generally be defined with *incoming* momenta. This definition is actually the most useful for the following reason: The tree level 1PI Green's functions correspond precisely to the inverse propagator and the interaction vertices of the theory. When momenta are interpreted as incoming, the interaction vertex in momentum space corresponding to particles φ_1, φ_2, and φ_3 with incoming momenta p_1, p_2, and p_3, respectively, is obtained as

$$\Gamma_{\varphi_1(p_1)\varphi_2(p_2)\varphi_3(p_3)} \quad . \tag{2.97}$$

Had we chosen outgoing momenta, this functional derivative would correspond to an interaction vertex of three conjugate particles $\bar{\varphi}_1$, $\bar{\varphi}_2$, and $\bar{\varphi}_3$.

For 1PI Green's functions, the correct momentum space Feynman rules for the inhomogeneous parts in the BRST transformation laws are then, with momenta interpreted as incoming,

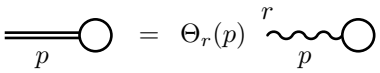

(2.98)

(2.99)

Observe that the momentum dependence of Θ and $\bar{\Theta}$ in these Feynman rules is consistent with our earlier definitions for the action of these operators on connected and 1PI Green's functions. Indeed, the respective definitions differ by a sign in the derivative part, which in momentum space translates into a sign change of the momentum. If we replace incoming by outgoing momenta in the Feynman rules for 1PI Green's functions, this sign change is apparent. The usefulness of these definitions can be appreciated in the next chapter, where we discuss the expansion of STIs at tree level.

—3—
Tree Level STIs and Gauge Flips

As mentioned before, the ultimate aim of our work is to show how minimal gauge invariant classes of Feynman diagrams with loops for connected Green's functions in gauge theories can be constructed by employing a set of graphical manipulations, called *gauge flips*. Due to the intricacies of multi-loop diagrams, this is a complicated task. Therefore, it is essential that we decompose this task into manageable parts, using an appropriate notation. The purpose of the present chapter is to introduce the corresponding decomposition and notation. To this end, we first state the STIs for the tree level vertices of the theory. Next, we demonstrate how minimal gauge invariant classes of *tree* Feynman diagrams can be constructed using the STIs for tree level vertices, and then provide the link to gauge flips.

The essence of this chapter is the realization that STIs can be proven in a purely diagrammatical way, dispensing completely with any explicit analytical expressions. We will first demonstrate this on specific examples, then go on to develop a systematic approach implementing this strategy for the general case.

The present chapter has some overlap with [5]. However, since our approach to the diagrammatical proof of STIs differs significantly from the one presented in [5], we consider the inclusion of this material necessary for a self-contained presentation of the subject.

3.1 STIs and Effective BRST Vertices

In this section we derive all STIs for the tree level vertices of the gauge theory. These identities are crucial for our later work, because we will be using tree level identities to show how minimal gauge invariant classes of Feynman diagrams can be constructed in higher orders of perturbation theory, i. e. for diagrams with loops.

We begin by discussing the STIs for propagator and inverse propagator, which, of course, are closely related. Then, we derive all STIs for tree level 1PI Green's functions, which we shall refer to simply as *vertices*, because they are identical to the interaction vertices of the gauge theory. Note that the tree level STIs derived in this section are collected in appendix B.

3.1.1 Propagator and Inverse Propagator STIs

The STIs for the full propagator and the full inverse propagator have been derived in (2.77) and (2.87). In both cases, the homogeneous parts in the BRST transformation laws do not contribute at tree level. Consequently, the tree level STIs read, respectively

(3.1)

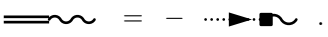
(3.2)

Since we have chosen the gauge fixing term to eliminate tree level mixing between gauge and Goldstone bosons, these STIs actually relate gauge boson and Goldstone boson two-point functions to the ghost two-point functions.

Of course, the STIs for propagator and inverse propagator are not independent. In fact, one could have been obtained from the other by applying the identies

(3.3)

For good measure, we state explicitely the analytical expressions corresponding to the STIs for the inverse propagators. These are given, for gauge bosons and Goldstone bosons, respectively, by

$$(-\mathrm{i}p_\mu)(-\mathrm{i})\left((p^2-M_a^2)g^{\mu\nu}-\left(1-\frac{1}{\xi^a}\right)p^\mu p^\nu\right)=-\left(\frac{1}{\xi^a}(-\mathrm{i}p^\nu)\right)\left(\mathrm{i}(p^2-\xi^a M_a^2)\right) \tag{3.4}$$

$$(-M^a)\left(\mathrm{i}(p^2-\xi^a M_a^2)\right)=-\left(M_a\right)\left(\mathrm{i}(p^2-\xi^a M_a^2)\right)\ . \tag{3.5}$$

3.1.2 Cubic Vertices

In the STIs for cubic vertices, there will be terms involving tree level inverse propagators multiplying tree level BRST vertices. To make the notation unambiguous, we cannot but introduce an extra piece of notation to make inverse propagators recognizable. We choose to do this by adding a cross at one end of the line representing the inverse propagator:

(3.6)

The STIs for *physical* cubic vertices, i. e. vertices without ghost lines,[1] are obtained by taking two functional derivatives of the master identity (2.86). The result is

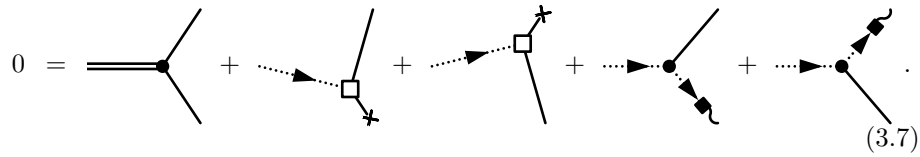
(3.7)

[1] This definition of "physical" is, of course, not compatible with the notion of physical external states. However, in the present context we find it convenient to use the term "physical" for all fields but ghosts or antighosts.

At this point, we emphasize that the last two terms are present only for gauge boson and Goldstone boson lines. This feature will prove very important in the next chapters.

We shall also need the STIs for the ghost vertices. This is evident, because we are interested in diagrams with loops, where ghost lines can occur. The relevant STIs must be derived from the original Lee identity (2.85), because in the master identity (2.86) the ghost sources are already set to zero. We obtain:

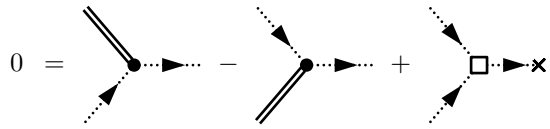

(3.8)

The minus sign in this STI is essential.

3.1.3 Quartic Vertices

The STI for a quartic vertex involving only physical fields is obtained by taking three derivatives of the master identity (2.86):

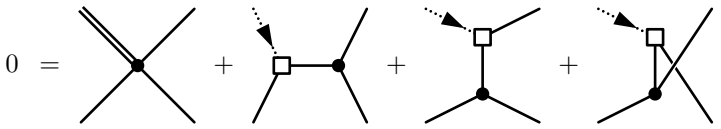

(3.9)

In the context of STIs for 1PI Green's functions, the three rightmost diagrams are likely to be interpreted correctly, namely, as the (sum over fields of a) multiplication of a tree level BRST vertex by a cubic tree level vertex. However, when we are going to use tree level STIs inside larger diagrams contributing to connected Green's functions, there is considerable potential for confusion, because then the lines connecting the cubic vertex to the BRST vertex could be mistaken for propagators.

However, observe that each of the three diagrams with BRST vertex behaves effectively like a quartic vertex. Therefore, it is convenient to introduce an *effective BRST vertex* by defining

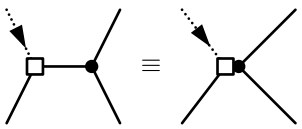

(3.10)

In this work, we shall use effective BRST vertices mainly in the graphical evaluation of STIs. However, nothing prevents us from associating an analytical expression with an effective BRST vertex and using it as a Feynman rule. We will demonstrate this on some examples below for illustration purposes. Notice that an effective BRST vertex is not symmetric under permutations of external lines. In particular, the direction present in the original diagram is kept.

Using the notation for effective BRST vertices, the STI for the quartic vertex with physical fields becomes

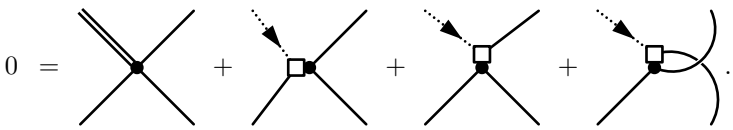

(3.11)

Now, for some fields there may not be a quartic tree level vertex with a gauge boson or Goldstone boson. In such cases, the first diagram in (3.11) is absent. Concerning physical fields, this condition is met for the fermion fields Ψ and $\bar{\Psi}$. Consequently, for these fields we have the STI

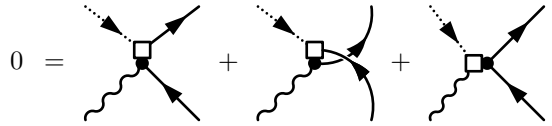

(3.12)

Inserting the corresponding analytical expressions this is seen to be the closure condition on the Lie algebra of generators in the fermion representation:

$$0 = g^2\gamma^\mu t^a t^b - g^2\gamma^\mu t^b t^a - \mathrm{i}g^2\gamma^\mu f^{abc}t^c = g^2\gamma^\mu\left([t^a,t^b] - \mathrm{i}f^{abc}t^c\right) \tag{3.13}$$

If unphysical vertices are taken into account, we can appeal to the absence of quartic ghost vertices. The corresponding STI is obtained by taking three derivatives of the Lee identity (2.85):

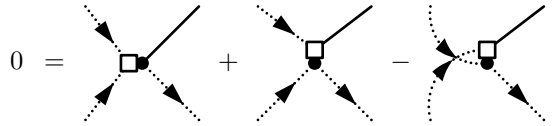

(3.14)

If the non-ghost line corresponds to a gauge boson, this identity is just the Jacobi identity for the structure constants of the Lie algebra:

$$\begin{aligned} 0 = (-gf^{abe})(gf^{ced}p^\mu) + (-gf^{ead})(gf^{cbe}p^\mu) - (-gf^{ebd})(gf^{cae}p^\mu) \\ = g^2p^\mu\left(f^{abe}f^{cde} + f^{bce}f^{ade} + f^{ace}f^{bde}\right) \end{aligned} \tag{3.15}$$

Then, if the non-ghost line corresponds to a Goldstone boson, we get the upper left component of the Lie algebra relation for the generators X^a (cf. (2.53)):

$$0 = g^2\xi^c M_c\left(-f^{abe}t^e_{cd} - t^a_{ce}t^b_{ed} - u^a_{cj}(-u^b_{jd}) + t^b_{ce}t^a_{ed} + u^b_{cj}(-u^a_{jd})\right) \tag{3.16}$$

In a similar manner, taking the non-ghost line to be a Higgs boson line, we would get the lower right component of the Lie algebra relation for X^a.

In any event, we see that the minus sign in the identity (3.14) is essential.

3.1.4 Five-Point Vertices

Of course, in a renormalizable theory, there are no five-point vertices. However, like in the case of quartic ghost vertices, the STI resulting from taking four derivatives of the Lee identity (2.85) (or, equivalently, three derivatives of the master identity (2.86), since only physical vertices are involved) is nontrivial and reads:

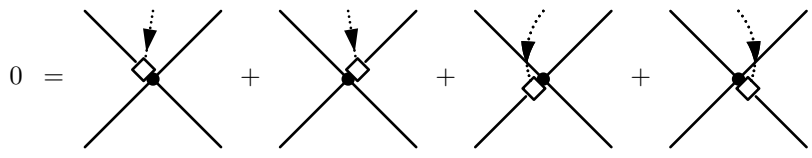

(3.17)

Here, we have again used the notion of effective BRST vertices to rewrite

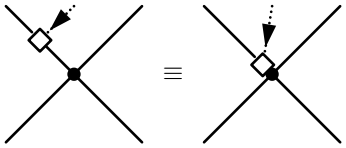

(3.18)

3.2 STIs of Connected Green's Functions: Examples

3.2.1 The STI for the Connected Three-Point Function

Denote by G_3 the generic connected three-point Green's function with at least one external gauge boson or Goldstone boson line and only physical external lines on tree level. In terms of Feynman diagrams, G_3 can be written

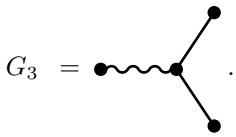

(3.19)

The STI for G_3 is obtained by expanding (2.76) for three external lines at tree level:

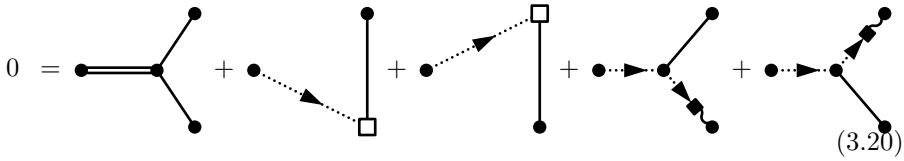

(3.20)

Actually, we could take this identity as a starting point for the analysis of STIs of Green's functions with more external lines, instead of deriving it from STIs for the tree level vertices. However, using this STI has the advantage of keeping the number of Feynman diagrams very small, making it easier to see what happens.

To begin with, we use (3.1) to replace the double line, corresponding to an insertion of B^a, in the first diagram on the RHS. This leads to

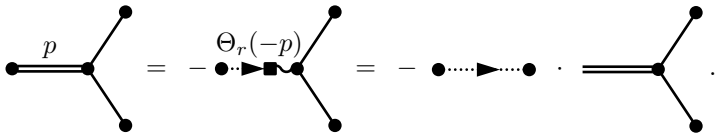

(3.21)

To understand this important relation, remember that the Feynman rules for vertices were defined for incoming momenta. On the other hand, the momentum p must be interpreted as outgoing. Therefore, according to (2.98), the contraction of $\Theta_r(-p)$ with the cubic vertex produces the first term on the RHS of the STI (3.7).

We will encounter this pattern, which does apply at a quartic vertex in the same way, over and over again in subsequent chapters. Therefore, it is useful to introduce a concise and intuitive notation for the above relation. To this end, we define

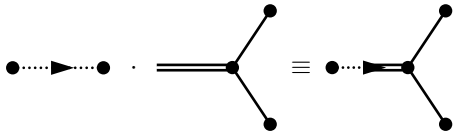

(3.22)

With this notation, the replacement of the B^a insertion becomes simply

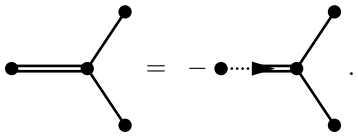

(3.23)

This relation, incidentally, explains the usefulness of the definitions (2.66) and (2.65) of Θ and $\bar{\Theta}$, respectively, in chapter 2.

Now, when we apply the STI (3.7), the inverse propagators in the terms with homogeneous BRST vertices will cancel the propagators connected to the two external lines on the right. The inhomogeneous terms, on the other hand, will contain expressions of the form

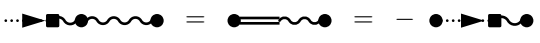

(3.24)

where the left end of the line is attached to the cubic vertex. This proves (3.20).

In practice, we will be going to use this STI inside larger diagrams in the following form:

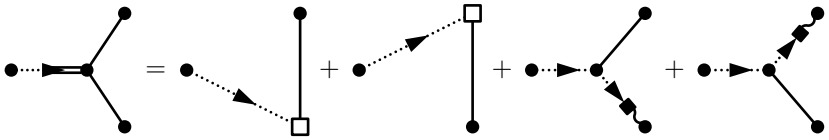

(3.25)

Likewise, we shall use an STI for the connected three-point function with two external ghost lines, which can alternatively be derived from (3.8) or directly as an STI for the connected Green's function:

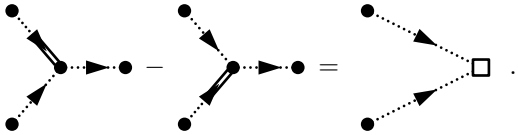

(3.26)

3.2.2 The STI for the Connected Four-Point Function

To see the identities (3.25) and (3.26) at work, and to provide an example for the use of STIs for the quartic vertices, we consider the connected four point Green's function.

Denote by G_4 the connected four-point Green's function with at least one external gauge boson or Goldstone boson line, and only physical external lines, expanded on tree level. We represent G_4 by a sum of Feynman diagrams as follows:

$$G_4 = s_4 + t_4 + u_4 + q_4$$

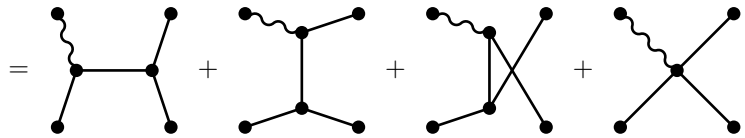

(3.27)

However, since G_4 is intended to represent the most general connected Green's function with one external gauge field line, each of the displayed diagrams has

to be interpreted as a *sum over all possible Feynman diagrams with the given topology*. This sum may be zero if no Feynman diagram exists according to the Feynman rules. For instance, if two external lines correspond to fermions, the diagram with quartic vertex will be absent. On the other hand, there may be more than one Feynman diagram for a particular topology, if the propagator may correspond to more than one field. (Remember in this context that, for our present purposes, gauge bosons and Goldstone bosons count as members of a *single* field A^a_r.)

We shall adopt this interpretation of diagrams for the remainder of this work, unless we explicitely state something else.

Correspondingly, the STI for G_4 can be represented, using (3.1), as:

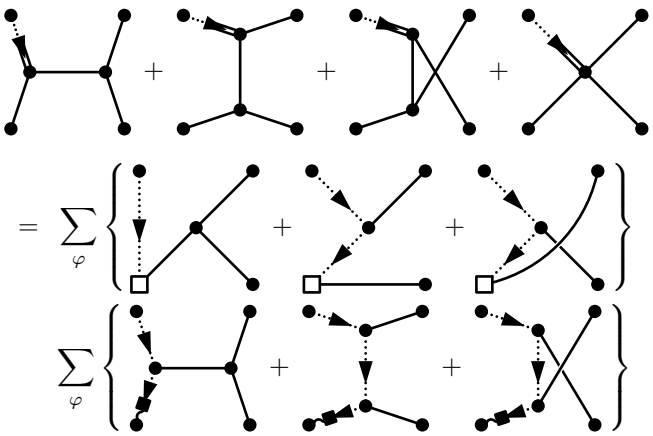

(3.28)

The sum is over the three external lines other than one with the double line.

We concentrate on the first diagram on the LHS. Employing (3.25), we can replace this diagram by

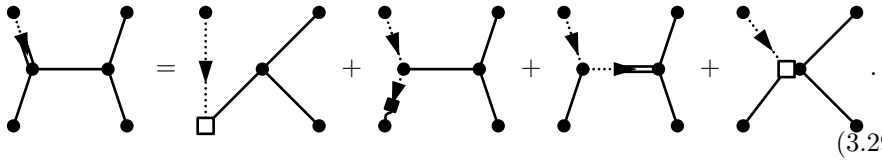

(3.29)

The first two diagrams on the RHS are required for the four-point STI (3.28). In the third diagram, we can apply (3.25) again, yielding

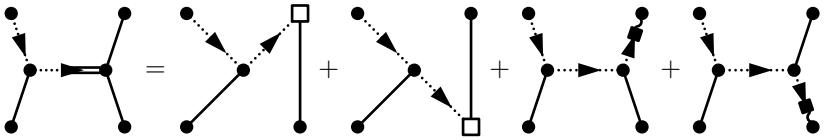

(3.30)

All terms are required for the four-point STI (3.28). We are left with the last diagram in (3.29). Proceeding in a similar manner for the second and third diagram on the LHS of (3.28), we see that the STI is satisfied up to the sum

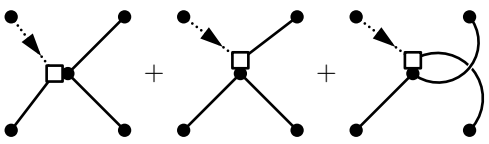

(3.31)

This sum is precisely cancelled by the contribution of the diagram with quartic vertex in (3.28). To see this, just multiply the STI (3.11) by one ghost propagator at the upper left line, and three propagators for the remaining, unspecified external lines.

3.3 Diagrammatical Relations

In the last section, we demonstrated on several examples how tree level STIs for connected Green's functions can be derived from the STIs for the vertices. Remarkably, although analytical expressions could have been inserted in each intermediate step, we did not have to write out a single formula in order to prove the validity of the STIs. Rather, we demonstrated that a sum of diagrams could be obtained by making replacements in other diagrams, the ones with double lines, according to the rules specified by vertex STIs.

In this section we will put this strategy on a sound basis. This will enable us to think and calculate entirely in terms of diagrams instead of analytical expressions, using an appropriate terminology. Once we have done this, we are in a good position to attack the really interesting case of Green's functions in higher orders of perturbation theory.

We introduce the necessary terminology in the next subsection. After that, we will define the replacement of a diagram with a double line by applying STIs as a map among linear combinations of diagrams. We are then going to investigate the properties of this map. Having established the formalism, we treat, as our last tree level example, the connected four-point Green's function with two external ghost lines. Once we have finished this, we are ready to make the connection to gauge flips as a means of constructing gauge invariant classes of Feynman diagrams.

3.3.1 Sums and Sets

Consider an arbitrary Green's function G. At a particular order of perturbation theory, G has an expansion in terms of Feynman diagrams with a fixed number of loops. We denote by $\mathcal{F}(G)$ the set of all diagrams contributing to this expansion, leaving the number of loops implicit. $\mathcal{F}(G)$ is called the *forest* of G.

Given the forest $\mathcal{F}(G)$ of Feynman diagrams, we define the Green's function G itself as

$$G = \sum_{d \in \mathcal{F}(G)} \chi(d) d \ . \tag{3.32}$$

In this expression, the *weight factor* $\chi(d)$ is the product of symmetry factors and fermion loop signs pertaining to the diagram d according to the Feymman rules. Note, that we really define G as a linear combination of diagrams, not of the corresponding analytical expressions. (Although the transition from the former to the latter is, of course, trivial.)

Now consider a Green's function G with an external gauge boson line. In general, we can extract from G a contribution to a scattering amplitude of a physically polarized gauge boson. Replace the gauge boson by the unphysical linear combination B^a (the gauge fixing functional), and call the resulting Green's function $\Theta(G)$.[2] There is a corresponding STI, in which $\Theta(G)$ is set

[2]The use of the symbol Θ will be justified in the next subsection.

equal to a sum over Green's functions with insertion of a single BRST transformed operator. We denote this sum by $\mathcal{W}(G)$ and refer to it as the *contact terms* of the STI. For instance, in the STI for the propagator $\langle W_\mu^a W_\nu^b \rangle^c$,

$$0 = \langle B^a W_\nu^b \rangle^c + \langle \bar{c}^a (s W_\nu^b) \rangle^c \quad , \tag{3.33}$$

we have

$$\Theta(G) = \langle B^a W_\nu^b \rangle^c \quad \text{and} \quad \mathcal{W}(G) = \langle \bar{c}^a (s W_\nu^b) \rangle^c \quad . \tag{3.34}$$

We define the expansions of $\Theta(G)$ and $\mathcal{W}(G)$ in complete analogy to the expansion (3.32) of G:

$$\Theta(G) = \sum_{d \in \mathcal{F}(\Theta(G))} \chi(d) d \tag{3.35}$$

$$\mathcal{W}(G) = \sum_{d \in \mathcal{F}(\mathcal{W}(G))} \chi(d) d \tag{3.36}$$

The point of these definitions is that they allows us to formally consider contributions to Green's functions or STIs as elements in the free vector space of Feynman diagrams, with rational coefficients. This construction is well defined, because the Feynman rules instruct us to sum over topologically different Feynman diagrams only, such that the underlying Feynman diagrams are really linearly independent. The statement that a certain linear combination of Feynman diagrams vanishes has a precise and unambigous meaning in this context: The coefficient of every diagram in the linear combination must vanish separately.

On the other hand, for some purposes it is convenient to be able to use set terminology for the Green's functions G, $\Theta(G)$ or $\mathcal{W}(G)$. A particular example, which we shall encounter in this work, concerns the question whether a given diagram can be produced by replacing the contracted external line in another diagram according to the vertex STIs, irrespective of the coefficients. We will soon define this replacement as a map in the free vector space of Feynman diagrams. The question could then be formulated in the language of linear combinations as follows: d is contained in a sum S of diagrams if it appears in S with a nonvanishing coefficient. Such phrases could only avoided by defining the abovementioned map for sets of Feynman diagrams, too.

Therefore, we shall use set terminology in connection with G, $\Theta(G)$ and $\mathcal{W}(G)$ in an intuitive sense. In particular, we will say that a diagram d is contained in a Green's function G. Also, we will say that a set of Feynman diagrams satisfies an STI, implying that the STI is satisfied by the sum over all diagrams with corresponding coefficients.

Note, however, that relations among linear combinations of diagrams will *never* be understood in the set theoretical sense. Thus, if we write down an equality between two expansions in Feynman diagrams, we *always* mean equality of coefficients for every Feynman diagram in the sum.

As a simple example, consider the gauge boson self energy $\Pi^{\mu\nu}$ in a pure Yang-Mills theory. In dimensional regularization, there are just two nonzero diagrams. Thus,

$\mathcal{F}(\Pi^{\mu\nu}) \;=\; \Big\{$ 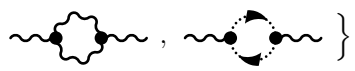 $\Big\}$ (3.37)

The Green's function itself is expanded as

$\Pi^{\mu\nu}$ = $\frac{1}{2}$ 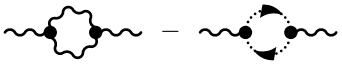 . (3.38)

$\Pi^{\mu\nu}$ satisfies the STI (2.86), evaluated at one-loop level. The statement that the set (3.37) satisfies the STI will be taken to mean just that.

3.3.2 Contraction as Map

In the previous section, we have defined the Green's function $\Theta(G)$ as the Green's function obtained from G by replacing a certain gauge boson by the unphysical linear combination B^a of gauge bosons and Goldstone bosons. We refer to this replacement as *contraction*, since it amounts to contracting the operator $\bar{\Theta}_r$ or Θ_r with a Green's function of the (formally) five dimensional gauge field A_r.

The STI for the Green's function G expresses the statement that the sum of the contraction $\Theta(G)$ and the contact terms $\mathcal{W}(G)$ is a vanishing linear combination of Feynman diagrams. We have already seen in the explicit tree level examples of section 3.2, that the contraction produces a sum of diagrams from each diagram contributing to G. It is therefore natural to consider the contraction as a linear map Θ in the space of linear combinations of Feynman diagrams. We use the same symbol here as for the operators Θ_r and $\bar{\Theta}_r$ to emphasize the close relationship.[3] The use of different symbols for connected and 1PI Green's functions is unnecessary here, because it will always be clear from the context which one applies.

We now have to give a definition of the map Θ. Since Θ is assumed to be linear, it suffices to define it for a single diagram d contributing to G. Recall how, in the derivation of the STI for the four-point function, we had to use the STI (3.7) repeatedly (cf. the discussion around (3.29) and (3.30)). This is the general pattern: The sum of diagrams $\Theta(d)$ will always be obtained by repeatedly applying contractions at vertices of d.

To formalize this observation, we define the *elementary contraction* θ of a vertex to extract the homogeneous parts in the tree level STIs:

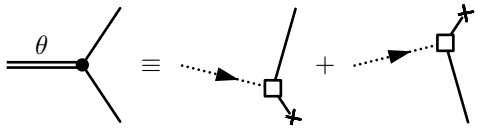 (3.39)

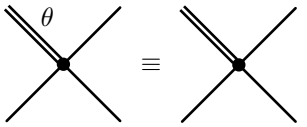 (3.40)

In particular, for the quartic vertex θ is equal to the full contraction. On the other hand, for the cubic vertex we have

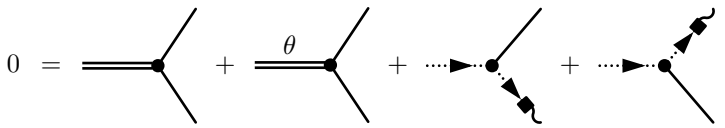 (3.41)

[3] In fact, for the analytical expressions corresponding to G, the operators Θ_r and $\bar{\Theta}_r$ do the same as the operator Θ for the formal linear combination of Feynman diagrams.

In a similar manner, the elementary contraction can be defined for the STI of the ghost vertex:

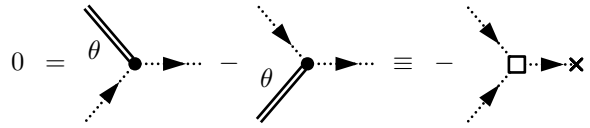

(3.42)

Thus, at a ghost vertex θ is equal to the full contraction.

Again, for use inside larger diagrams, the following versions of the cubic vertex-STI are actually more convenient:

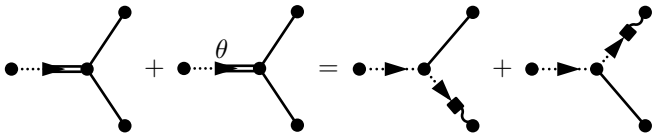

(3.43)

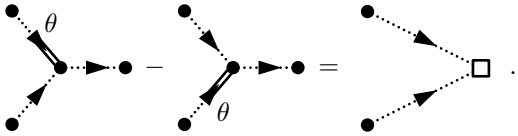

(3.44)

Let us rewrite the evaluation of the contraction in (3.29) using our new terminology:

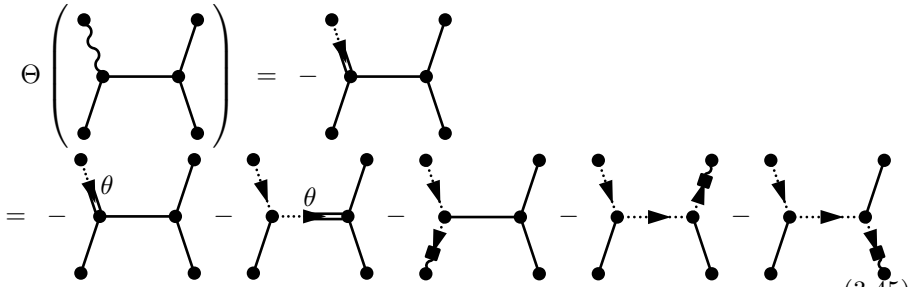

(3.45)

We can make this result even more uniform by defining θ to be the identity map for the endpoints of external lines:[4]

(3.46)

We can now describe precisely the action of the contraction map Θ on a single diagram d. Θ is given by the contraction of a gauge field line at some vertex e. At e, an STI can be used to replace the contracted vertex by a sum of other terms. Independent of the nature of e, there will always be a contribution to this sum by evaluating the elementary contraction θ at e. However, if e is a cubic physical vertex, the use of the STI (3.43) will produce a new contraction at a

[4] In principle, this is not a contraction, because the external line carries a five dimensional index. This could be remedied by defining a Feynman rule associating with an external vertex with index r the tensor δ^s_r and then contracting θ into s. However, the meaning of (3.46) should be intuitively clear without this complication.

neighboring vertex v, if e is connected to v by a gauge boson or Goldstone boson line. At v, we can evaluate the contraction in exactly the same way. Observe that, in this process, the gauge boson or Goldstone boson line connecting e and v is replaced by a ghost line. This process is recursively iterated. The recursion terminates, when no more cubic vertex with outgoing gauge field lines can be reached from another contracted vertex.

When the recursion stops, $\Theta(d)$ will be expressed as a sum of diagrams, each of which can be characterized uniquely in the following way. Define a *path* in d as a sequence of gauge field propagators, connecting e to some vertex v of d *via* cubic vertices, such that no propagator appears twice. In particular, this implies that a path always starts at an external vertex. Evidently, the recursive evaluation of $\Theta(d)$ will eventually proceed along every path in d. Also, if a vertex w cannot be reached by a path, there will be no term in $\Theta(d)$ corresponding to a contraction at w. As an example, consider the following diagram, where all gauge bosons have been made explicit:

$d \;=$ 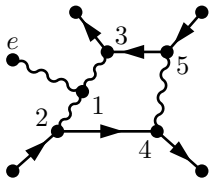

(3.47)

There are three paths in this diagram, which we indicate in by drawing the corresponding gauge field propagators in a bold line style:

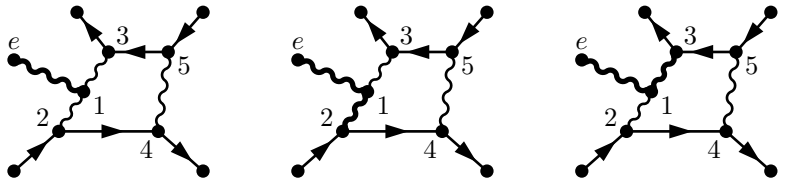

(3.48)

$P_1 = \{e, 1\}$ $P_2 = \{e, 1, 2\}$ $P_3 = \{e, 1, 3\}$

The vertices 4 and 5, on the other hand, cannot be reached by any path. Thus, the contraction $\Theta(d)$ will decompose into a sum over contributions of the paths P_1, P_2, and P_3.

Consider now the evaluation of the elementary contraction θ at the endpoint v of a path P. If v is an external vertex, θ will produce a single term according to (3.46). If v is a cubic vertex, θ produces a sum of two diagrams:

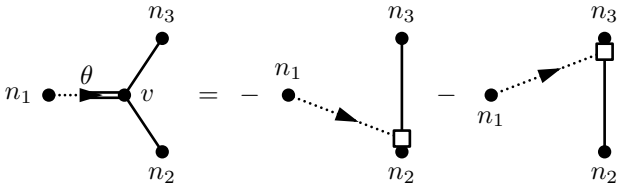

(3.49)

Either of the two diagrams on the RHS can be identified uniquely by specifying the second propagator, apart from the ghost propagator, coincident with the effective BRST vertex. These are (n_3, n_2) for the first diagram as well as (n_2, n_3)

for the second diagram. Note that, in general, it is really necessary to specify the propagator, even though one might be tempted to think that specifying the vertex n_2 or n_3 would be sufficient. However, n_2 may be equal to n_3, in which case the vertex does not provide enough information. The propagators, on the other hand, can be distinguished if necessary by an additional label, e. g. their momentum.

If v is a quartic vertex, it gets replaced by a sum of terms with an effective BRST vertex:

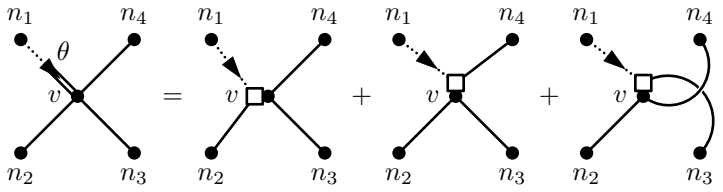

(3.50)

Also in this case, either of the three diagrams on the RHS is uniquely identified by specifying the second propagator connecting to the BRST vertex, which is (n_2, v), (n_4, v), and (n_3, v), respectively.

In any event, an arbitrary diagram in $\Theta(d)$ can be characterized uniquely by a path P and, if the path does not end at an external vertex or a ghost line, an additional edge specifying the *direction* of the resulting BRST vertex.

As an example, consider the path P_1 of the diagram d in (3.47). Evaluating the elementary contraction θ at the vertex 1, we obtain the following two terms:

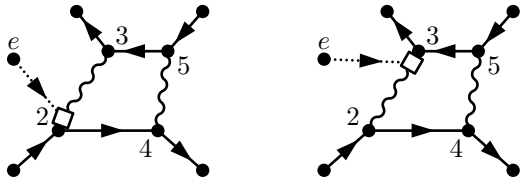

(3.51)

$n_1 = (3, 2)$ $\qquad$ $n_1' = (2, 3)$

Now let a path P and a direction n in a diagram d be given. A contribution to $\Theta(d)$ can be obtained by replacing P with a ghost line and performing θ in the direction of n. Call this operation an *elementary contraction of the diagram* d, denoted by $\theta_{(P,n)}(d)$. With this notation, the two elementary contractions in (3.51) would be denoted as $\theta_{(P_1,n_1)}(d)$ and $\theta_{(P_1,n_1')}(d)$, respectively.

Let $\mathcal{P}(d)$ be the set of all possible combinations (P, n) of paths and directions for the diagram d. Then, the complete contraction $\Theta(d)$ can be written as a sum of elementary contractions of d:

$$\Theta(d) = \sum_{\mathcal{P}(d)} \theta_{(P,n)}(d) \tag{3.52}$$

The sum is over all possible paths and directions. At tree level, all diagrams in this sum are distinct. However, as we shall see, in higher orders different choices of P and n may lead to the same diagram. One of the major tasks in the proof of STIs for higher order diagrams will be to demonstrate that the occurrence of nontrivial coefficients does not spoil the required cancellations.

For further illustration, we may look back at the example of section 3.2.2. For instance, in (3.45) the paths are visible as ghost lines. The evaluation of

the elementary contraction θ in the first and second diagram can be read from relations (3.29) and (3.30). As an example of an elementary contraction at a quartic vertex, cf. (3.31).

Equation (3.52) defines the action of Θ on a single diagram. Its action on a linear combination of diagrams is then defined in an obvious way by linearity.

Evidently, we do not learn anything new about the STI of G_4 in this terminology. The point of the decomposition of $\Theta(d)$ in terms of elementary contractions is that it allows for a reorganization which will simplify the diagrammatical proof of STIs immensely.

3.3.3 Decomposing the Contraction Map Θ

In this section, we show how the contraction Θ as well as the elementary contraction θ, of diagrams as well as vertices, can be decomposed in such a way that the production of contact terms can be disentangled from the cancellations occurring in the diagrammatical proofs of STIs.

In section 3.2.2 we showed how the diagrams in the four point Green's function G_4 conspire to produce the contact terms $\mathcal{W}(G_4)$ of the STI when the contraction $\Theta(G_4)$ is evaluated. In general, $\Theta(d)$ for a single diagram d contained contact term diagrams as well as diagrams that had to cancel in order for the STI to be satisfied. The cancellation was then achieved by picking appropriate terms from the contributions of all diagrams.

While this approach ultimately worked, the proof of the STIs can be arranged much clearer by separating the production of contact term diagrams from the cancellations. The basic idea is the following: Let G be some connected Green's function and $\mathcal{W}(G)$ the sum of contact terms. The contraction $\Theta(G)$ is given by

$$\Theta(G) = \sum_{d \in G} \chi(d)\Theta(d) = \sum_{d \in G} \chi(d) \sum_{\mathcal{P}(d)} \theta_{(P,n)}(d) \ , \tag{3.53}$$

with $\chi(d)$ the weight factor of the diagram d.

We now decompose $\Theta(G)$ as follows:

$$\Theta(G) = \Omega(G) + \mathrm{B}_4(G) + \mathrm{B}_5(G) + \mathrm{B}_c(G) \tag{3.54}$$

We define the various maps in this sum for single diagrams and then extend by linearity. Then, let G be some Green's function and d a diagram in d. If G has no external ghost lines, $\Omega(d)$ is the sum over all diagrams in $\Theta(d)$ with one of the following subdiagrams at the end of external lines:

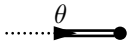

(3.55a)

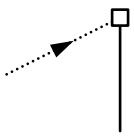

(3.55b)

For Green's functions with external ghost lines, we include, in addition, diagrams with an elementary contraction at a ghost line, if the outgoing ghost line is an

external line (indicated here by an open circle):

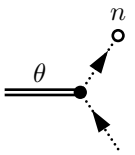

(3.55c)

$B_4(d)$ is the sum over all diagrams in $\Theta(d)$ with a quartic effective BRST vertex without extra ghost lines:

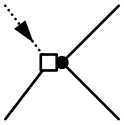

, (3.56)

$B_5(d)$ is the sum over all diagrams in $\Theta(d)$ with a five-point effective BRST vertex:

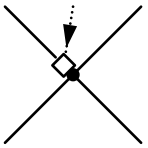

. (3.57)

Finally, $B_c(d)$ is the sum over all diagrams in $\Theta(d)$ with either an elementary contraction at a ghost line or an effective BRST vertex with extra ghost lines, but not if the outgoing ghost line is an external line:

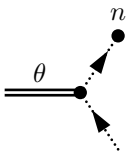

(3.58a)

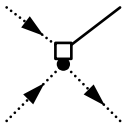

(3.58b)

Given the decomposition (3.54) of $\Theta(G)$, the STI $\Theta(G) + \mathcal{W}(G) = 0$ can be verified by proving separately $\Omega(G)+\mathcal{W}(G) = 0$ and $B_4(G)+B_5(G)+B_c(G) = 0$. We will do this in the next chapter.

First, however, we show how the various terms in the decomposition can be expressed quite naturally as sums over decomposed elementary contractions. To this end, consider again a single diagram d. Clearly, it is possible to express $\Omega(d)$ as a sum over paths and directions. Now, however, only those combinations (P, n) are selected, for which the contraction $\theta_{(P,n)}$ satisfies the corresponding criteria. Denote the set of such combinations (P, n) by $\mathcal{P}_\Omega(d)$. Then

$$\Omega(d) = \sum_{\mathcal{P}_\Omega(d)} \theta_{(P,n)}(d) \ . \tag{3.59}$$

It is possible to eliminate the restriction on the summed paths by defining an elementary contraction ω as follows:

$$\omega_{(P,n)}(d) = \begin{cases} \theta_{(P,n)}(d) & \text{for } (P,n) \in \mathcal{P}_\Omega(d) \\ 0 & \text{for } (P,n) \notin \mathcal{P}_\Omega(d) \end{cases} \tag{3.60}$$

In complete analogy, we define the restricted path sets $\mathcal{P}_{\mathrm{B}_4}(d)$, $\mathcal{P}_{\mathrm{B}_5}(d)$, and $\mathcal{P}_{\mathrm{B}_c}(d)$, as well as the elementary contractions β_4, β_5 and β_c. Obviously, $\mathcal{P}$ is the disjoint union of the restricted path sets:

$$\mathcal{P}(d) = \mathcal{P}_\Omega(d) \cup \mathcal{P}_{\mathrm{B}_4}(d) \cup \mathcal{P}_{\mathrm{B}_5}(d) \cup \mathcal{P}_{\mathrm{B}_c}(d) \tag{3.61}$$

Therefore, we have the following decomposition of the elementary contractions θ of d:

$$\theta_{(P,n)}(d) = \omega_{(P,n)}(d) + (\beta_4)_{(P,n)}(d) + (\beta_5)_{(P,n)}(d) + (\beta_c)_{(P,n)}(d) \ . \tag{3.62}$$

For every pair (P, n), exactly one of the terms in this sum is nonzero.

Finally, the decomposition (3.62) of elementary contractions $\theta_{(P,n)}(d)$ of diagrams induces a corresponding decomposition of the elementary contraction θ of a single vertex. For instance, β_4 will perform only replacements that lead to a subdiagram of the form (3.56).

For many purposes, it is useful to decompose the elementary contraction β_4 further into β_{43} and β_{44} according to the origin of the quartic BRST vertex. In particular, β_{43} will act only at a cubic vertex:

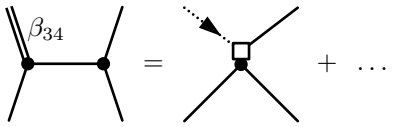

(3.63)

β_{44}, on the other hand, will produce quartic BRST vertices from quartic vertices:

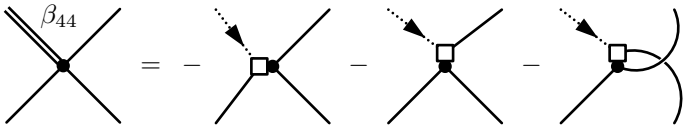

(3.64)

Accordingly, we decompose the elementary contraction $(\beta_4)_{(P,v)}$ into $(\beta_{43})_{(P,v)}$ and $(\beta_{44})_{(P,v)}$. Likewise, B_4 is split into B_{43} and B_{44}.

The foregoing discussion might appear very formal. However, there is a very intuitive explanation for what our definitions achieve. Suppose we are interested in how the diagrams in $\mathrm{B}_4(G)$, i. e. with subdiagrams of the form (3.56), can be produced by applying STIs in the diagrams of G. Of course, we could just recursively evaluate the contraction $\Theta(d)$ as described in the last subsection, throwing away all undesired diagrams. A better approach would be to just produce the desired contractions, ignoring paths (P, n) which would not contribute to $\mathrm{B}_4(G)$. The neglected elementary contractions can then be picked up later by one of the remaining maps. The above definitions just formalize this simple idea.

3.4 The STI for the Two-Ghost Four-Point Function

In this section, we use the formalism developed in the last section to verify the STI (2.90) for the connected four-point Green's function G_{12} with two external ghost lines at tree level. This will enable us to derive gauge flips for diagrams external ghost lines.

First, we write down the expansion of G_{12} at tree level:

$$G_{12} \;=\; s_{12} + t_{12} + u_{12} \;=\;$$ 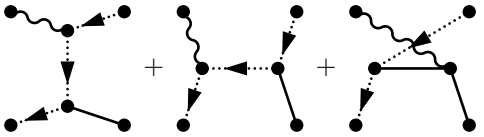 (3.65)

The names have been introduced for future reference. G_{21} is obtained from G_{12} by exchanging the gauge field line with the incoming ghost line:

$$G_{21} \;=\; s_{21} + t_{21} + u_{21} \;=\;$$ 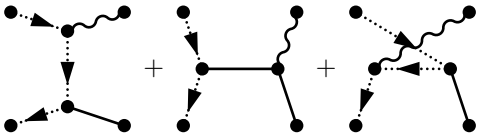 (3.66)

The contact terms of the STI (2.90), evaluated at tree level, are given by

$$\mathcal{W}(G_{12}) \;=\; -\;\mathcal{W}(G_{21}) \;=\; -$$ 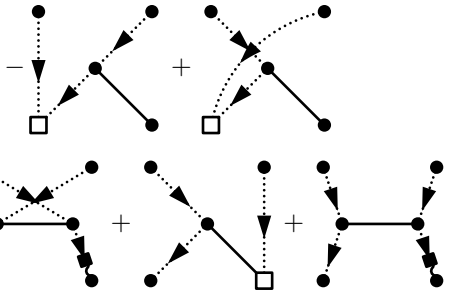 (3.67)

To verify the STI (2.90) at tree level, we have to show that

$$\Theta(G_{12}) - \Theta(G_{21}) = \mathcal{W}(G_{12}) \;. \tag{3.68}$$

To begin with, let us note that B_4 and B_5 are identically zero in this case, the former because every elementary contraction of a diagram will involve a ghost line, the latter because there are no five-point subdiagrams.

Next consider B_c. For s_{12}, we have

$$\mathrm{B}_c(s_{12}) = \Theta(s_{12}) = \;-$$ 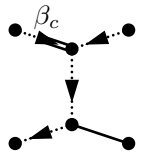 (3.69)

Doing the same for s_{21} and using the STI (3.26), we get

$$\mathrm{B}_c(s_{12}) - \mathrm{B}_c(s_{21}) = \;-$$ 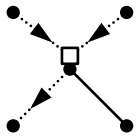 (3.70)

Then, we have

$$\mathrm{B}_c(u_{12}) \;=\; -$$ 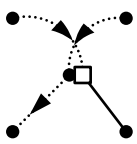 (3.71)

$$\mathrm{B}_c(t_{21}) \;=\; -$$ 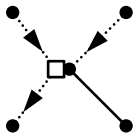 (3.72)

On the remaining diagrams, B_c gives zero. Collecting the contributions to B_c, we get a cancellation by making use of the STI (3.14):

$$\mathrm{B}_c(s_{12}) - \mathrm{B}_c(s_{21}) + \mathrm{B}_c(u_{12}) - \mathrm{B}_c(t_{21}) = 0 \tag{3.73}$$

Finally, we have to evaluate the contributions of Ω. From t_{21}, we get

$$\Omega(t_{21}) \;=\; -$$ 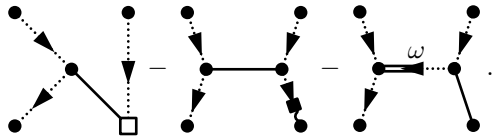 (3.74)

Next evaluate the contribution from t_{12}:

$$\Omega(t_{12}) \;=\; -$$ 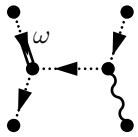 (3.75)

Using (3.26), we can add up the two contributions to get

$$\Omega(t_{12}) - \Omega(t_{21}) \;=$$ 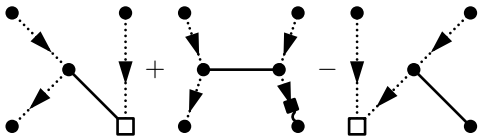 (3.76)

This is precisely one half of the contact terms. Doing the same manipulations for u_{12} and u_{21} we arrive at

$$\Omega(t_{12}) + \Omega(u_{12}) - \Omega(t_{21}) - \Omega(u_{21}) = \mathcal{W}(G_{12}) \ . \tag{3.77}$$

We have exhausted all nonzero contributions to $\Theta(G_{12})$ and $\Theta(G_{21})$. Therefore, the STI (3.68) is proven.

3.5 Gauge Cancellations and Gauge Flips

In this section, we want to make a connection between cancellations in the STIs for G_4 on the one hand and G_{12} as well as G_{21} on the other hand, and gauge flips. We have already established a notation for the diagrams in these Green's functions (cf. (3.27), (3.65), and (3.66)).

Let us briefly recall the derivation of the STI for G_4, using the terminology developed above: The contact terms $\mathcal{W}(G_4)$ are produced by Ω, i. e. we have $\Omega(G_4) + \mathcal{W}(G_4) = 0$. $\mathrm{B}_5(G_4)$ and $\mathrm{B}_c(G_4)$ are identically zero, the former due to lack of a sufficient number of external lines, the latter due to the absence of ghost lines. B_4 is split into B_{43} and B_{44} according to (3.63) and (3.64). Now

B_{43} yields zero on q_4, while B_{44} yields zero on s_4, t_4 and u_4. The remaining nonzero contributions cancel precisely:

$$\mathrm{B}_{43}(s_4) + \mathrm{B}_{43}(t_4) + \mathrm{B}_{43}(u_4) + \mathrm{B}_{44}(q_4) = 0 \tag{3.78}$$

This relation clearly shows that no real subset S of G_4 can satisfy the STI on its own.[5] For this to be true, S would have to satisfy

$$\Theta(S) = \Omega(S) \ . \tag{3.79}$$

But this implies

$$\mathrm{B}_4(S) = 0 \ , \tag{3.80}$$

which is impossible for a real subset of G_4 according to (3.78).

We can put it another way. If we start with one diagram, s_4 say, and require that diagrams be added until (3.79) holds, we see that we are successively forced to add t_4, u_4, and q_4 as well. Now elementary gauge flips are defined as the possible transformations among elements of $\mathcal{F}(G_4)$. Therefore, we can express this result as the statement that *all possible elementary gauge flips must be applied to s_4 in order to obtain a set of diagrams satisfying* (3.79). This demonstrates the connection between gauge cancellations and elementary gauge flips for G_4.

Next we are going to derive elementary gauge flips for diagrams in G_{12} by considering the cancellations in the STI (3.68) for G_{12} and G_{21}. Since this is an STI for two Green's functions at the same time, we need to find a generalization of the requirement (3.79) for a subset of diagrams to satisfy the STI by itself. Denoting by S_{12} and S_{21} subsets of G_{12} and G_{21}, respectively, a natural generalization would be to demand

$$\Theta(S_{12}) - \Theta(S_{21}) = \Omega(S_{12}) - \Omega(S_{21}) \ . \tag{3.81}$$

However, this requirement is actually not sufficient to guarantee that the RHS is a subset of the contact terms $\mathcal{W}(G_{12})$. To see this, observe that, for diagrams with ghost lines, ω does not produce a contact term directly when applied to a single diagram in G_{12}. Rather, we must subtract the contribution of a corresponding diagram in G_{21} to get a contact term. We have seen this explicitely in (3.76). Therefore, (3.81) has to be supplemented by the constraint that the RHS must be contained in the contact terms $\mathcal{W}(G_{12})$.

A glance at (3.73) shows that the cancellations alone already select two diagrams each from G_{12} and G_{21}. The supplementary constraint then forces us to choose all of G_{12} and G_{21}. Since elementary gauge flips for diagrams with two external ghost lines are precisely the transformations among diagrams in G_{12} (or, equivalently, G_{21}), this is again equivalent to the statement that (3.81) can only be satisfied by a set which is invariant under elementary gauge flips.

Before closing this section, let us comment on two points. First, the reader familiar with the literatur on gauge flips may wonder why we did not discuss elementary gauge flips among four-point diagrams with four external ghost lines. The reason is that, as we shall see in the next chapters, these are really not needed to prove the STIs we consider. However, for more general STIs (e. g.

[5] Here and in the rest of this section, we make extensive use of set terminology for Green's functions. For a justification, cf. section 3.3.1.

STIs with several contractions), or in the study of the gauge parameter dependence of Green's functions, the situation may be different. As a second remark, we note that the STI for the (non-existent) five-point vertices has not been used up to this point, because we only considered four-point Green's function on tree level. However, this STI plays a crucial rôle in the gauge cancellations already at tree level [5]. Likewise, it will have to do its part in the case of higher order diagrams.

3.6 Projections

Before we enter into the discussion of gauge cancellations in higher order diagrams, we introduce yet one more useful tool. Clearly, it would be desirable if we did not have to consider all diagrams of a Green's function at once. To this end, observe that an elementary contraction θ of a diagram d preserves many properties of d. In particular, although θ exchanges cubic gluon vertices by ghost gluon vertices (and propagators accordingly) on the path to the contracted vertex, this does not change the total number of cubic vertices. When θ acts on a vertex inside d, it may remove a propagator, joining two cubic vertices into an effective BRS vertex. Essentially, this produces a quartic vertex from two cubic ones. But this can happen only once for every elementary contraction of d. Consequently, cancellations can only take place among diagrams for which the number of quartic vertices differs by one. We have seen an example of this in the discussion of the STI for G_4 in section 3.2.2.

Therefore, it makes sense to consider for a Green's function G the subset of diagrams with exactly ν quartic vertices. More precisely, since G is an element of the free vector space over Feynman diagrams, we can consider the projection of G onto the subspace of diagrams with ν quartic vertices. We will denote this projection as

$$[G]^\nu \quad . \tag{3.82}$$

There is another important property of a diagram d that can only be changed in a very controlled way, namely, the number ρ of ghost loops. Of course, this is irrelevant on tree level. However, decomposing a connected Green's function according to the number of ghost loops will simplify the proof of cancellations involving the STIs for ghost vertices a lot. Therefore, we introduce a projection of G on the subspace of diagrams with ρ ghost loops, denoted as

$$[G]_\rho \quad . \tag{3.83}$$

Clearly, both projections are independent. Therefore we can consider the subspace of diagrams with ν quartic vertices and ρ ghost loops. The projection of G onto that subspace is then

$$[G]^\nu_\rho \quad . \tag{3.84}$$

The contact terms $\mathcal{W}(G)$ can be projected in the same way.

If the theory contains physical fermions, the number of fermion loops is actually preserved by elementary contractions. In principle, then, we could introduce a further projection onto the subspace of diagrams with a fixed number of fermion loops. However, because this number does not change at all, all relations among diagrams will hold separately in each subspace. We can therefore leave this decomposition implicit.

—4—
Groves of General Connected Green's Functions

In this chapter, we demonstrate, how the multi-loop Feynman diagrams corresponding to an expansion of a general connected Green's function G (without external ghost lines) at an arbitrary order of perturbation theory can be decomposed into *groves*, i. e. subsets of Feynman diagrams satisfying the STI by themselves (in a sense to be made precise below). As a byproduct, we obtain a full diagrammatical proof of the STI for G.

This chapter is organized as follows. First, we briefly discuss the prerequisites and introduce the necessary terminology for a diagrammatical proof of the STI. Then we prove the STI to one-loop order. The one-loop proof will already show many general features of the gauge cancellations in higher orders of perturbation theory. In particular, we are then ready to make the connection between the cancellations occuring in the proof of the STI and gauge flips. After that we extend the proof of the STI to arbitrary loop order and argue that the groves can still be constructed by the set of gauge flips derived from the one-loop proof.

4.1 Preliminaries

The STI for a single contraction of a connected Green's function G without external ghost lines has been given in (2.76). Using the terminology developed in chapter (3), this STI can be written as

$$0 = \Theta(G) + \mathcal{W}(G) \ , \tag{4.1}$$

This identity has to be considered at a fixed order of perturbation theory, corresponding to a fixed number L of loops. Proving (4.1) is equivalent to demonstrating that the recursive evaluation of $\Theta(G)$ equals the contact terms $\mathcal{W}(G)$ with the opposite sign. We assume that the divergencies generally occuring in higher order diagrams are regularized using dimensional regularization, so that $\Theta(G)$ can be evaluated by using tree level STIs naively even in divergent parts of Feynman diagrams, which is justified because dimensional regularization preserves gauge invariance.

We can reduce the combinatorial complexity by decomposing G and $\mathcal{W}(G)$ according to the number of ghost loops and the number of quartic vertices, because, as we shall soon demonstrate, the map Θ changes these numbers by at most one. Once we have determined how the gauge cancellations work, we can

use this information to define the correct set of gauge flips for the construction of minimal gauge invariant subsets of $\mathcal{F}(G)$.

4.2 STI at One-Loop

In this section we take G and $\mathcal{W}(G)$ to refer to their respective expansions in one-loop Feynman diagrams. Using the decomposition (3.54), we will verify the STI (4.1) by successively proving the following statements:

$$\Omega(G) + \mathcal{W}(G) = 0 \tag{4.2a}$$
$$\mathrm{B}_4(G) = 0 \tag{4.2b}$$
$$\mathrm{B}_5(G) = 0 \tag{4.2c}$$
$$\mathrm{B}_c(G) = 0 \tag{4.2d}$$

4.2.1 Production of Contact Terms

We begin by proving (4.2a), which states that the production of contact terms is entirely described by the action of Ω. From the defining contractions (3.55) of Ω it is obvious that these contractions can change neither the number of quartic vertices nor the number of ghost loops. For the elementary contraction ω is zero at a quartic vertex or ghost vertex. Therefore, (4.2a) must hold separately for every projection $[G]^\nu_\rho$ of G. Since we can project the contact terms $\mathcal{W}(G)$ in the same way, we have to show

$$\Omega\left([G]^\nu_\rho\right) + [\mathcal{W}(G)]^\nu_\rho = 0 \ . \tag{4.3}$$

For notational convenience, however, we shall continue to write G instead of $[G]^\nu_\rho$, and likewise for $\mathcal{W}(G)$, in the remainder of this section, the decomposition being implicitely understood. We can do so safely, because Ω preserves ν and ρ.

We are going to verify (4.3) in two steps. First, we demonstrate that for every diagram d in G, $\Omega(d)$ is contained in $\mathcal{W}(G)$ with the opposite sign. (Formally, this means that the projection of $\Omega(d) + \mathcal{W}(G)$ onto $\Omega(d)$ vanishes.) In the second step, we show that every diagram in $\mathcal{W}(G)$ can be produced by applying an elementary contraction ω to some d in G. These two statements clearly imply the relation (4.3).

Every diagram produced by applying an elementary contraction $\omega_{(P,v)}$ to d in G constitutes a valid Feynman diagram for $\mathcal{W}(G)$. This is clear, because the forest $\mathcal{F}(\mathcal{W}(G))$ consists of *all* diagrams with a subdiagram (3.55a) or (3.55b) in place of an external line, with the ghost line replacing a gauge field line originating at the contracted external gauge field line. Note that this argument is actually independent of the number L of loops. Furthermore, the relative sign between $\omega_{(P,v)}(d)$ and the corresponding contribution to $\mathcal{W}(G)$ is caused by the relation (3.23). Consequently, we need only show that every nonzero $\omega_{(P,v)}(d)$ is produced with the correct symmetry factor. (Since the number ρ of ghost loops is preserved by ω, the sign of the weight factor is automatically correct.)

Let $d' = \omega_{(P,v)}(d)$. d' will have the same symmetry factor as d unless the ghost line in d' destroys an automorphism of d. This can happen because a ghost line is always directed while the gauge field line it replaces may be not, if

the gauge field is neutral. Examples are provided by the gluon ghosts in QCD or the ghosts of photon and Z^0 in the SM.

At one loop level, d can only have a nontrivial automorphism if it contains one of the following tadpole or self energy diagrams as subdiagram:

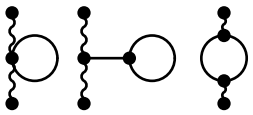

(4.4)

Among these, only in the rightmost diagram, i. e. the self energy, can the path P pass through the loop. For definiteness, we consider the case of the gluon self energy in QCD. Now, while the gluon self energy has a symmetry factor $1/2$, the ghost self energy has not. On the other hand, there are two equivalent paths through the gluon self energy. Both paths are appear in the sum $\Omega(d)$, whence the ghost self energy is produced twice:

(4.5)

Thus, the symmetry factor is cancelled, and consequently d' will be produced with the correct symmetry factor of unity. This shows that $\Omega(G)$ is contained in $\mathcal{W}(G)$.

We are not yet ready, however, because in principle it would be possible that there exists a diagram d' in $\mathcal{W}(G)$, which is not in $\Omega(G)$. This is, however, impossible, because given d' in $\mathcal{W}(G)$ we can always reverse the contraction by replacing the ghost line by a gauge field line and reading the definition of the elementary contraction ω backwards. This process will give us a valid Feynman diagram for G. (Although not necessarily with the correct weight, but that does not matter here.) Consequently, d' must be in $\Omega(G)$. This completes the proof of (4.3), hence (4.2a).

In the next sections, we will verify the remaining relations of (4.2). The proof of these relation is actually at the heart of this work, because it will disclose the gauge cancellations among various diagrams, thus allowing us to justify the use of gauge flips in constructing gauge invariant classes of Feynman for one loop processes.

4.2.2 Cancellations in $\mathrm{B}_4(G)$

In this section, we are going to verify the validity of (4.2b). We have seen an explicit example of the cancellations in $\mathrm{B}_4(G_4)$ in the derivation of the STI for the four-point Green's function G_4 on tree level in chapter 3. This identity is a relation for offshell values of the external momenta. Therefore, the same cancellation would take place among four larger diagrams related to each other by the exchange of a single four-point subdiagram, chosen from the set $\{s_4, t_4, u_4, q_4\}$ of diagrams constituting $\mathcal{F}(G_4)$. Indeed, this observation is the basis for the construction of gauge invariant classes of Feynman diagrams in the tree level case.[4][5]

It is reasonable to expect that in the one loop case, too, similar cancellations take place among diagrams for which the number of quartic vertices differs by one, irrespective of the number of ghost loops. Indeed, we shall now prove that

$$\mathrm{B}_{43}\Big([G]^{\nu}\Big) + \mathrm{B}_{44}\Big([G]^{\nu+1}\Big) = 0 \ . \tag{4.6}$$

Since B_{43} increases the number of quartic vertices by one, this means that the sector of $B_4(G)$ with ν quartic vertices (not counting the effective BRST vertex) receives contributions from diagrams with ν and $\nu+1$ quartic vertices, and that these contributions cancel precisely.

For the proof of (4.6), consider a diagram d_t in $[G]^\nu$:

d_t =

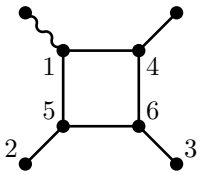

(4.7)

For definiteness, we have chosen $\nu = 0$ here. Our arguments will, however, not depend on this choice. We have labeled the vertices for easier referencing.

Now apply the contraction B_{43} to d_t. B_{43}, like all contraction maps, can be expressed as a sum of elementary contractions over all possible paths and directions of d_t. The nonzero contributions to B_{43} come from paths for which endpoint and direction are given by two cubic vertices. These two vertices define a four-point subdiagram of d_t. To illustrate this point, we choose the path $P_t = \{1, 5\}$ and direction $n_t = 2$.[1] The corresponding subdiagram is drawn in bold style in the following diagram:

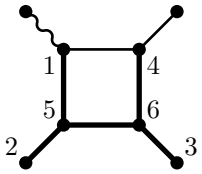

(4.8)

We shall refer to this subdiagram as t. We use the letter "t" here to indicate one of the three possible topologies of a four-point subdiagram with two cubic vertices. The remaining two ones will be introduced in a moment.

The elementary contraction of d_t corresponding to the above choice of path and direction is given by

$(\beta_{43})_{(P_t,n_t)}(d_t)$ = $-$

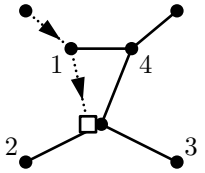

. (4.9)

Now from d_t we can obtain two diagrams d_s and d_u in $[G]^\nu$ by replacing the subdiagram t with the subdiagrams s and u, respectively, as follows:

d_s =

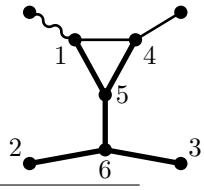

d_u =

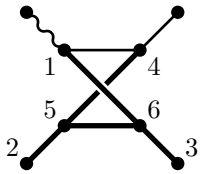

(4.10)

[1] Note that paths were actually defined as sequences of edges, not vertices. However, since the endpoint of one edge in the path always is the initial point of its successor, it suffices to specify the vertices, unless the path crosses a double edge. In the same spirit, we shall denote the direction by a vertex, rather than an edge, if this identifies the direction uniquely.

We have argued above, that a choice of path and direction, with endpoint and direction two cubic vertices, defines a four-point subdiagram. The converse is also true. In particular, if a four-point subdiagram d and a path P are given, the direction is uniquely determined. This has the important implication that B_{43} can be written as a sum of elementary contractions over paths and four-point subdiagrams instead of paths and directions. Note further, that the second last vertex in P specifies the point where the ghost line enters the subdiagram d.

For instance, given the path $P_s = \{1, 5\}$ and the subdiagram s for d_s, the direction vertex must necessarily be $n_s = 4$. Likewise, for choosing $P_u = \{1, 6\}$ and u for d_u, we obtain $n_u = 3$. The corresponding elementary contractions yield

$$(\beta_{43})_{(P_s,n_s)}(d_s) \;=\; -$$

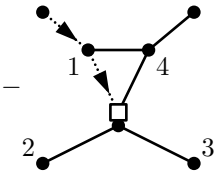

(4.11)

$$(\beta_{43})_{(P_u,n_u)}(d_u) \;=\; -$$

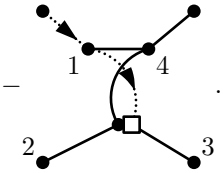

. (4.12)

Depending on the nature of the three uncontracted external lines, there may or may not exist a diagram with a subdiagram containing a quartic vertex in place of t in d_t (equivalently, s in d_s or u in d_u). As an example of the latter case, take two external lines of the subdiagram to correspond to physical fermions. In this case, as well as all other cases where a quartic vertex does not exist, the sum of elementary contractions (4.9), (4.11) and (4.12) cancels by an STI like (3.12).

On the other hand, if a subdiagram q with quartic vertex does exist for the given set of external lines of the subdiagram, we obtain a diagram d_q in $[G]^{\nu+1}$ by replacing t in d_t with q:

$$d_q =$$

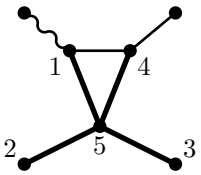

(4.13)

We are interested in those contractions in $\mathrm{B}_{44}(d_q)$, for which the ghost line enters the subdiagram at the vertex 1. To this end, we have to chose the path $P_q = \{1, 5\}$. There are three possible choices of direction, namely, 2, 3 and 4. Evaluating the corresponding elementary contractions yields

$$(\beta_{44})_{(P_q,2)} + (\beta_{44})_{(P_q,3)} + (\beta_{44})_{(P_q,4)}$$

$$=$$

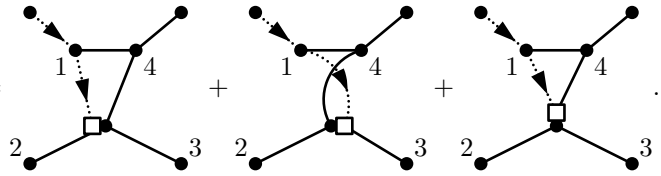

. (4.14)

This cancels precisely with (4.9), (4.11) and (4.12), just as we anticipated at the beginning of the section. It is easy to see why there is no difference to the tree level case in our present example: The four-point subdiagram under consideration has four distinct external points 1, 2, 3, and 4. Locally, then, there is essentially no difference to the tree level case, if we use a regularization scheme with shift invariance, like dimensional regularization.

Since the choice of path and subdiagram was arbitrary, our proof is complete once we can show that, for every choice of four-point subdiagram and path, the contributions of the elementary contractions β_{43} and β_{44} add up with equal weight. For one-loop diagrams, this is a nontrivial assertion, because four-point subdiagrams may have coincident external vertices. When the four-point subdiagram is transformed in all possible ways as above, some of the diagrams so obtained may be identical. In this situation, it is not obvious that the gauge cancellations still work as before.

We must now investigate the implications of symmetries which affect the chosen four-point subdiagram d. (If a symmetry does not affect d, since we always pick diagrams that differ at most in d, the effect of the symmetry can be at most a global factor.) We begin with the four-point subdiagram q with a quartic vertex, because this subdiagram evidently has the highest symmetry. The three ways to replace q by a subdiagram with a pair of connected cubic vertices correspond precisely to the three different ways to group the four external edges of q in pairs:

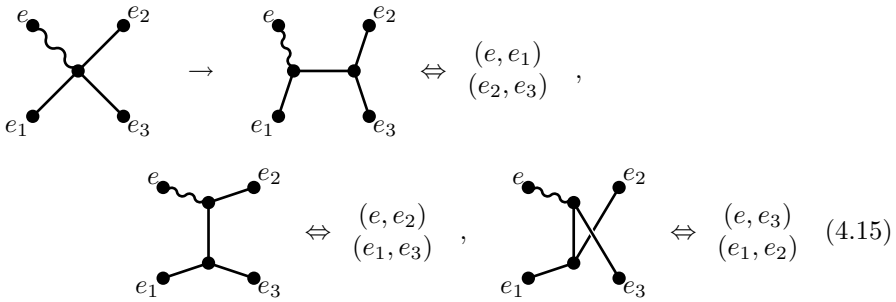

(4.15)

In fact, the edge e is distinguished because it is part of the path leading to the quartic vertex. Therefore, it actually suffices to specify the second member of the pair containing e or, equivalently, the second pair.

Now consider applying the elementary contraction β_{44} to q. According to the STI (3.11), we get a sum of three diagrams with an effective BRST vertex:

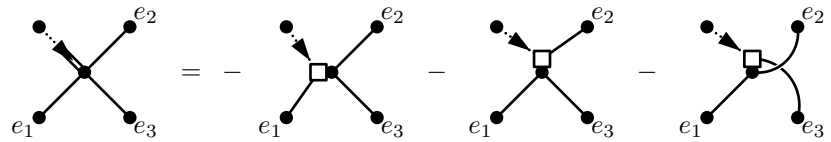

(4.16)

Inside a larger diagram, the three diagrams with effective BRST vertex correspond to three elementary contractions with the same path but different directions. Evidently, these directions can be characterized by the same pairings of edges as the three subdiagram topologies above. Therefore, the relevant symmetries of the four-point subdiagram are automorphisms of the three undistinguished edges. Furthermore, *an elementary contraction characterized by the*

pair (e, e_k) *will automatically have the same symmetries as the corresponding four-point subdiagram.*

At one-loop level, there are only two such automorphisms. On one hand, two edges may connect to the same vertex:

V_q =

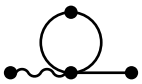

(4.17)

On the other hand, two edges may actually coincide:[2]

S_q =

(4.18)

When the quartic vertex in V_q and S_q is expanded, the edge automorphism of the subdiagram can be either preserved or spoiled. In the latter case, due to the automorphism of the original diagram, there must be different pairings leading to the same expanded diagram. All this can clearly be seen in the expansions of V_q and S_q:

$V_q \to \{V_s, V_t, V_u\}$ =

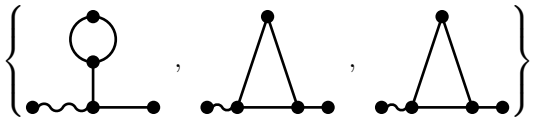

(4.19)

$S_q \to \{S_s, S_t, S_u\}$ =

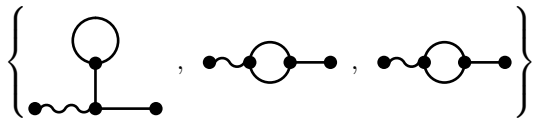

(4.20)

V_s and S_s have the same automorphism as V_q and S_q. V_t and V_u are identical because V_q is invariant under a permutation of the two edges which connect to the same vertex. A similar argument explains the equality of S_t and S_u. In this case, however, the resultant subdiagrams still have an automorphism.

Now we have to evaluate the contractions of these diagrams and look whether symmetry factors are global ones. First, consider the vertex diagrams:

$\frac{1}{2}\beta_{44}(V_q) = \frac{1}{2}$

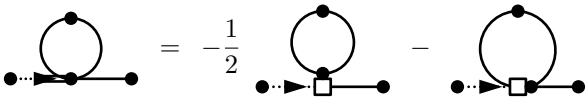

(4.21)

$\frac{1}{2}\beta_{43}(V_s) = \frac{1}{2}$

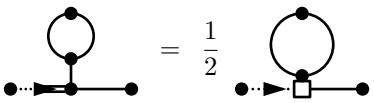

(4.22)

$\beta_{43}(V_t) =$

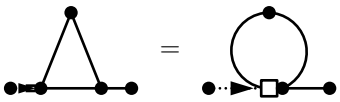

(4.23)

[2]The symbols V and S stand for "vertex" and "self energy".

The sum of all contributions cancels. Since $V_t = V_u$, we could write this in a more symmetric way as follows:

$$\frac{1}{2}\beta_{44}(V_q) + \frac{1}{2}\beta_{43}(V_s) + \beta_{43}(V_t) = \frac{1}{2}\big(\beta_{44}(V_q) + \beta_{43}(V_s) + \beta_{43}(V_t) + \beta_{43}(V_u)\big) \ . \tag{4.24}$$

We see that the symmetry factor has turned into a common prefactor.

In a similar way, we get for the contractions of the self energy diagrams S_q and S_s:

$\frac{1}{2}\beta_{44}(S_q) \ = \ \frac{1}{2}$  $= \ -\frac{1}{2}$ 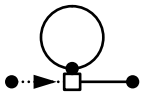 $-$ 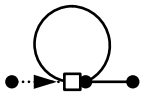 (4.25)

$\frac{1}{2}\beta_{43}(S_s) \ = \ \frac{1}{2}$ 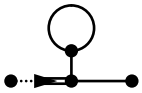 $= \ \frac{1}{2}$ 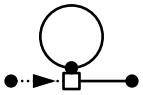 (4.26)

To evaluate the contraction of V_t, we must be a little more precise about the definition of elementary contractions. Actually, the elementary contractions considered here should be contractions of diagrams, hence carry a direction. In the previous cases the direction was always clear, so we could safely omit it. Now, however, there are two choices:

$\frac{1}{2}$  $= \ \frac{1}{2}$  $+ \ \frac{1}{2}$ 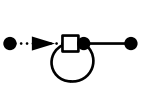 $=$ 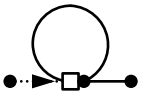 (4.27)

Both choices lead to equal diagrams. The reason is the same symmetry under permutation of edges that led to the coefficient of unity in (4.27). Again, we can use $S_t = S_u$ to turn the symmetry factor into a common prefactor:

$$\frac{1}{2}\big(\beta_{44}(S_q) + \beta_{43}(S_s) + 2\beta_{43}(S_t)\big) = \frac{1}{2}\big(\beta_{44}(S_q) + \beta_{43}(S_s) + \beta_{43}(S_t) + \beta_{43}(S_u)\big) \tag{4.28}$$

On the other hand, in both cases the potential problems with the symmetry factors produced by automorphisms were resolved again through these automorphisms. As we shall see when we investigate the multi-loop case, this is a general scheme.

The demonstration of the cancellations in the four-point subdiagrams with nontrivial symmetry factors completes the proof of (4.6). We emphasize that, in order to produce the cancellations we do *not* have to match diagrams in $[G]^\nu$ and $[G]^{\nu+1}$, which is in general impossible because four-point subdiagrams can overlap. Rather, we need only match diagrams in $\mathrm{B}_{43}\big([G]^\nu\big)$ and $\mathrm{B}_{44}\big([G]^{\nu+1}\big)$ to make sure that the required gauge cancellations take place. This works because the contractions B_{43} and B_{44} produce separate additive contributions for every possible choice of four-point subdiagram. Thereby, overlapping subdiagrams are disentangled.

Pictorially speaking, $\mathrm{B}_{43}\big([G]^\nu\big)$ and $\mathrm{B}_{44}\big([G]^{\nu+1}\big)$ each produce a pile of diagrams with effective BRST vertex. These can be sorted according to the subdiagrams that contain the effective BRST vertex. It then turns out that both piles

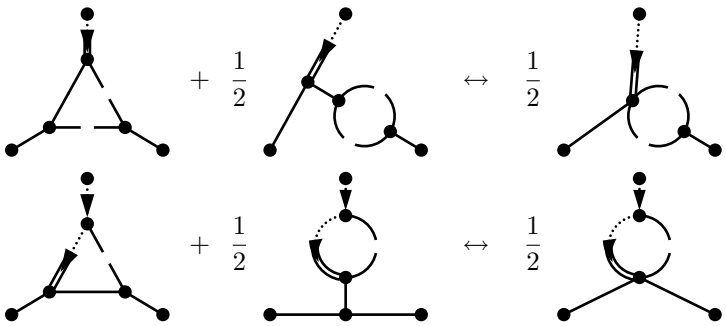

Figure 4.1: Matching terms in $\mathrm{B}_{43}\big([G_3]^0\big)$ (on the LHS of the arrow) and $\mathrm{B}_{44}\big([G_3]^1\big)$ (on the RHS). The four-point subdiagrams are indicated by cuts in the propagators. We have displayed only one half of all terms. The second half is obtained by taking the mirror images of the displayed diagrams.

consist of the same set of diagrams, with matching coefficients, but opposite sign.

We illustrate the matching of terms in $\mathrm{B}_{43}\big([G_3]^0\big)$ and $\mathrm{B}_{44}\big([G_3]^1\big)$ for the connected three-point Green's function G_3 at one-loop in figure 4.1.

4.2.3 Cancellations in $\mathrm{B}_5(G)$

Our next task is to demonstrate the gauge cancellations leading to (4.2c). Since B_5 does not change the number of ghost loops we can leave the corresponding decomposition of the forest implicit. Moreover, B_5 uniformly reduces the number of quartic vertices by one. Therefore, we claim that

$$\mathrm{B}_5\big([G]^\nu\big) = 0 \ . \tag{4.29}$$

In the following, we omit the index ν for simplicity. The five-point effective BRST vertex in a diagram of $\mathrm{B}_5(G)$ defines a five-point subdiagram. Therefore, cancellations must be expected to take place among diagrams that are identical up to changes in a five-point subdiagram. However, not all five-point subdiagrams will produce a contribution to $\mathrm{B}_5(G)$, but only five-point subdiagrams containing one cubic and one quartic vertex:

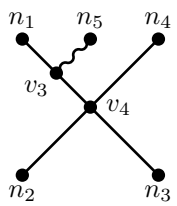

(4.30)

In this section, we will use the term "five-point subdiagram" for diagrams in G exclusively in this restricted sense.

Presumably, cancellations in $\mathrm{B}_5(G)$ are directed by the five-point STI (3.17). Let d_1 be a diagram in G. In analogy with the last section, we want to rewrite

$\mathrm{B}_5(d_1)$ as a sum over choices of paths and five-point subdiagrams instead of directions. For this to be true, the direction vertex of the elementary contraction must be uniquely determined by specifying a path and a five-point subdiagram. Now let s_1 be a five-point subdiagram of d_1 as above, characterized by the two vertices v_3 and v_4, and choose the path to enter s_1 at n_5, i. e. $P = \{\ldots, n_5, v_3\}$, where the ellipsis represents possible further vertices in omitted parts of d_1. Then, the direction vertex is uniquely determined to be v_2, since v_4 and n_5 cannot be direction vertices, the latter because it is in the path, the former because the contraction will push the BRST vertex onto v_4. Thus, we can characterize the corresponding elementary contraction of d_1 as $(\beta_5)_{(P,s_1)}(d_1)$:

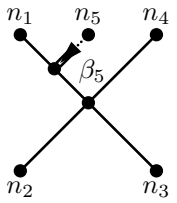

(4.31)

As in the last section, the line through which $(\beta_5)_{(P,s_1)}$ enters s_1 is distinguished.

Now, there are exactly four choices of five-point subdiagrams possible with the given set of external lines, corresponding to the four ways to choose the external neighbor of the cubic vertex from n_1 through n_4. The choice n_1 corresponds to s_1. Denoting the remaining subdiagrams as s_2 through s_4, we obtain three diagrams d_2 through d_4 by replacing s_1 in d_1 by s_2 through s_4, respectively. d_2 through d_4 constitute valid Feynman diagrams for G, for which P is one possible path. Consequently, in $\mathrm{B}_5(G)$ we can pick the sum of elementary contractions

$$(\beta_5)_{(P,s_1)}(d_1) + (\beta_5)_{(P,s_2)}(d_2) + (\beta_5)_{(P,s_3)}(d_3) + (\beta_5)_{(P,s_4)}(d_4)$$

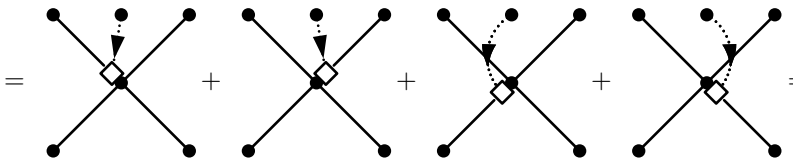

(4.32)

which indeed cancels by the STI (3.17). Since the choice of path and subdiagram was completely arbitrary, we are done, if we can show that symmetry factors do not destroy the combinatorics.

Like in the last section, we only have to consider symmetries of contracted five-point subdiagrams. At one-loop level, the only possible symmetries are two kinds of symmetries under edge permutations: Either two edges on the quartic vertex connect to the same vertex, or else two edges actually coincide.

When two edges of the subdiagram connect to the same external vertex, two of the four possible subdiagrams will have an automorphism under permutations of these edges and come with a symmetry factor of 1/2. The other two subdiagrams are identical and can be added as one half each, such that the

symmetry factor turns into a global prefactor:

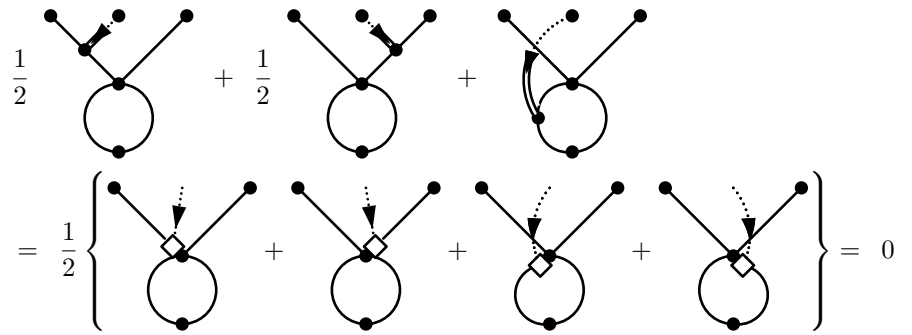

(4.33)

In the second case, two of four subdiagrams have a tadpole edge and come with symmetry factor 1/2. The other two subdiagrams are identical, having a double edge between cubic and quartic vertex, and consequently carry a symmetry factor 1/2, too. For the latter subdiagrams, the contraction yields two identical terms, making up for the symmetry factor, such that only a global factor is left:

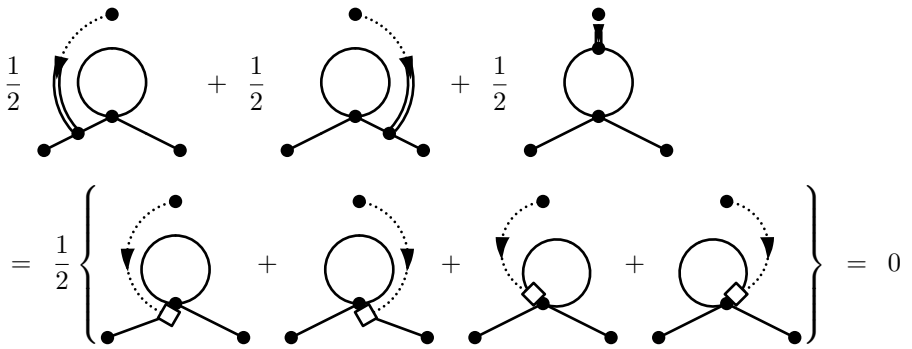

(4.34)

Thus, we have proved (4.29).

4.2.4 Cancellations in $\mathrm{B}_c(G)$

In this section we will demonstrate the cancellation of diagrams with contractions at ghost lines. Since we are presently considering only diagrams without external ghost lines, it would appear that such contractions can only be generated in diagrams with a ghost loop. This guess is, however, wrong. Indeed, in the one-loop case, we shall find that diagrams without ghost loop provide cancellations for diagrams with ghost loop.

In this section, we can leave the decomposition of the forest according to the number of quartic vertices implicit, because the elementary contraction β_c cannot change this number. On the other hand, the decomposition of G into $[G]_0$ and $[G]_1^0$ according to the number of ghost loops is essential.

First, let us demonstrate how a diagram d in $[G]_0$ can produce a contribution to $\mathrm{B}_c(G)$ even though by definition it does not contain a ghost line. To this end, recall that the action of the complete contraction map Θ can be described as a

recursive operation: Θ enters d through the contracted external line, performing the elementary contraction θ at every vertex on its way, and then forking at every cubic vertex in all possible ways. Thereby, Θ replaces each gauge field line by a ghost line. Pictorially speaking, Θ drags a ghost line behind while forking through the d. The action of B_c on d can be described in exactly the same way, with the elementary contraction θ replaced by β_c.

Now let d_t be a diagram in G with a closed gauge field loop containing only cubic vertices:

$d_t \;=$ 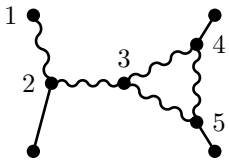

(4.35)

If B_c can enter the loop, it will circle the loop until it reaches the entry point again. But since B_c drags a ghost line behind, the contraction will now encounter a ghost line. This corresponds to an elementary contraction with a path P_t the endpoint of which is already contained in P_t. For definiteness, we choose $P_t = \{1, 2, 3, 4, 5, 3\}$. For our present purposes, it is convenient to split P_t into a subpath $P = \{1, 2, 3\}$, connecting the start point of the path to the entry point into the loop, and a subpath $L_t = \{4, 5, 3\}$, passing through the loop. Denoting composition of subpaths by $P \circ L_t$, the corresponding elementary contraction $(\beta_c)_{P_t}$ reads:[3]

$(\beta_c)_{P_t}(d_t) \;=\; -$ 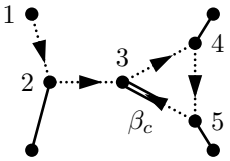

(4.36)

(The minus sign is the obligatory one from (3.23).) As the tree level example in section 3.4 suggests, a diagram in $\mathrm{B}_c(G)$ with an elementary contraction at a ghost line must be combined with a similar diagram, producing a ghost BRST vertex according to the STI (3.8) (or, equivalently, (3.26)).

From the above example, it is clear that a matching diagram can always be found in $\mathrm{B}_c\big([G]_1\big)$, i. e. among the contributions of diagrams with one ghost loop. In particular, replace the loop in d_t by a ghost loop, choosing the direction of the ghost arrow identical to that in $(\beta_c)_{P_t}(d_t)$, to obtain a diagram c_t in $[G]_1$:

$c_t \;=$ 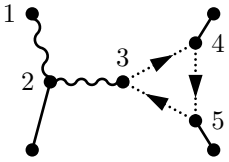

(4.37)

The subpath P is a valid path for an elementary contraction in $\mathrm{B}_c(c_t)$. Evalu-

[3] Remember that no direction needs to be specified if β_c is applied directly at a ghost line.

ating this contraction yields

$(\beta_c)_P(c_t) \;=\; -$ 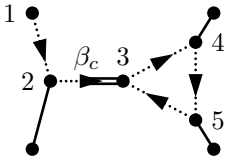

. (4.38)

Adding both contributions using (3.26) we get, remembering to add the minus sign for the fermion loop,

$(\beta_c)_{P\circ L_t}(d_t) - (\beta_c)_P(c_t) \;=$ 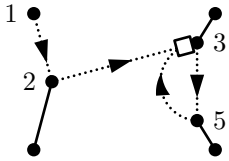

. (4.39)

The effective BRST vertex in this diagram defines a four-point subdiagram, together with a direction. Presumably, a cancellation will take place with two other contributions to $\mathrm{B}_c(G)$ according to the STI (3.14). Therefore, we have to look whether such contributions can be found.

Go back to the original diagram d_t. Consider the four-point subdiagram defined by the vertices 3 and 4. These vertices are actually uniquely determined by the path P_t, as entry point into the loop and its successor, respectively. Transform this subdiagram as follows to obtain a diagram d_u:

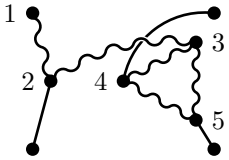

(4.40)

In $\mathrm{B}_c(d_u)$, we can find an elementary contraction with path $P \circ L_u$, $L_u = \{3,5,4\}$:

$(\beta_c)_{P\circ L_u}(d_u) \;=\; -$ 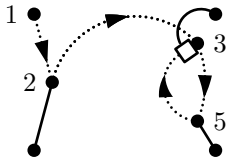

(4.41)

Evidently, the ghost effective BRST vertex is contained in the same four-point subdiagram as the one in (4.39). Since, in addition, the path P to the subdiagram is the same in both diagrams, we have found the first of the two matching contributions.

The second one should be the same as (4.41) except for an interchange of the two incoming ghost lines at the BRST vertex. This elementary contraction can be found in $\mathrm{B}_c(c_s)$, where

$c_s \;=$ 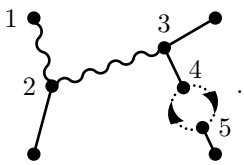

. (4.42)

Observe that c_s can be obtained from c_t by a transformation of the four-point subdiagram defined by the vertices 3 and 4, which are again uniquely determined by the path P_t.

The desired elementary contraction in $\mathrm{B}_c(c_s)$ is obtained by choosing the path P:

$$(\beta_c)_P(c_s) \;=\; -$$

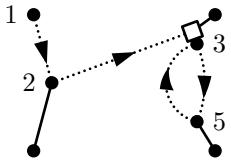

(4.43)

Adding up all contributions, with appropriate fermion loop signs, we get a complete cancellation:

$$(\beta_c)_{P\circ L_t}(d_t) - (\beta_c)_P(c_t) + (\beta_c)_{P\circ L_u}(d_u) - (\beta_c)_P(c_s) = 0 \tag{4.44}$$

It may seem that the indicated cancellation depends on the properties of the chosen example diagram. This is, however, not the case. With one exception, to be treated in a moment, the above proof covers the general one-loop case. To see this, first note that all *changes* in the diagrams are confined to a single four-point subdiagram. All parts of the diagrams outside this subdiagram were completely arbitrary and did not change at all. Also, the number of vertices in the loop was (almost) not essential. Indeed, we could have added any number of vertices to the loop in almost all places without affecting the proof. The only necessary constraint is, that the vertices 3 and 4 have to be neighbors. But if they were not, 3 and 4 could by no means be contracted into an effective BRST vertex anyway.

There is, however, one point we have to be careful about. In particular, observe that the diagram c_s in the above example has one vertex less in the loop than d_t, d_u and c_t. Since this will be the case for any number of vertices in the loop, this opens the possibility that there are unmatched contributions for the maximum and minimum possible numbers.

Concerning the maximum possible number of vertices, observe that, if the path P contains only the external line, no diagram of the form (4.43) is actually produced. To see this, consider the following example:

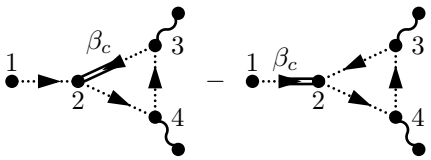

(4.45)

When the two contractions are combined like in (4.39), they will contribute to a cancellation among diagrams in $\mathrm{B}_c(G)$ with *two* ghost propagators in the loop, not three. In fact, there is no diagram at all in $\mathrm{B}_c(G)$ with three ghost propagators. Now observe that the number of vertices in the loop is actually irrelevant for this argument, which depends only on the fact that the subpath P from the external contraction to the loop is a trivial path consisting of just a single external line. Therefore, we may conclude that no unmatched contributions remain for one-loop diagrams with the maximum possible number of vertices in the loop.

On the other hand, the minimum possible number of vertices in a loop is one, corresponding to a one-point Green's function. The relevant contractions come from the one-loop diagrams with a gauge field or ghost in the loop, respectively:

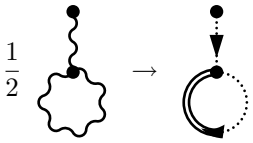

(4.46)

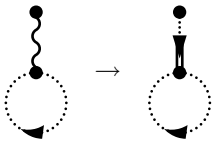

(4.47)

When the two contractions are combined using the STI (3.8), the ghost propagator in the loop is cancelled, rendering the integrand of the loop integral independent of the loop momentum:

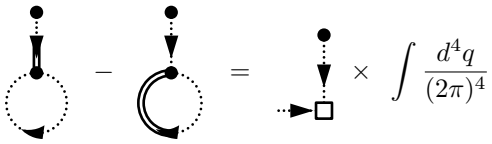

(4.48)

But in dimensional regularization, this integral vanishes identically.

Consequently, we have proven $\mathrm{B}_c(G) = 0$. This completes the proof of the STI (4.1) for the one-loop case.

4.3 Groves and Gauge Flips

In the last three sections, we have demonstrated how the STI for the one-loop expansion of a connected Green's function (without external ghost lines) follows from STIs for the tree level vertices. In the course, we conducted a detailed analysis of the cancellations among the diagrams contributing to $\Theta(G)$. In particular, we have shown that the cancellations of a single contribution $\Theta(G)$ in general require the existence of several diagrams in G. We can use this information now to construct minimal subsets $\mathcal{F}(S)$ of the forest $\mathcal{F}(G)$ satisfying the condition that $\Theta(S)$ contains nothing but contact terms, i. e. diagrams in $\mathcal{W}(G)$.[4]

To make this notion precise, recall that, according to (4.2a), the contact terms $\mathcal{W}(G)$ coincide with the contractions $\Omega(G)$ at external vertices. Since Ω is a linear map, it makes sense to consider $\Omega(S)$ for a projection S of G onto a subspace.[5] Now we *define* the contact terms $\mathcal{W}(S)$ of S by

$$\mathcal{W}(S) \equiv \Omega(S) \ . \tag{4.49}$$

Evidently, if $G = \sum_j S_j$ for several projections S_j, then the contact terms of G are the sum over contact terms of S_j, i. e. $\mathcal{W}(G) = \sum_j \mathcal{W}(S_j)$.

[4] For the definition of the symbol $\mathcal{F}(\,)$, cf. 3.3.1.

[5] For the definition of a projection of a Green's function, cf. 3.3.1.

An *invariant subset* of the forest $\mathcal{F}(G)$ is defined as the set $\mathcal{F}(S)$, where S is a projection of G satisfying

$$\Theta(S) = \mathcal{W}(S) \ . \tag{4.50}$$

If $\mathcal{F}(G)$ is the (disjoint) union of $r > 1$ invariant subsets $\mathcal{F}(S_j)$, this means that all cancellations required to satisfy the STI for G take place separately within each invariant subset.

If the Green's function G has several external gauge boson lines, the contraction Θ can be applied to each gauge boson line. Denoting by $\Theta_\ell(G)$ the contraction of G at the ℓ-th gauge boson line and by $\mathcal{W}_\ell(G)$ the corresponding contact terms, we must then extend the definition of an invariant subset S to include all possible contractions:

$$\Theta_\ell(S) = \mathcal{W}_\ell(S) \quad \text{for all } \ell \tag{4.51}$$

In the following, (4.50) is always understood in this sense, so we will continue to omit the label for the external gauge boson line.

In analogy to the tree level case [4], we now define the *groves* of $\mathcal{F}(G)$ as the elements of the finest possible partitioning of $\mathcal{F}(G)$ into invariant subsets, which in addition we require to be independent of the gauge parameters, once onshell matrix elements are extracted from G.[6]

If $\mathcal{F}(G_r)$ is a grove, then no diagram can be omitted from $\mathcal{F}(G_r)$ without violating the condition $\Theta(G_r) = \mathcal{W}(G_r)$ or the gauge parameter independence. It is in this sense, that groves are the minimal gauge invariant classes of Feynman diagrams.

We are now going to demonstrate that the groves of a connected Green's function G can be constructed by performing graphical operations, called gauge flips, on Feynman diagrams.

4.3.1 Constructing Groves

To construct a grove, we start with a set $\mathcal{F}(S)$ containing a single diagram d in the connected Green's function G. (This means $S = \chi(d)d$.) Applying Θ to S, we get

$$\Theta(S) = \Omega(S) + \mathrm{B}_4(S) + \mathrm{B}_5(S) + \mathrm{B}_c(S) \ . \tag{4.52}$$

In general, the B terms will be nonzero. Therefore, in order to satisfy $\Theta(S) = \Omega(S)$, we must add diagrams of G which provide the necessary cancellations.

First, consider $\mathrm{B}_4(S)$. According to the discussion in 4.2.2, the required cancellations will come from diagrams which differ from d in a single four-point subdiagram. Specifically, call a subdiagram with at least one external gauge field line a *gauge subdiagram*. A gauge subdiagram which can be reached by a path is denoted as a *reachable gauge subdiagram*. Remember in this context that, by definition, a path always starts at an *external* line.

We have seen that $\mathrm{B}_4(d)$ can be written as a sum of elementary contractions over reachable four-point gauge subdiagrams. Therefore, we have to add to

[6] The proper framework for the discussion of the gauge parameter dependence of Green's functions is provided by the so-called *Nielsen identities* [22]. A detailed discussion of the gauge parameter dependence is, however, beyond the scope of this work and therefore left to a separate publication [23]. We give a more intuitive definition here instead.

S all diagrams obtained from d by replacing every reachable four-point gauge subdiagrams by all possible four-point gauge subdiagrams.

The possible four-point gauge subdiagrams are precisely given by the forest $\mathcal{F}(G_4)$ of the tree level connected Green's function G_4 (which we discussed in 3.2.2):

$$\mathcal{F}(G_4) = \{s_4, t_4, u_4, q_4\}$$

$$= \left\{ \quad , \quad , \quad , \quad \right\} \tag{4.53}$$

Transformations among these subdiagrams are called *elementary gauge flips* [4]. Consequently, in order to get cancellations for $\mathrm{B}_4(d)$, we have to add to $\mathcal{F}(S)$ all diagrams constructed from d by applying elementary gauge flips to every reachable gauge subdiagram in all possible ways. Denote the set so obtained by $\mathcal{F}(S_1)$. The projection of $\mathrm{B}_4(S_1)$, and hence also of $\Theta(S_1)$, onto $\mathrm{B}_4(d)$ is now zero by construction.

However, S_1 does not necessarily satisfy $\mathrm{B}_4(S_1) = 0$. This condition may be violated through the contributions of the newly added diagrams. Therefore, we have to iterate the procedure: For every diagram in S_1, perform elementary gauge flips in reachable gauge subdiagrams in all possible ways, and add the resulting diagrams to $\mathcal{F}(S_1)$, thus producing a set $\mathcal{F}(S_2)$. Continue in this fashion until no more new diagrams are produced by applying the elementary gauge flip. The resultant set $\mathcal{F}(S')$ will satisfy $\mathrm{B}_4(S') = 0$. Moreover, $\mathcal{F}(S')$ is a *minimal* subset of $\mathcal{F}(G)$ satisfying $\mathrm{B}_4(S') = 0$, because no diagram could be omitted without violating this condition.

Next, we consider $\mathrm{B}_5(S')$. As we have seen, cancellations in $\mathrm{B}_5(d)$ require that for every diagram d in S' there exist in S' all diagrams, which are obtained from d by performing all possible transformations in reachable five-point gauge subdiagrams of the form

$$F_5 = \{f_1, f_2, f_3, f_4\}$$

$$= \left\{ \quad , \quad , \quad , \quad \right\} . \tag{4.54}$$

Fortunately, with one exception, all such diagrams are already present in $\mathcal{F}(S')$. To see this, note that in a renormalizable gauge theory quartic couplings can only involve gauge bosons, Goldstone bosons, and Higgs bosons. In the above five-point diagrams, if the line connecting the cubic to the quartic vertex is a gauge field line, the quartic vertex is reachable if the cubic vertex is. But if the quartic vertex is reachable, the diagrams obtained by applying an elementary gauge flip to the quartic vertex are already in S'. We demonstrate this for one

elementary gauge flip:

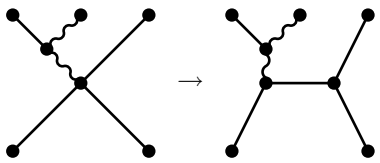

(4.55)

In this case, it can be shown that all diagrams in (4.54) are obtained by performing all possible elementary gauge flips in the diagram on the RHS.[5]

On the other hand, if in one of the four diagrams of (4.54) the quartic vertex is a four-Higgs vertex, elementary gauge flips of the corresponding five-point subdiagrams really have to be introduced.[5] Thus, the transformations among the following five-point subdiagrams, where dashed lines denote Higgs boson lines, have to be included among the elementary gauge flips:

$$F_5 = \{f_1, f_2, f_3, f_4\}$$

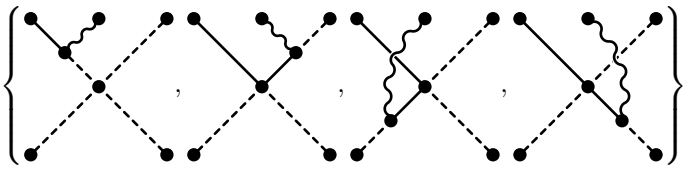

(4.56)

Finally, we have to care about $\mathrm{B}_c(S')$. Note that all cancellations discussed so far were independent of the number of ghost loops. The cancellations in $\mathrm{B}_c(G)$, however, were shown to take place among contributions of diagrams with and without ghost loop. In particular, in section 4.2.4 we found that the following four-point subdiagrams were required in order to produce a cancellation:

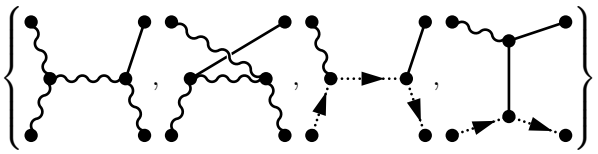

(4.57)

Of these, the first two are present anyway because they are connected by an elementary gauge flip. If in the last two diagrams we replace the ghost line by a gauge boson line, the resulting diagrams are connected to the first two by elementary gauge flips, too. Thus, if the diagrams in S' do not contain a ghost loop, we simply have to add those diagrams of $\mathcal{F}(S')$ with a gauge field loop with the loop replaced by a ghost loop in both possible directions, clockwise and counterclockwise. On the other hand, if the diagrams in S' all contain a ghost loop, we can obtain $\mathcal{F}\left(\tilde{S}\right)$ by replacing the ghost loop by a gauge field loop in all diagrams of $\mathcal{F}(S')$, perform elementary gauge flips of reachable subdiagrams in $\tilde{S}$ until it is invariant, and then proceed as in the first case. In this way, we could avoid introducing elementary flips of ghost diagrams altogether.

However, for practical purposes the replacement of a gauge field loop by a ghost loop and *vice versa* is very inconvenient. In particular, in contrast to the elementary gauge flips, which are local transformations of a diagram in the sense that nothing but the respective subdiagram is changed, the exchange of fields in

a loop is not a local operation, because the loop may possibly pass through all vertices of the diagram. It is therefore desirable to reduce the number of loop replacements in favor of local operations.

This can be achieved by introducing elementary gauge flips of four-point gauge subdiagrams with two ghost lines as follows. First, note that a single loop replacement is unavoidable, or else we could never get a diagram with a ghost loop if the diagrams in S' had none, and *vice versa*. But once we have two matching diagrams with and without ghost loop, all effects of elementary gauge flips in the diagram with the gauge field loop can be simultaneously transferred to the diagram with the ghost loop by defining elementary gauge flips as transformations among the following four-point gauge subdiagrams:

$$\mathcal{F}(G_{12}) \;=\; \{s_{12}, t_{12}, u_{12}\} \;=\; \left\{ \quad , \quad , \quad \right\} \tag{4.58}$$

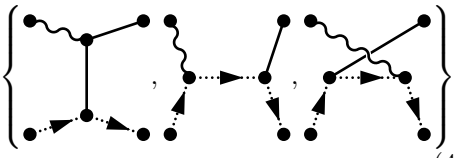

Observe that, as indicated, this is just the forest $\mathcal{F}(G_{12})$ of the tree level two-ghost connected Green's function, for which we proved the STI in 3.4. Thus, this definition of elementary ghost gauge flips is consistent with the verification of STIs for tree level connected Green's functions with external ghost lines. Similar to the case of the tree level STI for G_{12}, we do not need a flip of a four-point subdiagram with four external ghost lines in the proof of the ghost cancellations (4.2d).

Let us summarize what we have shown. Given a diagram d in G, the minimal invariant subset S of G containing d can be constructed by the following procedure: Initially, take $S = \{d\}$. Then, add to S all diagrams obtained from d by applying elementary gauge flips, as defined in (4.53), (4.56), and (4.58), in reachable subdiagrams. After that, add all diagrams obtained from diagrams in S by replacing a ghost loop with a gauge field loop and *vice versa*. This step is necessary, because a gauge field loop containing a quartic vertex becomes replacable by a ghost loop if the quartic vertex is eliminated through an elementary gauge flip. Repeat this process until no more new diagrams are created by either elementary gauge flips or replacements.

We would now like to conclude that, apart from the necessary replacements of a ghost loop by a gauge field loop, and *vice versa*, the groves of G can be found by repeatedly applying *gauge flips* to every diagram in S in all possible ways, until no more new diagrams are found. A gauge flip of a *diagram* is defined as the operation of applying an elementary gauge flip to an *arbitrary* four-point gauge subdiagram. On the other hand, the proof of the STI (4.1) does only require that we include elementary gauge flips of *reachable* four-point gauge subdiagrams. Thus, in principle the invariant subsets constructed by applying all gauge flips to S may not be minimal invariant subsets, through the inclusion of elementary gauge flips in non-reachable subdiagrams.

To provide a concrete example of how this might happen, consider the fol-

lowing gauge flip:

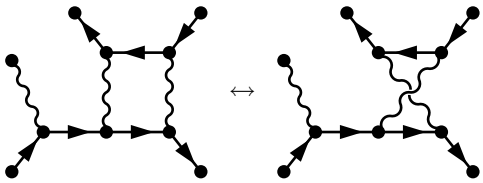

(4.59)

Clearly, this is not an elementary gauge flip in a reachable four-point gauge subdiagram, because the box subdiagram in which the flip takes place is not connected to any external gauge boson. Yet, it constitutes a valid gauge flip by definition.

In this particular example, the two displayed diagrams are connected by a sequence of elementary gauge flips in reachable subdiagrams as follows:

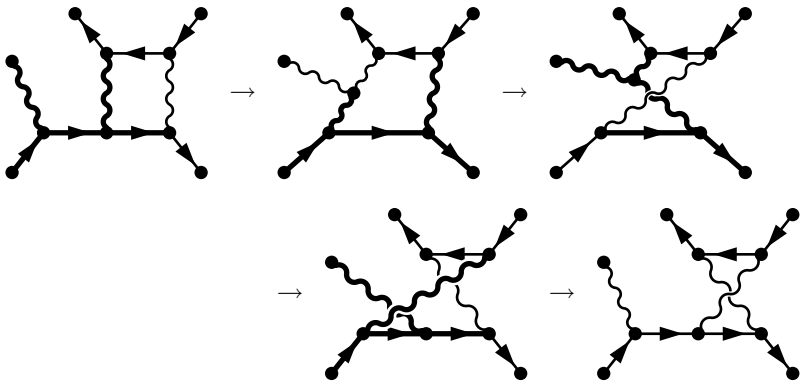

(4.60)

We have drawn in bold style the lines corresponding to the subgraphs in which the next elementary gauge flip is performed. Evidently, each of these subdiagrams is reachable. Thus, provided all intermediate diagrams are allowed by the Feynman rules, the addition of diagrams produced by gauge flips in a non-reachable subdiagram will not result in a non-minimal invariant subset.

However, the intermediate diagrams need not exist. For instance, if the diagrams in (4.59) were contributions to a Green's function in QED, the diagrams with a cubic gauge boson vertex do not exist. Consequently, the displayed gauge flip cannot be achieved by a sequence of elementary gauge flips in reachable subdiagrams.

On the other hand, the gauge flip (4.59) is necessary in QED to guarantee the gauge parameter independence of the complete amplitude. This can be readily seen from the diagrammatical proof of the Ward-Takahashi identies of QED [24], which requires a summation over all possible insertions of a contracted gauge boson along a fermion line. Neighboring insertions are connected by gauge flips, so the Ward-Takahashi identities instruct us to sum over all gauge flips of contracted gauge bosons. In particular, this applies to the longitudinal components of the photon propagator, which bear the gauge parameter dependence. Consequently, the flip in (4.59) is not required for the construction of an invariant subset in the sense of the definition (4.50), but it *is* required if we want groves to be gauge parameter independent when contributions to a physical amplitude are extracted.

For the case of a general non-abelian gauge theory, broken or unbroken, this result has also been proven for the tree level case [5]. Its extension to the one-loop or multi-loop order will be discussed in [5]. In any event, we shall take the groves of G from now on to denote the *equivalence classes of G under sequences of gauge flips*, i. e. two diagrams d and d' in G belong to the same grove if and only if d' can be obtained by successively applying a sequence of gauge flips to d, and *vice versa*. With this definition, groves are always invariant subsets, because the elementary gauge flips in reachable subdiagrams are a subset of all possible gauge flips.

In the next section, when we extend the above proof of the STI (4.1) to the multi-loop case, it will be seen that no new elementary gauge flips have to be introduced in order to satisfy the STI. Therefore, the set of elementary gauge flips is already the complete set even in the multi-loop case.

4.4 STI at n-loop

When we proved the general STI (4.1) at one-loop level in (4.2), only some of our arguments depended on the fact that the diagrams in the Green's function G contained exactly one loop. Thus, in order to generalize to the multi-loop case, we do not need to repeat the complete proof.

However, we shall organize the generalization in the same way as we organized the proof in the one-loop case. We claim that, in the multi-loop case, the production of contact terms and the gauge cancellations can still be separated into the statements of (4.2). We are now going to consider each statement in turn, indicating the modifications required to transfer the proof from the one-loop case to the multi-loop case.

4.4.1 Production of Contact Terms

The proof of the statement (4.2a) was based on the observations that all diagrams produced by the elementary contraction ω (cf. (3.55)) are in $\mathcal{W}(G)$, and that, conversely, every diagram in $\mathcal{W}(G)$ was given as the elementary contraction ω of a diagram in G. These statements are clearly true in the multi-loop case, too. Therefore, like in the one-loop case, we only have to worry about symmetry factors.

For one-loop diagrams, there was only one potential source for a mismatch of symmetry factors, which we could easily treat explicitely. In the multi-loop case, we can no longer treat all possible cases by exhaustion. Rather, we have to provide general arguments. However, to keep our discussion concrete, we will illustrate our arguments on specific examples. For simplicity, we shall choose our examples from a pure Yang-Mills theory, drawing gauge bosons as *straight* lines for ease of notation. None of our arguments will depend on this choice.

Relation (4.2a) can be written, using the definition of elementary contractions of diagrams, as

$$\Omega(G) = \sum_{\mathcal{P}(d)} \chi(d)\omega_P(d) = \sum_{\mathcal{F}(\mathcal{W}(G))} \chi(c)c = \mathcal{W}(G) \ . \tag{4.61}$$

We know already that both sums are linear combinations of the same set of diagrams. We now have to show that, if c is contained in $\omega_P(d)$ (in the set

theoretical sense), then

$$\chi(d)\omega_P(d) = \chi(c)c \ . \tag{4.62}$$

If the symmetry factor $\chi(d)$ is nontrivial,[7] i. e. $\chi(d) \neq 1$, then the diagram d is invariant under the action of an automorphism group A of edge permutations with $\chi(d) = 1/|A|$. Evidently, we need only consider paths P that are affected by the permuations in A. Otherwise, $\omega(d)$ will have the same automorphism group and hence the same symmetry factor as d.

As an example, we choose the following two-point diagram:

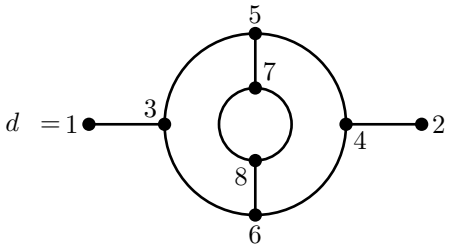

(4.63)

The automorphism group $A(d)$ of d is the direct product of two independent automorphisms, the first one a permutation of the two edges connecting 7 and 8, the second one a vertex permutation simultaneously taking 5 in 6 and 7 in 8, and *vice versa*. Pictorially, both independent automorphisms can be interpreted as an invariance under rotation about the axis defined by the external lines of a two point function. Since $A(d)$ contains four elements, we have $\chi(d) = 1/4$.

No matter which path P we choose in d, the diagram $\omega_P(d)$ will be less symmetric than d, because the ghost line dragged through d introduces a direction. In the present example, there are essentially two different choices, $P_1 = \{1, 3, 5, 4, 2\}$ and $P_2 = \{1, 3, 5, 7, 8, 6, 4, 2\}$, of path possible, leading to two diagrams c_1 and c_2 in $\mathcal{W}(G)$, respectively:

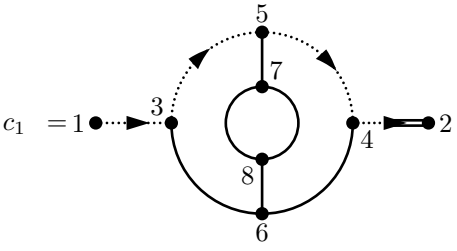

(4.64)

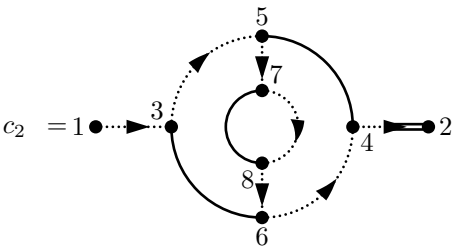

(4.65)

[7] Fermion loop signs can be ignored, because the elementary contraction ω preserves the number of fermion loops.

c_1 is still invariant under the permutation of the double edge, and consequently has $\chi(c_1) = 1/2$, while c_2 no longer has an automorphism.

Now, consider choosing $P_1' = \{1, 3, 6, 4, 2\}$ instead of P_1:

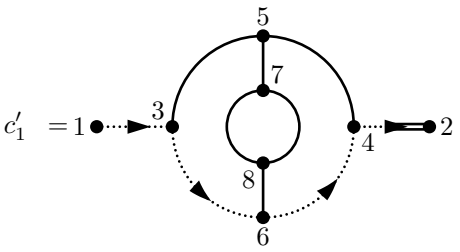

(4.66)

c_1 and c_1' are actually *identical* Feynman diagrams, because one is obtained from the other by a mere index relabeling simultaneously taking 5 in 6 and 7 in 8, and *vice versa*. But this is precisely the action of the original automorphism of d, which has been destroyed by the contraction.

In a similar way, we can find three more paths leading to a diagram identical to c_2:

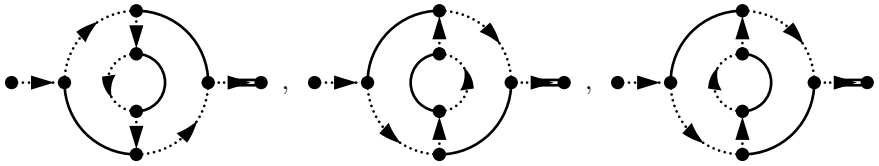

(4.67)

Again, these are identical Feynman diagrams, once vertex labelings are removed, while the respective vertex labelings are obtained from the one of c_2 by applying the automorphisms $A(d)$ of the original diagram. Altogether, we get

$$\Omega(d) = \chi(d) \sum_{\mathcal{P}(d)} \omega_P(d) = \frac{1}{4}\,(2c_1 + 4c_2) = \frac{1}{2}c_1 + c_2 = \chi(c_1)c_1 + \chi(c_2)c_2 \ . \quad (4.68)$$

Thus, the automorphism ensure that the symmetry factors come out correct in this example.

This is also true in the general case: Given a diagram d with automorphism group $A(d)$ and a path P in d, we can consider the action of the elementary contraction $\omega_P(d)$, leading to a contact term diagram c. We say that ω_P preserves the symmetries corresponding to a subgroup H of $A(d)$, if H is equal to the automorphism group $A(c)$ of c. In terms of diagrams, this means that the path P does not pass through the parts of d affected by the automorphisms in H. The remaining automorphisms can be parametrized by the set $A(d)/H$ of (left or right) cosets. Now choose an α in $A(d)/H$. By definition, α must affect the path P. Let us denote by P_α the path obtained from P by applying α to the vertices in P. Then, we have

$$\omega_{P_\alpha}(d) = \omega_P(\alpha(d)) = \omega_P(d) = c \ . \quad (4.69)$$

The coefficient of c in the contact term sum $\mathcal{W}(G)$ is given by the sum over elementary contrations and paths that produce c:

$$\chi(d) \sum_{P':c\in\omega_{P'}(d)} \omega_{P'}(d) = \frac{1}{|A(d)|} \sum_{\alpha\in A(d)/H} \omega_{P_\alpha}(d)$$
$$= \frac{1}{|A(d)|} \sum_{\alpha\in A(d)/H} \omega_{P_\alpha}(d) = \frac{1}{|A(d)|}\frac{|A(d)|}{|H|}c = \frac{1}{|H|}c = \frac{1}{|A(c)|}c = \chi(c)c \quad (4.70)$$

This calculation shows that every diagram c in the contact term sum $\mathcal{W}(G)$ is produced with the correct weight, proving (4.62), and hence (4.2a), in the multi-loop case.

4.4.2 Cancellations in $\mathrm{B}_4(G)$ *and* $\mathrm{B}_5(G)$

For the cancellations in $\mathrm{B}_4(G)$ and $\mathrm{B}_5(G)$ to work, the contracted four-point or five-point gauge subdiagrams must come with the correct symmetry factor. We would now like to give a general argument that this is always the case.

First, recall that the relevant symmetries are the symmetries of the *contracted* diagrams. These are given as a sum of elementary contractions over paths and subdiagrams. Consider a particular diagram d in G, as well as a path P and a subdiagram s in d. Denote by $H(d,P)$ the subgroup of all automorphisms $A(d)$ of d which leaves the path P unaffected. The remaining automorphisms can be parametrized as in the last section by the set of (left or right) cosets $A(d)/H(d,P)$. By an argument identical to the one given in the last section, the automorphisms affecting the path just make sure that the original symmetry factor $1/|A(d)|$ is reduced to the factor $1/|H(d,P)|$, in accordance with the symmetries remaining when the ghost line has been dragged along the path P. Now the cancellations in $\mathrm{B}_4(G)$ and $\mathrm{B}_5(G)$ take place among diagrams that differ only in the subdiagram s, but, in particular, not in the part containing P. Therefore, we need only take into account the automorphisms in $H(d,P)$.

We discuss the cancellations in $\mathrm{B}_4(G)$ first. For fixed P and four-point subdiagram s, consider, as in (4.16), the contraction of the diagram d_q in G, which is obtained from d by replacing s with a quartic vertex:

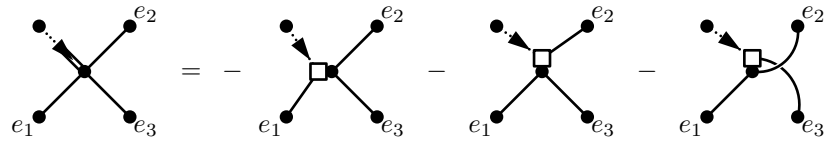

(4.71)

We display the four-point subdiagram only. It should be understood that the diagram d_q extends further, and that some of the displayed edges may coincide or connect to the same vertex.

Denote by $K(d_q)$ the subgroup of $H(d_q)$ which leaves the edges e_1 through e_3 unaffected.[8] We must assume that $K(d_q)$ is really smaller than $H(d_q)$, or else the symmetry factor $1/|H(d_q)|$ is just a global factor for each of the three diagrams on the RHS of (4.71). The automorphisms in the cosets $H(d_q)/K(d_q)$ will then necessarily permute one of the edges e_1 through e_3. However, for the permutation to be an *automorphism*, it can at most permute the three edges among themselves. (Remember that the edge with the contraction is invariant

[8] we omit the path argument in $H(P,d_q)$, because we consider a *fixed* path P.

under $H(d_q)$, because it belongs to the path.) Since the three diagrams with effective BRST vertex coincide outside the subdiagram s, we have reduced the problem to the investigation of automorphisms under permutations of the edges e_1 through e_3.

We can exclude the possibility that two of the three edges coincide, because this case has already been treated in section 4.2.2, in the discussion following (4.16). This leaves only two cases to consider, namely, an automorphism under permutation of either a pair of edges or all three edges. As an example of the former case, consider the following two-loop diagram:

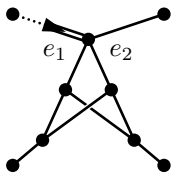

(4.72)

Now, remember that the three elementary contractions on the RHS of (4.71) are characterized uniquely by the pair of edges not connected to the effective BRST vertex. In the present case, if we choose the pair (e_1, e_2), the corresponding elementary contraction will still be invariant under the automorphism. On the other hand, the two remaining choices lead to identical diagrams, owing to the action of the automorphism. Therefore, all symmetry factors turn into a global prefactor. The argument is really the same as in our discussion of V_q in section 4.2.2, so there's no need to repeat the details here.

As an example for an invariance under permutation of all three edges, consider

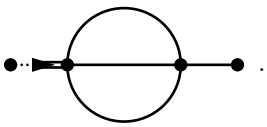

(4.73)

In this case, all three elementary contractions are identical owing to the automorphism, leaving an invariance under permutation of two out of the three edges. Thus, taking symmetry factors into account, we have

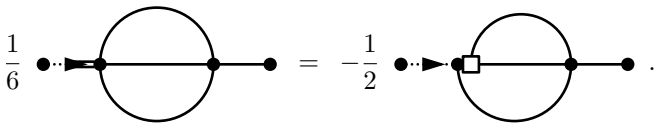

(4.74)

By the same argument, expanding the quartic vertex in d_q into a pair of cubic vertices leads to three identical diagrams with an invariance under permutation of two out of three edges. Evaluating the corresponding contraction yields

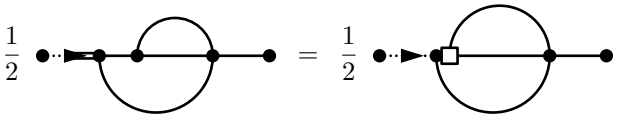

(4.75)

Thus, the sum of all contributions cancels. This proves (4.2b) for arbitrary numbers of loops.

For the cancellations in $\mathrm{B}_5(G)$, we can proceed in an analogous manner. The subdiagram s is then a five-point subdiagram as in (4.30), with one out of five external edges distinguished as lying on the path. The elementary contraction β_5 produces a five-point effective BRST vertex, which singles out one more out of the remaining four edges (cf. (4.32)). Thus, the relevant automorphisms in H/K are those permuting two or three edges at the quartic vertex of the five-point subdiagram. (The case of a tadpole edge, i. e. a pair of coincident edges, has already been treated as a special case in 4.2.3.) If at most two edges are permuted by the automorphism, the symmetry factors work out exactly as in (4.33).

As an example for the case of three permuted edges, consider the elementary contraction

$\frac{1}{6}$ 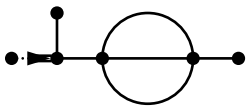 $= \frac{1}{6}$ 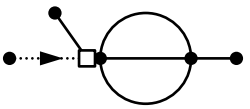 . (4.76)

Owing to the invariance under permutations of the three symmetric edges at the quartic vertices, the remaining three elementary contractions, characterized by connecting one of the symmetric edges to the cubic vertex, are all equal, still having an automorphism under permutation of two out of the symmetric edges:

$\frac{1}{2}$ 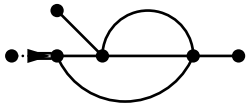 $= 3 \cdot \frac{1}{6}$ 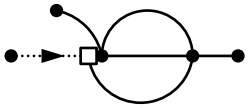 (4.77)

Thus, the four elementary contractions contribute with a common factor $1/6$, hence cancel according to (4.32). This proves (4.2c) for an arbitrary number of loops.

4.4.3 Cancellations in $\mathrm{B}_c(G)$

In contrast to the case of cancellations in $\mathrm{B}_4(G)$ and $\mathrm{B}_5(G)$, symmetry factors play no rôle for cancellations in $\mathrm{B}_c(G)$. This is easily seen from the structure of the relevant four-point subgraphs in the STI (3.14): Of the three ghost effective BRST vertices, only the one where two incoming ghost lines meet at the BRST vertex can potentially support a symmetry under edge permutations. However, in our applications there can be no automorphism under permutation of the two incoming ghost lines, because one of them will circle a loop, while the other begins at an external line. Of course, automorphisms affecting the path may exist, but these can be treated exactly as in the last two sections. Consequently, we can forget about symmetry factors altogether.

On the other hand, if we consider diagrams with L loops, there are now diagrams with any number of ghost loops from 0 to L. Recall that, in the one-loop case, the cancellations took place among diagrams with zero and one ghost loop. In the multi-loop case, we shall now prove that

$$\Big[\mathrm{B}_c\big([G]_\rho + [G]_{\rho+1}\big)\Big]_{\rho+1} = 0 \ . \tag{4.78}$$

That is, cancellations take place in the $(\rho+1)$-ghost-loop sector of Feynman diagrams with effective BRST vertices, with contributions coming from ρ-loop and $(\rho+1)$-ghost-loop sector of G. As in the one-loop case, the number of quartic vertices is preserved and can be left implicit.

We begin our discussion with an explicit example. Choose a diagram in $[G]_1$, i. e. a diagram with a single ghost loop:

$d \;=$ 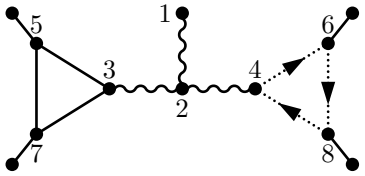

(4.79)

Since the contraction $\mathrm{B}_c(d)$ can be written as a sum of elementary contractions over paths and directions, it suffices to consider a single path at a time. Consider, for instance, the path $P_1 = \{1,2,3,5,7,3\}$. The corresponding elementary contraction is given by

$(\beta_c)_{P_1}(d) \;=$ 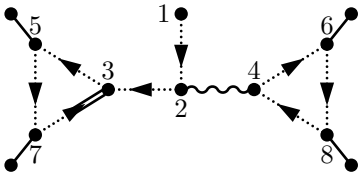

. (4.80)

Ignoring the right ghost loop, this is exactly the same as the contraction (4.36) in the one-loop case. Therefore, we can repeat all the steps leading to the cancellation in (4.44). This works because all diagrams required for the cancellation differ, aside from the necessary replacement of a gauge field loop by a ghost loop, in a single four-point subdiagram only, with the remaining parts of the diagram kept fixed. In our specific example, the cancellation takes place in the sector of diagrams with two ghost loops, with contributions coming from diagrams in $[G]_1$ and $[G]_2$. However, our example diagram d could actually contain many more loops, ghost or other, without affecting our arguments.

We have yet to consider two more paths with a nonzero contribution to $\mathrm{B}_c(d)$, namely, $P_2 = \{1,2\}$ with direction 4 and $P_3 = \{1,2,4\}$. The corresponding elementary contractions read:

$(\beta_c)_{(P_2,4)}(d) \;=$ 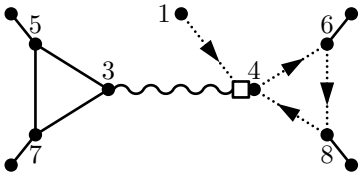

(4.81)

$(\beta_c)_{P_3}(d) \;=$ 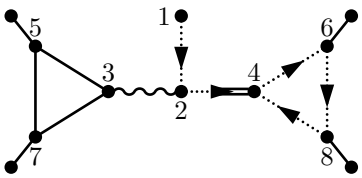

(4.82)

However, this time we can just ignore the left loop and proceed as in the one-loop case. The displayed elementary contractions will then combine with elementary contractions of diagrams in $[G]_0$ without a ghost loop to form a cancellation in the sector of diagrams with a single ghost loop. (Note that $(\beta_c)_{(P_2,4)}(d)$ and $(\beta_c)_{P_3}(d)$ contribute to *different* cancellations.) Again, the structure of the unaffected parts of the diagrams is actually arbitrary.

Finally, since cancellations take place among diagrams for which the number of vertices in the contracted ghost loop differs by one, the cases of ghost loops with the maximum or minimum possible number of loops can be treated in exactly the same way as in the one-loop case. (Cf. the discussion at the end of section 4.2.4.) Concerning cancellations in $\mathrm{B}_c(G)$, there is then essentially no difference between the one-loop diagrams and multi-loop diagrams.

Given the possibility of overlapping gauge field loops, this result might appear a little surprising. Therefore, we will give a further illustration of the combinatorics of the cancellations. To this end, we consider the action of the contraction B_c on a diagram d as a recursive map. The contraction is propagated into the diagram along gauge field lines, forking at every cubic vertex, dragging a ghost line behind. Nonzero contributions require that the contraction encounters a ghost line. This happens in two ways: The contraction can either hit a ghost loop, or it can traverse a gauge field loop completely, until it hits the ghost line it dragged behind itself.

The latter case is particularly interesting, because then the contraction increases the number of ghost loops by one. To see what this means for the case of overlapping gauge field loops, suppose d has a two-point subdiagram of the form

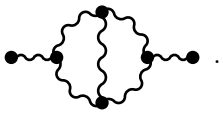

(4.83)

When the contraction propagates into this subdiagram from the left, it will produce the following elementary contractions:

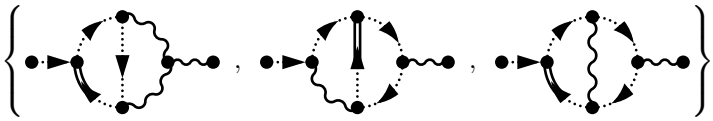

(4.84)

Evidently, the contraction B_c produces a separate elementary contraction for every possible choice of a single gauge field loop. But to each choice there corresponds precisely a diagram with one more ghost loop than d, identical to d up to the displayed two-point subdiagrams:

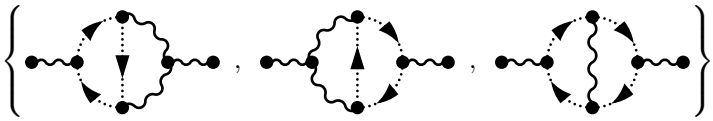

(4.85)

This property of the contraction B_c generalizes immediately to the case of an arbitrary number of overlapping loops: *The contraction* B_c *produces for a diagram* d *a separate elementary contraction for every possible choice of a traversable gauge field loop in* d. Traversable here means that a path circling the loop must

exist. Consequently, since the number of ghost loops of d was arbitrary, there is a correspondence between the elementary contractions with $\rho+1$ ghost loops in $\mathrm{B}_c\big([G]_\rho\big)$ and the diagrams in $[G]_{\rho+1}$.

To see how this correspondence can be exploited to simplify the combinatorics of cancellations in $\mathrm{B}_c(G)$, consider the diagrams without ghost loop, i. e. $[G]_0$. Suppose of B_c circles a gauge field loop L_0 along path P_0 in a diagram d_0 in $[G]_0$, producing $(\beta_c)_{P_0\circ L_0}(d_0)$. Then, the corresponding diagram d_1 in $[G]_1$ is obtained simply replacing the ghost line leading to L_0 in $(\beta_c)_{P_0}(d_0)$ by the original gauge field line that was present in d_0. The existence of the elementary contraction $(\beta_c)_{P_0}(d_1)$ is then automatically guaranteed. The existence of the other elementary contractions required for the cancellation follows from the discussion above. Since B_c can do nothing else but pick a ghost loop in $[G]_0$, $\mathrm{B}_c\big([G]_0\big)$ is cancelled completely. The same applies to all diagrams with a single ghost loop in $\mathrm{B}_c\big([G]_1\big)$, because these were all required to cancel $\mathrm{B}_c\big([G]_0\big)$.

However, we have not yet exhausted the action of B_c on $[G]_1$. In fact, given d_1 in $[G]_1$,[9] B_c may circle a gauge field loop L_1 along a path P_1 in d_1. By the same arguments as before, the existence of matching contributions in $\mathrm{B}_c\big([G]_1\big)$ and $\mathrm{B}_c\big([G]_2\big)$ can be inferred.

Evidently, we can continue this process up to an arbitrary number ρ of ghost loops. The process will terminate when there is no more gauge field loop that could be circled by B_c. Thus, we have proven that the cancellations in B_c take place as claimed in (4.78). This completes the proof of the STI (4.1) for an arbitrary number of loops.

4.4.4 Groves and Gauge Flips

Having completed the diagrammatical proof of the STI (4.1) for an arbitrary number of loops, we can now extend the notions of groves and gauge flips to the multi-loop case. Let G denote the expansion of a connected Green's function into Feynman diagrams at n-loop order. The definition (4.50) of invariant subsets of the forest $\mathcal{F}(G)$ is taken over unchanged. Also, the groves of $\mathcal{F}(G)$ are again the elements of the finest possible partitioning of $\mathcal{F}(G)$ into invariant subsets.

A priori, the cancellations in the multi-loop case could require the introduction of further gauge flips, in addition to the ones constructed for the one-loop case (cf. 4.3). However, the cancellations in $\mathrm{B}_4(G)$, $\mathrm{B}_5(G)$, and $\mathrm{B}_c(G)$ still involve the same reachable four-point or five-point gauge subdiagrams as in the one-loop case. Indeed, the multi-loop case just introduced additional combinatorial factors, but not new kinds of cancellations. Therefore, we conclude that the elementary gauge flips as defined in (4.53), (4.56), and (4.58) constitute the correct set of elementary gauge flips for the construction of invariant subsets of $\mathcal{F}(G)$ at an arbitrary order of perturbation theory.

On the other hand, in the multi-loop case we need a more general procedure to make sure that diagrams with all possible numbers of ghost loops are produced. Recall that, if overlapping gauge field loops are present, mutually exclusive choices of ghost loops are possible (cf. (4.84)). Therefore, we start from a diagram d without ghost loop. (If d contains ghost loops, we just replace them by gauge field loops.)

[9] Of course, this d_1 is not the same as the one in the last paragraph.

Given d without ghost loop, we apply all possible elementary gauge flips in reachable subdiagrams as in the one-loop case. This will produce all required diagrams without ghost loop. After that, choose a *single* diagram without ghost loop and replace an arbitrary gauge field loop by a ghost loop, if there is any. All other required diagrams with a ghost loop are then produced by applying gauge flips to this single diagram. This is true, because the ghost-gauge boson subdiagrams have the same gauge flips as pure gauge boson subdiagrams.

Therefore, in order to construct the diagrams with all possible numbers of ghost loops, we need only repeat the procedure just described: Having added all gauge flipped diagrams with one ghost loop, we choose a single diagram with one ghost loop and replace some gauge field loop by a second ghost loop. After that, we apply gauge flips again to obtain all diagrams with two ghost loops. This process is continued until the maximum possible number of ghost loops is reached.

Having determined a general procedure for the construction of minimal invariant subsets of a connected Green's function G in the multi-loop case, we emphasize again that we have defined groves as the equivalence classes of $\mathcal{F}(G)$ under sequences of *all* gauge flips, not only gauge flips in reachable subdiagrams. Therefore, also in the multi-loop case the groves of $\mathcal{F}(G)$ are not necessarily the minimal subsets satisfying (4.50). However, as will be demonstrated in [23], the inclusion of elementary gauge flips in non-reachable subdiagrams is necessary to make the contribution of a single grove to a physical amplitude gauge parameter independent.

Before closing this chapter, we remark that, for practical purposes, a different but equivalent strategy for the construction of groves may be more efficient. In particular, once we have determined all diagrams without ghost loop, the required diagrams with n ghost loops can be obtained by replacing, in *each* diagram without ghost loop, n non-overlapping gauge field loops in all possible ways (which, of course, can be done recursively, increasing the number of ghost loops by one in each step). This procedure will lead to the same set of diagrams as the one described above, because the gauge flips performed in the diagrams with ghost loops occur also in the diagrams without a ghost loop.

—5—
Unflavored Flips

Having described an algorithm for the construction of groves in gauge theories by means of gauge flips, as defined in section 4.3, the logical next step would be that we apply this algorithm to investigate the forest of connected Green's functions in the Standard Model, which is our paradigm for a spontaneously broken gauge theory. However, flips, when interpreted as graphical operations on Feynman diagrams, have a meaning independent of the context of gauge theories. In particular, they can be used for the construction of Feynman diagrams in general perturbative quantum field theories with renormalizable interactions. In this chapter, we shall develop a formalism for flips of unflavored diagrams. We shall derive a number o derive a number of results on the structure of the forest of unflavored n-loop diagrams with certain properties, e. g. 1PI diagrams or amputated diagrams. Gauge theories are then taken up again in the next chapter.

5.1 Flips Without Flavor: The Basic Tool

In the previous chapter, we have proven that the groves of a connected Green's function at an arbitrary loop order can be constructed by applying gauge flips to Feynman diagrams, i. e. exchanging a certain four-point gauge subdiagram by another one. Thus, a gauge flip transforms Feynman diagrams into each other, an operation that can be described in purely graphical terms, where no more reference to the meaning of a Feynman diagram as a representative for an analytical expression is made.

We can go even further and detach the notion of flips completely from the context of gauge theories. To this end, we forget about the field types, i. e. the quantum numbers, of the lines in a Feynman diagram and consider transformations in an *arbitrary* four-point subdiagram. That is, we consider the possible *topologies* of Feynman diagrams in a general renormalizable gauge theory, and how they can be transformed into each other by exchanging four-point subdiagrams.

The relevant topologies of Feynman diagrams can easily be generated from the Feynman rules corresponding to the theory of a self-interacting real scalar field with cubic and quartic interactions. Such a theory has no quantum numbers connected with internal degrees of freedom, and the interaction degrees cover all renormalizable interactions in non-abelian gauge theories. It can be described

by a Lagrangian of the form:

$$\mathcal{L} = -\frac{1}{2}\phi\left(\partial^2 - m^2\right)\Phi - \frac{g}{3!}\phi^3 - \frac{\lambda}{4!}\phi^4 \tag{5.1}$$

This theory will be referred to in the remainder of this chapter as *unflavored ϕ-theory*. We will frequently consider the case $\lambda \equiv 0$ to eliminate the quartic coupling, which is then referred to as *unflavored ϕ^3-theory*. Of course, such a theory is unsound as a fundamental theory, since the Hamiltonian is not bounded from below. On the other hand, all we need is the Feynman rules of these theories, so that the choice $\lambda = 0$ corresponds to omitting any diagram with quartic vertices. In this section, the attribute "unflavored" will usually be omitted, because we do not deal with flavored theories here.

5.1.1 Forest and Flips in Unflavored ϕ-Theory

We are about investigating Feynman diagrams as graphical objects without reference to a particular analytical expression. Therefore, we first have to clarify what kinds of Feynman diagrams we are going to consider. Ultimately, we are interested in connected Green's functions in gauge theories. Therefore, also in the unflavored case, we restrict our attention to connected diagrams. Furthermore, we do not consider vacuum-to-vacuum diagrams, i. e. the Feynman diagrams are required to have at least one external line. Finally, we do not take into account diagrams with counter terms. Thus, our Feynman diagrams correspond to unrenormalized expressions.

In unflavored ϕ-theory, the connected Feynman diagrams can then be characterized completely by the number E of external lines and the number L of loops. The set of all connected Feynman diagrams with E external lines and L loops, called *forest*, is denoted by $F(E, L)$. If diagrams with quartic vertices are omitted, i. e. in ϕ^3-theory, we denote the forest as $F_3(E, L)$. For tree level forests, we omit the number of loops, writing $F(E, 0) \equiv F(E)$ and $F_3(E, 0) \equiv F_3(E)$.

An *elementary flip* is defined as a transformation between two diagrams in the tree level forest $F(4, 0) \equiv F(4)$:

$F(4) \;=\; \{s, t, u, q\} \;=$ 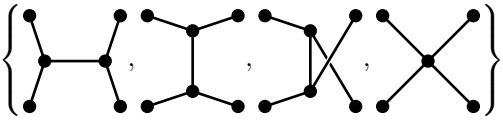 (5.2)

It turns out that it is useful to subdivide the set of all possible elementary flips further into the transformations among $\{s, t, u\}$, called *elementary rotations*, the transformations from q to $\{s, t, u\}$, called *elementary expansions*, and the transformations from $\{s, t, u\}$ to q, called *elementary contractions*.

The elementary flips define a relation $\circ$ on $F(4)$, which is true if two diagrams d and d' from $F(4)$ are connected by an elementary flip. Clearly, on $F(4)$ this relation is trivially true for any pair of diagrams. The important point is that it can be extended to an arbitrary forest $F(E, L)$. To this end, a *flip* of a diagram d in $F(E, L)$ is defined as an elementary flip in some four-point subdiagram of d. The flips are divided into *rotations*, *expansions*, and *contractions* according to the type of elementary flip involved.

With this definition, d and d' in $F(E, L)$ are said to satisfy $d \circ d'$ if d and d' are connected by a single flip. Two *diagrams* are said to be *connected*, if one

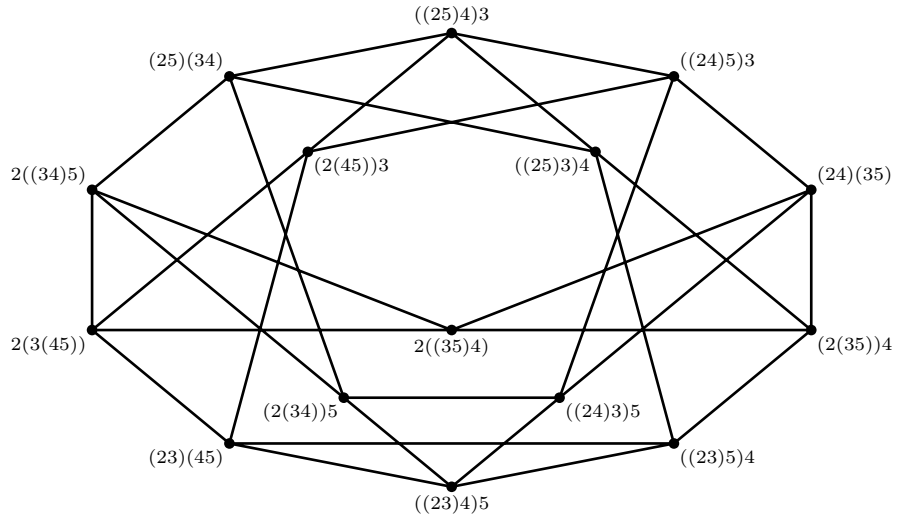

Figure 5.1: The forest $F(5)$ of the 15 five point tree diagrams in unflavored ϕ^3-theory. (For the notation, cf. the footnote on page 76.)

can be transformed into the other by a sequence of flips. A *subset* S of the forest $F(E, L)$ is said to be connected if any two diagrams d_1 and d_2 in S are connected and if, in addition, the sequence of flips connecting d_1 and d_2 does not leave S. In other words, there should be at least one sequence of flips such that every diagram produced by the flips is in S.

As an example of connected diagrams, we display all flips of a diagram in $F(5)$ which take place in a single four-point subdiagram. The dashed lines in the diagrams are unchanged.

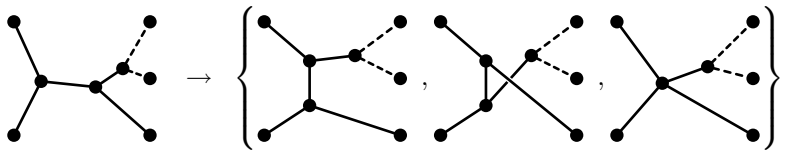

(5.3)

The relations imposed by the flips on the forest $F(E, L)$ can be represented as a graph where a node is assigned to each member of the forest (each Feynman diagram, that is) and nodes are connected by an edge if the corresponding diagrams are connected by a single flip. The forest $F(5)$ is displayed in figure 5.1.[1]

For large values of E and L, the forest $F(E, L)$ is large and, correspondingly, the number of edges in the graph representing the forest. It is an interesting question, then, whether $F(E, L)$ can fall into several disjoint subsets of Feynman

[1] Following [4], the fifteen diagrams of $F(5)$ are denoted as follows: External lines are labeled 1 through 5, subtrees are grouped in parentheses. The first external line is singled out as the root of the tree. Two examples may illustrate this:

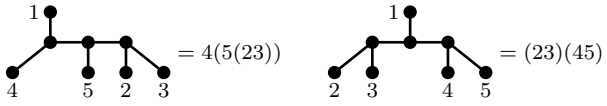

diagrams, so that diagrams from different subsets are not connected by any number of flips.

According to a theorem proven in [4], every tree level forest $F(E)$ is connected. This can intuitively be understood by noting that $F(E)$ can be constructed by successively inserting external lines into the three point diagram in all possible ways. However, neighboring insertions are connected by flips, hence the forest is connected. We will make use of this result below.

Before we go on to discuss flips of diagrams with loops, we would like to comment shortly on the issue of five-point subdiagrams. In the last chapter, we have seen that, for diagrams containing one of the five-point subdiagrams in (4.56), five-point flips are necessary. It might seem appropriate, then, that we discuss five-point flips in the present context of unflavored ϕ-theory as well. However, in unflavored ϕ-theory, flips of five-point subdiagrams are completely redundant, as the connectedness of F_5 under elementary flips of four-point subdiagrams clearly shows. Therefore, we defer the discussion of the flips of five-point subdiagrams to a later part of this chapter, where we discuss the structure of SM forests.

5.1.2 Forest and Flips for Higher Order Processes

We have already given the definitions of forest and flips for diagrams with an arbitrary number of loops. In this section, we intend to prove some general results about the forest $F(E, L)$ of L-loop diagrams and certain subsets. For this to make sense, the flips, as defined in the last section, should not change the number of loops. We will demonstrate shortly that this is indeed a property of flips.

First, however, we provide some explicit examples of flips in higher order diagrams. This is useful, because for some topologies of four-point subdiagrams it may be quite difficult to recognize the action of an elementary flip.

The action of an elementary flip in $F(E, L)$ is obvious if we consider four-point subdiagrams all external legs of which connect to *different* vertices:

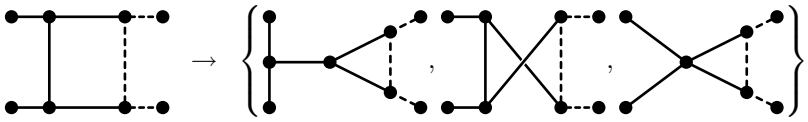

(5.4)

Next, consider the first flipped diagram of (5.4). It contains a four-point subdiagram with coincident external legs e_1 and e_2:

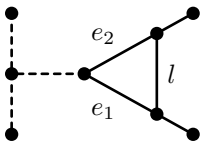

(5.5)

To perform elementary flips in this subdiagram, we first cut e_1 and e_2. As a result, we have a four-point subdiagram with four distinct external legs, which can be transformed in the same way as before. Finally, the cut edges are reconnected again. In the present example, this leads to (suppressing now the dashed parts of the diagram):

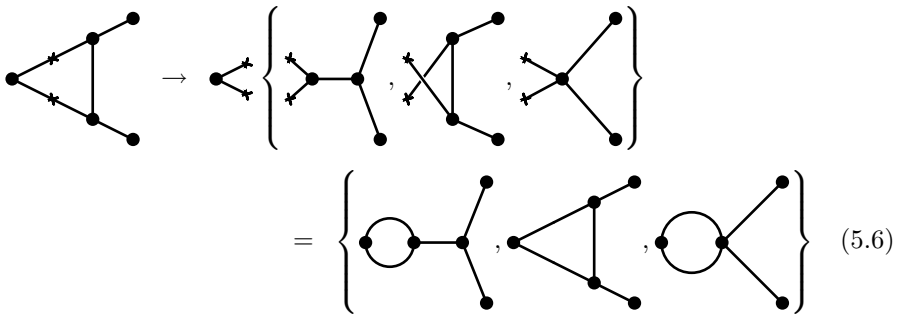

(5.6)

Note how the coincidence of the edges e_1 and e_2 at a single vertex leads to diagrams with a double edge, as in the first and third flipped diagram. Furthermore, we see that a flip can map a diagram onto itself, as is the case for the second of the flipped diagrams.

Let us finally consider the flips of the one-loop propagator:

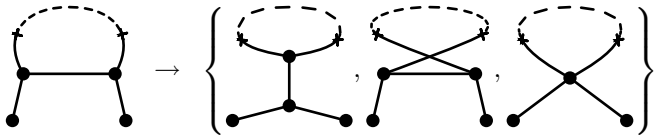

(5.7)

We have drawn the diagrams in a rather unconventional fashion to emphasize how the flipped four-point subdiagram is embedded in the whole diagram. In a more conventional drawing, the same flips look like this:

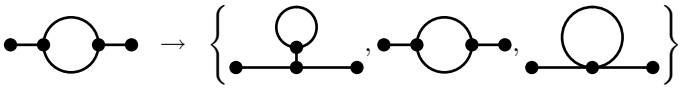

(5.8)

Note that we have chosen to cut the upper one of the double edges to perform the flips. In the unflavored case, cutting the lower edge would have led to the same set of flipped diagrams, of course. When we consider flavored diagrams at a later stage, both cases will in general lead to different results.

In all the examples discussed so far, it is apparent that a flip can *shrink* a loop, i. e. reduce the number of vertices in the loop. Since every flip can be reversed, the opposite is also true. Thus, flips of higher order diagrams can grow or shrink loops.

However, a flip can never change the number of loops. To see this, recall the topological formulae linking the number of loops L to the numbers of cubic and quartic vertices, V_3 and V_4, as well as the numbers of external and internal lines E and I. Since each internal line is connected to two vertices and each external line to one vertex, we have:

$$3V_3 + 4V_4 = 2I + E \tag{5.9}$$

Then, there is Euler's formula:

$$L = I - (V - 1) \tag{5.10}$$

Putting both equations together we get:

$$2L = 2V_4 + V_3 + 2 - E \tag{5.11}$$

Now look a the elementary flips among the diagrams in (5.2). The flips among s, t, and u just reorganize the given vertices and lines, so they do not change L. A flip to q decreases V_3 by two, I by one and increases V_4 by one, while leaving E invariant. Thus, the number of loops L and therefore the complete forest $F(E, L)$ is invariant under flips.

Since $F(E, L)$ is invariant, it makes sense to ask whether or not it is connected. As we shall now prove, it is:

Theorem 5.1 *The unflavored forest $F(E, L)$ of connected L-loop diagrams is connected for any number E of external lines and any number L of loops.*

To prove this statement, we note that from a diagram in $F(E, L)$ we can obtain a diagram of the tree level forest $F(E + 2L)$ by cutting L lines. Conversely, from every diagram in $F(E + 2L)$ we can get a diagram in $F(E, L)$ by joining $2L$ external lines. Now take d_1 and d_2 in $F(E, L)$. First, cut L external lines in d_1 and d_2 to obtain d_1' and d_2' in $F(E + 2L)$, respectively. Then, d_1' and d_2' are connected in $F(E + 2L)$, because all tree level forests are connected. But a sequence of flips in $F(E + 2L)$ defines a valid sequence of flips in $F(E, L)$, if we join the L cut lines again. Hence $F(E, L)$ is connected, as was to be proved. Of course, there is in general no unique prescription to perform the L cuts. This is, however, not necessary, because we need only demonstrate existence of at least one sequence of flips connecting d_1 and d_2.

This result is of practical importance, because it guarantees that the complete forest $F(E, L)$ can be produced from a single diagram by repeatedly applying flips. However, at higher orders of perturbation theory, constructing the complete forest of diagrams representing a connected Green's function is not always desired. For instance, if we are interested in scattering matrix elements, only amputated diagrams must be taken into account. At tree level, there is no difference between amputated and non-amputated diagrams, except for the different interpretation of external lines. For diagrams with loops, on the other hand, the amputated diagrams are a real subset of the complete forest $F(E, L)$. Also, we may or may not want to include one-point insertions, or we may require just the subset of 1PI diagrams.

This means that, in many cases, we will be interested in a *subset* S of the complete forest $F(E, L)$. If we want to produce the diagrams in S by performing flips, starting from a given diagram d in S, it would clearly be advantageous if we knew that every diagram in S can be generated from d by a sequence of flips leading only to diagrams *within* S. In other words, S should be a connected subset. For then we could throw away immediately any flipped diagram which is not in S.

Of course, an arbitrarily chosen subset of $F(E, L)$ need not necessarily be connected. In the remainder of this section, we want to study the connectedness of the aforementioned subsets of the complete forest $F(E, L)$. This study can be simplified by demonstrating that the four-point subdiagram q in (5.2) is actually meaningless for the connectedness of a forest. This is the reason why we divided the flips into rotations on one hand as well as expansions and contractions on the other hand. (Cf. the definitions below (5.2).)

Now, we can state and prove the connectedness of the forest $F_3(E, L)$, which is the subset of $F(E, L)$ of diagrams without quartic vertices:

Theorem 5.2 *The subset $F_3(E, L)$ is connected for any number E of external lines and any number L of loops.*

This statement can be proven in the same way as the connectedness of the complete forest. In particular, the tree level forest $F_3(E + 2L)$ is connected, because it can be constructed by performing successive insertions of an additional external line into the three-point diagram, omitting the production of quartic vertices. Neighboring insertions are then connected by rotations. Once we have the connectedness of $F_3(E+2L)$, the connectedness of $F_3(E, L)$ follows as before.

We can understand the connectedness of $F_3(E, L)$ intuitively in yet another way. Since we are starting from a diagram without quartic vertex, a quartic vertex can only be produced by a contraction. On the other hand, we end up again with a diagram without quartic vertex, so any contraction must eventually be balanced by a subsequent expansion. But then, the net effect of all subsequent elementary flips in an arbitrary four-point subdiagram must be a mere rotation.

The reason for the irrelevance of expansions and contractions for the connectedness of a forest becomes visible when we look at the example of a diagram in $F(5)$:

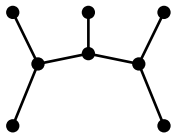

(5.12)

There are two *overlapping* choices of four-point subdiagrams:

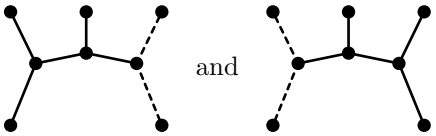

(5.13)

Performing successively a rotation in either of the subdiagrams will bring us away from the original diagram:

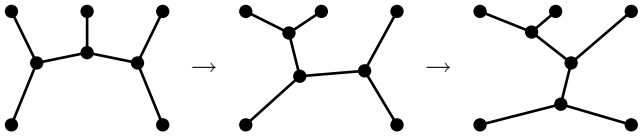

(5.14)

On the other hand, if we perform a contraction in the original diagram, there is no more room for a rotation:

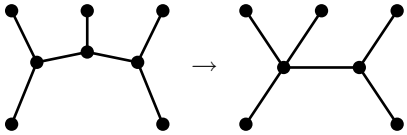

(5.15)

All we can do here is expand the quartic vertex again, with a result that could have obtained as well by performing a single rotation.

This argument has a straightforward generalization to other subsets of $F(E, L)$, which we state as a lemma:

Lemma 5.1 *A subset S of $F(E,L)$ is connected if its restriction $S_3 = S \cap F_3(E,L)$ to diagrams without quartic vertices is connected, as long as every diagram in S can be generated from a diagram in S_3 by a sequence of contractions.*

Indeed, given d_1 and d_2 in S, we can invert the respective contractions to get diagrams d_1' and d_2' in S_3. If S_3 is connected, d_1' and d_2' are connected, and consequently d_1 and d_2, too, are connected.

As a simple application, we note that the connectedness of $F(E,L)$ follows, by the lemma, from the connectedness of $F_3(E,L)$. To see this, note that a diagram d with quartic vertices can be produced from $F_3(E,L)$ by applying contractions if and only if the expansion of all quartic vertices in d leads to a diagram in $F_3(E,L)$. But this is obviously true.

5.1.3 1PI Diagrams

The above lemma suggests a two-step strategy to prove that a subset S of $F(E,L)$ is connected: First, prove that the restriction $S_3 = S \cap F_3(E,L)$ is connected, and then prove that every diagram in the remainder $S \setminus S_3$ can be generated from S_3 by a sequence of contractions.

In this section, we shall demonstrate, in the proof of connectedness for 1PI diagrams, that this strategy can be further refined as follows: Suppose we find a *connected* subset T_3 of S_3 such that every diagram in S_3 can be obtained from a diagram in T_3 by a sequence of rotations. Then, evidently S_3 is connected, which implies connectedness of S by the lemma.

We are further using the example of 1PI diagrams to introduce an interpretation of flips as *higher level graphical operations on Feynman diagrams*. That is, instead of thinking in terms of elementary flips in four-point subdiagrams, we will be thinking in terms of moving lines in diagrams around. In the present context of unflavored ϕ-theory, this may appear as a mere tautology, because after all neighboring insertions are connected by flips, and moving lines along other lines is actually equivalent to performing neighboring insertions. However, thinking in terms of higher level operations turns out extremely useful in unravelling the structure of the forest in gauge theories, (cf. 6.3.2).

Consider, then, the forest $F^I(E,1)$ of 1PI one-loop diagrams. We concentrate on the set $F_3^I(E,1)$, ignoring diagrams with quartic vertices. The diagrams in $F_3^I(E,1)$ have the E external lines immediately attached to the single loop. We demonstrate this for $E = 4$, but our arguments are completely general. Thus, consider d in $F(4,1)$:[2]

$d \;=$ 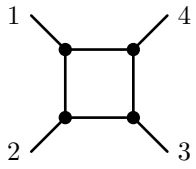

(5.16)

We have labeled the external lines for reference purposes.

For every possible four-point subdiagram, there is only one rotation keeping the flipped diagram irreducible. For instance, in the subdiagram containing 3

[2]Observe that, in this section, we omit the dots at the ends of external lines of diagrams, because 1PI diagrams are usually defined without including propagators for the external lines.

and 4 we get

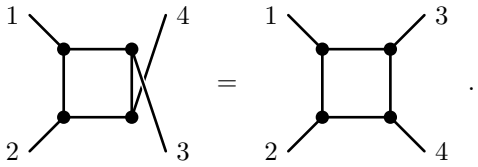

(5.17)

We can describe this operation by saying that the external line 3 has been moved past the external line 4. Thus, since flips can be applied repeatedly, elementary flips in $F_3^I(E,1)$ correspond to moving external lines along the loop in all possible ways. This observation shows that $F_3^I(E,1)$ is connected, because the diagrams in $F_3^I(E,1)$ can be characterized uniquely by the permutations of $E-1$ external lines.

In order to generalize this result to the case of an arbitrary number of loops, note that we did not actually make use of the fact that the permuted lines in (5.17) were external ones. They could just as well have been internal lines inside a larger diagram. Thus, quite generally, *rotations can be used to move a line connecting to a loop past other lines around that loop.*

This is actually all we need to know in order to prove that $F_3^I(E,L)$ is connected for arbitrary L. To this end, denote by T_3 the subset of $F_3^I(E,L)$ containing diagrams of the following form:

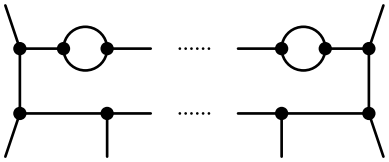

(5.18)

Evidently, every diagram in T_3 is uniquely characterized by a permutation of E external lines. (Not counting as different permutations that just reverse the order of external lines, because the diagrams in T_3 have a mirror symmetry.) By the same argument as in the one-loop case, T_3 is connected. Therefore, if we can show that every diagram in $F_3^I(E,L)$ can be transformed into a diagram in T_3 by moving lines along loops, then $F_3^I(E,L)$ is connected.

So let d be a diagram in $F_3^I(E,L)$:

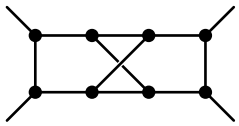

(5.19)

We use an example from the three-loop forest $F_3^I(4,3)$ for illustration purposes. However, our arguments are again completely general. It should be emphasized that even 1PI diagrams with 1PI one-point insertions, i. e. irreducible tadpole subdiagrams, fit into this scheme. The reason is the existence of the following rotation:

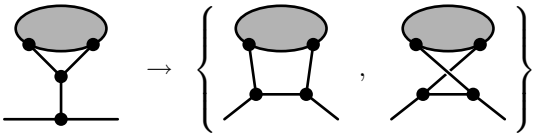

(5.20)

Here, the gray blobs denote a 1PI insertion. Evidently, then, the flipped diagrams are 1PI, too.

Now, it is crucial to note that in an 1PI diagram *every* internal line is part of at least one loop. For if it were not, the diagram could be separated by cutting this internal line, violating the condition of irreducibility. Therefore, we can move lines arbitrarily along internal lines without spoiling irreducibility. We use this freedom to first move all external lines next to each other:

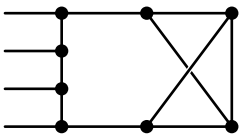

(5.21)

Then, we choose one of the internal lines next to the outermost external lines (it does not matter which one we choose), and move its endpoint along internal lines until it is located next to its starting point:

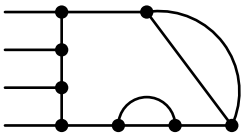

(5.22)

In the present example, we have completed the transformation to a diagram in T_3. In the general case, we can repeat this step with one of the internal lines next to the newly created one-loop self energy insertion. This shows that eventually every diagram in $F_3^I(E,L)$ can be transformed into a diagram in T_3, hence $F_3^I(E,L)$ is connected.

It remains to show that every diagram in $F^I(E,L)$ can be obtained from a diagram in $F_3^I(E,L)$ by performing a sequence of contractions. Equivalently, we can demonstrate that every diagram in $F^I(E,L)$ can be transformed into a diagram in $F_3^I(E,L)$ by a sequence of expansions *within* $F^I(E,L)$. We are thus led to consider the expansion of a quartic vertex that would lead to a reducible diagram. To this end, it suffices to take a look at the following two-loop example:

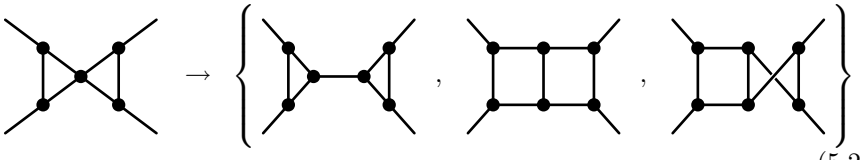

(5.23)

Obviously, the first expansion leads to a reducible diagram. However, the other two expansions can never produce a reducible diagram if the original diagram had been irreducible. Since the flip corresponding to the first expansion is the *only* way to produce a reducible diagram from an irreducible one, we conclude that it is always possible to choose expansions within $F^I(E,L)$. Thus, we have proven the connectedness of the set of 1PI diagrams:

Theorem 5.3 *The subset $F^I(E,L)$ of 1PI diagrams is connected for any number E of external lines and any number L of loops.*

5.1.4 *Amputated Diagrams*

We turn now to the subset of amputated diagrams. We shall assume $E \geq 3$ in this section, because otherwise the notion of an amputated diagram does not make sense.[3] Amputated diagrams are in general reducible. However, amputated diagrams are distinguished by the property that none of the two disconnected pieces obtained by cutting through a single internal line is a diagram with two external lines.

On the other hand, we do not exclude the possibility of one-point insertions. Therefore, we consider two subsets of amputated diagrams: the subsets $F^A(E,L)$ and $F^*(E,L)$ of amputated diagrams with and without one-point insertions, respectively.

We shall first prove that the restrictions $F_3^A(E,L)$ and $F_3^*(E,L)$ to diagrams without quartic vertices are connected. We begin with one-loop diagrams. A one-loop diagram is always amputated if the loop contains three or more vertices. If the loop contains exactly two vertices, the diagram is amputated if none of the two tree subdiagrams obtained by removing the loop consist of a single line. Finally, if the loop contains just a single particle, corresponding to a one-loop tadpole, the tree subdiagram obtained by removing the loop must have at least four external vertices.[4]

As an example, consider the following three diagrams from $F_3(4,1)$, successively linked by flips:

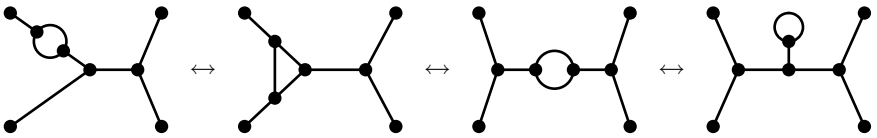

(5.24)

The latter three diagrams are amputated, while the former is not. This example again demonstrates a kind of a graphical higher order operation representing an elementary rotation. In particular, observe that the displayed flips correspond to moving a line from the loop onto an adjecent line and *vice versa*. Combined with the operation of moving lines along loops, this means that *sequences of rotations are equivalent to all possible motions of lines along other lines within a diagram.*

In the one-loop case, it is now easy to see that all diagrams in $F_3^A(E,1)$ are connected within $F_3^A(E,1)$ to the set of irreducible diagrams $F_3^I(E,1)$: We just have to move all external lines onto the loop. This can only fail if in the beginning the loop contains a single vertex, i. e. if the diagram contains a one-loop tadpole. In this case, for the original diagram to be amputated, it must contain the last diagram of (5.24) as subdiagram. But, reading the flips in (5.24) from right to left, we see that also in this case all intermediate diagrams are amputated. This proves the connectedness of $F_3^A(E,1)$. But $F_3^*(E,1)$ is also connected, because the flip to the one-loop tadpole is not required to connect the other diagrams, whence one-point insertions can be omitted without spoiling

[3] In principle, amputation could be defined for one-point diagrams, i. e. $E = 1$. However, an amputated one-point diagram is an 1PI diagram, and 1PI diagrams have been treated in the last section.

[4] We ignore here the one-loop self-energy diagrams, for which amputation is not actually defined. Anyway, these diagrams are 1PI, so they have been treated before.

the connectedness of the remaining diagrams.

We would like to use a similar line of reasoning in the multi-loop case. To this end, recall that connected diagrams, and hence amputated diagrams, have a skeleton expansion consisting of tree diagrams with 1PI functions for vertices, connected by full propagators. For our purposes, this means that an amputated diagram consists of 1PI subdiagrams linked by single lines, as e. g. the first flipped diagram in (5.23). Now, every single line connecting two 1PI subdiagrams defines a four-point subdiagram, the rotations of which will join the two 1PI subdiagrams into a single one:

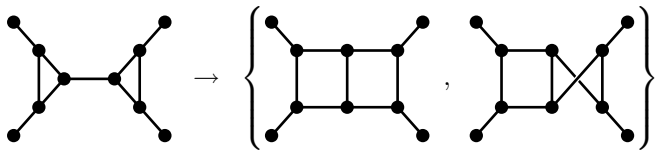

(5.25)

Consequently, every diagram in $F_3^A(E,L)$ can be transformed by rotations within $F_3^A(E,L)$ into an 1PI diagram in $F_3^I(E,L)$. Since the latter set is connected, $F_3^A(E,L)$ is connected, too. Again, the same applies if we omit one-point insertions, i. e. $F_3^*(E,L)$ is also connected.

We must now ask, whether all diagrams in $F^A(E,L)$ can be expanded within $F^A(E,L)$ into diagrams in $F_3^A(E,L)$, and similar for $F^*(E,L)$. Let us consider $F^*(E,L)$ first. By an argument similar to the one used in the last section, if one expansion of a quartic vertex leads to a non-amputated diagram, there is always another one that does not:[5]

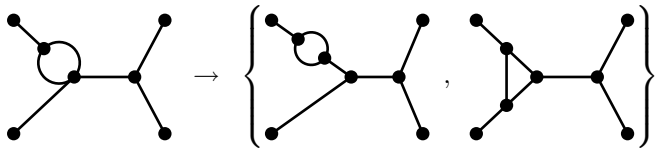

(5.26)

Thus, $F^*(E,L)$ is connected.

If one-point insertions are taken into account, these can be rotated away as in (5.20), *unless* they are inserted into a quartic vertex. In this case, the quartic vertex has to be expanded first, but this may lead to a non-amputated diagram if external lines are coupled to the quartic vertex:

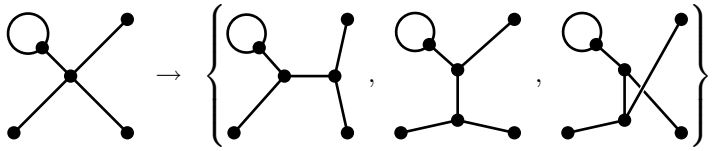

(5.27)

We have displayed the case of a one-loop tadpole, but clearly the argument applies to the general case as well. Now, if at least one of the three non-tadpole lines is not an external one, the insertion of the tadpole in this line is still an amputated diagram. The tadpole can then again be transformed away as in (5.20), and all our previous arguments remain valid. Only if *all* non-tadpole lines at the quartic vertex are external lines is it impossible to avoid a non-amputated intermediate diagram. This case, which must be noted as a special

[5] Due to coinciding vertices, two expansions are identical here.

exception, is, however, limited to diagrams with three external lines, i. e. $E = 3$. In fact, for $E > 3$ the additional external line provides the necessary escape route. In any event, for $E > 3$ we have unambigously proven the connectedness of $F^A(E, L)$.

As a corollary of the above proof, we note that the subset $F^T(E, L)$ obtained by omitting all one-point insertions from the *complete* forest $F(E, L)$ is also connected. To see this, recall that we have already shown that $F^A(E, L)$ is connected when one-point insertions are omitted. But from the example (5.24) it is clear that the flips leading to self energy insertions in external lines do not require intermediate diagrams with one-point insertions.

Finally, we summarize the results of this section:

Theorem 5.4

1. *The subset $F^A(E, L)$ of amputated diagrams is connected for $E \geq 4$ and any number L of loops.*

2. *The subset $F^*(E, L)$ of amputated diagrams without one-point insertions is connected for $E \geq 3$ and any number L of loops.*

3. *The subset $F^T(E, L)$ of connected diagrams without one-point insertions is connected for any number E of external lines and any number L of loops.*

4. *The subset $F^A(3, L)$ of amputated diagrams with three external lines and $L \geq 1$ loops is disconnected due to one-point insertions into a quartic vertex with three external lines.*

5.1.5 An Explicit Example

To illustrate the ideas developed in the foregoing subsections, we discuss the connectedness in the forest $F(3, 2)$ of connected two-loop three-point diagrams. $F(3, 2)$ itself contains 217 diagrams, too many to provide a practical example. Therefore, we restrict ourselves to the subset $F^*(3, 2)$ of amputated diagrams without one-point insertions. Doing so will render this example manageable and at the same time confirm the results derived above.

$F^*(3, 2)$ contains 40 diagrams, still a lot of diagrams to draw. Fortunately, in unflavored ϕ-theory many diagrams will differ only by permutations of external lines. If we consider external lines as indistinguishable, we can choose one diagram to represent all permutations. This will give us the possible *topologies* of diagrams in $F^*(3, 2)$. It turns out that there are thirteen topologies. Furthermore, since we know that $F^*(3, 2)$ is connected, we need only demonstrate the connectedness of the topologies without a quartic vertex (i. e. the topologies of $F_3^*(3, 2)$), of which there are just three. The diagrams with quartic vertices are necessarily given by performing all possible contractions in $F_3^*(3, 2)$.

We first illustrate in detail how the three topologies of $F_3^*(3, 2)$ are connected

by flips:

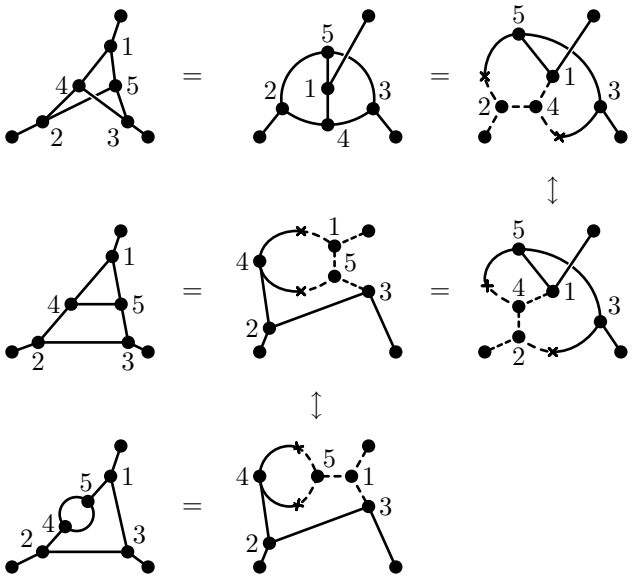

(5.28)

The diagrams are drawn in the left column in what could be called a conventional style. The middle and right column show how the flipped four-point subdiagrams—displayed in dashed line style—are embedded in these diagrams, leading to rather unconventional drawings. We denote the three topologies of $F_3^*(3,2)$ from top down as *crossed ladder*, *ladder* and *self energy* topology, respectively.

Note that the vertices are labeled in the above diagrams only only to ease recognition of the topologies. When *comparing* topologies, these labels have to be forgotten. On the other hand, when we discuss the diagrams in $F_3^*(3,2)$, the labels 1, 2, and 3 must be kept to distinguish external lines.

Let us first count the number of diagrams in $F_3^*(3,2)$: The permutations of external lines (i. e. of the labels 1, 2, and 3) produce three different diagrams for the ladder and self energy topology. On the other hand, every permutation of external lines leaves the crossed ladder invariant. Thus, $F_3^*(3,2)$ consists of seven diagrams, one crossed ladder, three ladders and three self energies.

Next we need the flips in $F_3^*(3,2)$. We begin with the most symmetric diagram, the crossed ladder, which we abbreviate as C. Due to the symmetry of C, every flip must lead to a ladder:

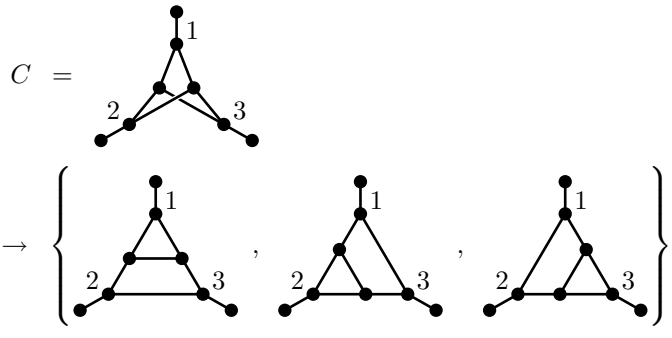

$\equiv \{L_1, L_2, L_3\}$

(5.29)

We have introduced the notation L_1, L_2, and L_3 for the ladder diagrams, where the index refers to the label of the external line at the "top" of the ladder.

Next, consider the flips of a ladder diagram. We shall ignore flips which leave the diagram invariant. Of course, we can flip back to the crossed ladder C. Furthermore, from (5.28) we know that a ladder can be flipped to a self energy diagram, where the self energy can appear on both "sides" of the ladder. But a ladder can also be flipped into another ladder, e. g.

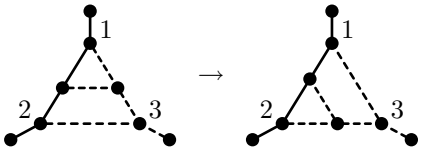

(5.30)

Clearly, a similar flip can be performed at the opposite side of the ladder. Thus, every ladder diagram can be flipped into every other ladder diagram, the crossed ladder, and two self energy diagrams:

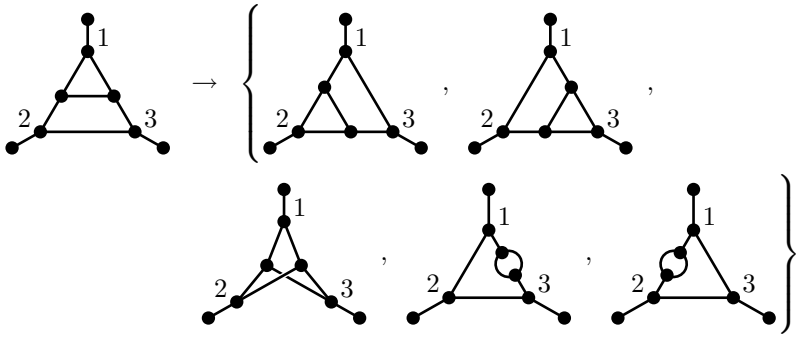

(5.31)

Denoting by S_j the self energy diagram with external line j opposite to the self energy insertion, this can be written symbolically as

$$L_1 \to \{L_2, L_2, C, S_2, S_3\} \quad . \tag{5.32}$$

Finally, we have to determine the flips of a self energy diagram. From the symmetries of the diagrams and the above discussion we see that there must be flips to two different ladders. In addition, every self energy diagram is connected with every other self energy diagram, as demonstrated by the flip below:

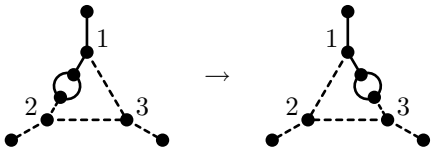

(5.33)

Altogether, the flips of the self energy diagram S_1 are given by

$$S_1 \to \{L_2, L_3, S_2, S_3\} \quad . \tag{5.34}$$

We have now determined the structure of the subset $F_3^*(3,2)$. In figure 5.2 it is represented as a graph, nodes corresponding to the diagrams and edges corresponding to a single flip. Figure 5.3 then displays how the topologies

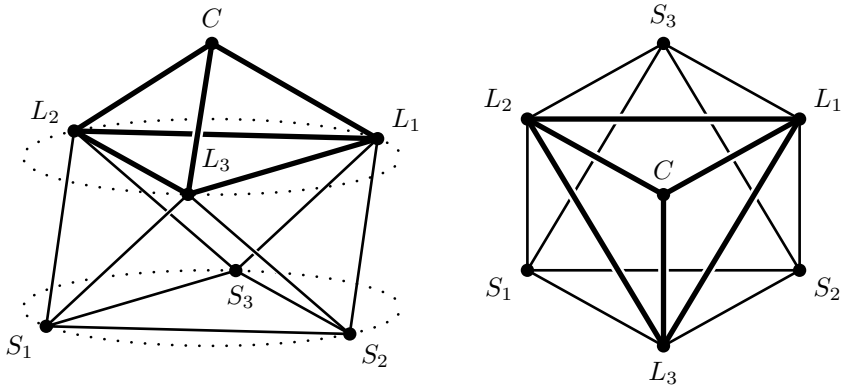

Figure 5.2: Two views on the graph of the subset $F_3^*(3,2)$. On the left hand side, the triangles in the planes indicated by the dotted circles correspond to the three ladder diagrams (top layer) and the three self energy diagrams (bottom layer), respectively. The top node represents the crossed ladder diagram, which is completely symmetric under permutation of external lines. The right hand side then represents a view "from above". The edges of the upper tetrahedron have been drawn in bold style to ease recognition.

with quartic vertices can be obtained from $F_3^*(3,2)$ by performing contractions. Arrows indicate a single flip, and the pair of contracted cubic vertices is indicated by white dots, reading flips from left to right. Of course, the displayed topologies are connected by more flips than the ones explicitely shown. The graph of the complete subset $F^*(3,2)$ can be viewed in figure 5.4.

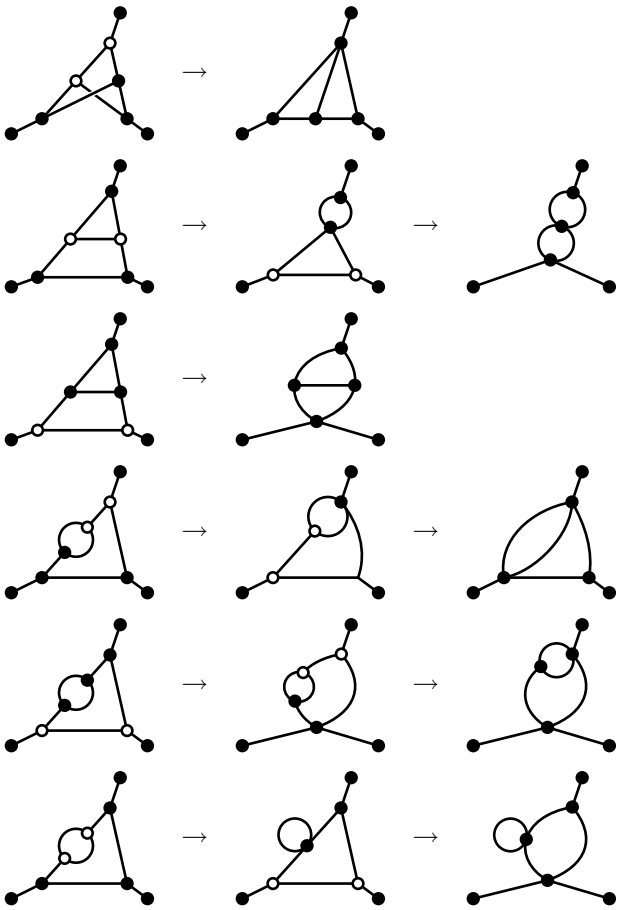

Figure 5.3: Contractions yielding the complete subset $F^*(3,2)$. White dots indicate the contracted pair of cubic vertices.

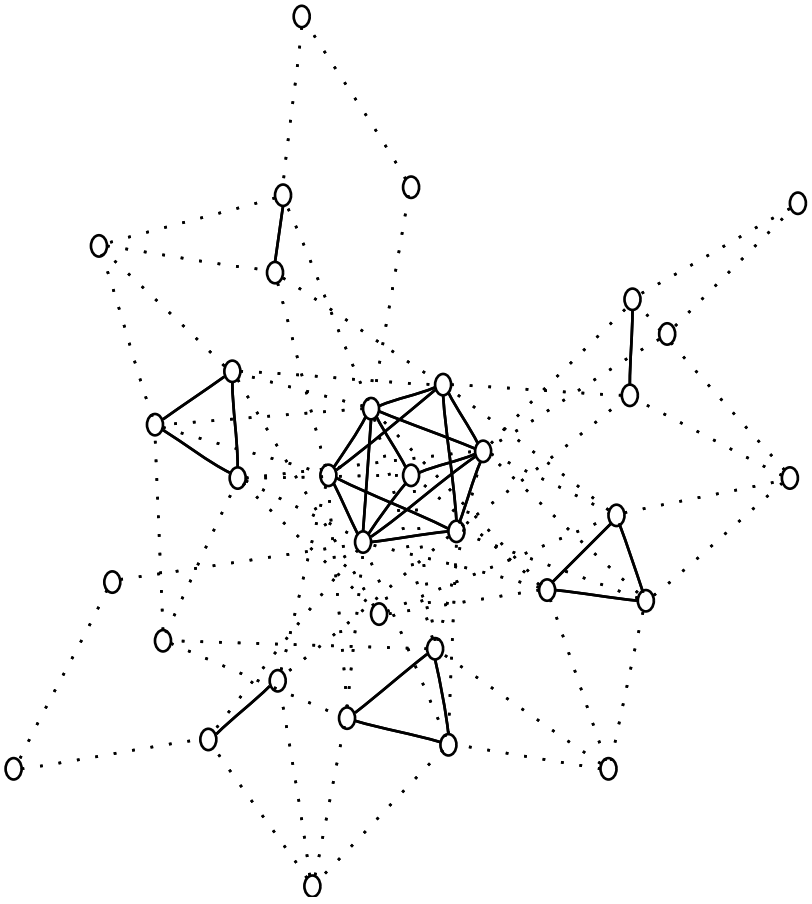

Figure 5.4: The graph of the complete subset $F^*(3,2)$. Solid lines correspond to rotations, dotted lines to contractions or expansions. In the center of the forest, we recognize the subset $F_3^*(3,2)$. The view corresponds to the one displayed in the right hand side of figure 5.2.

—6—
Flips and Groves in Gauge Theories

In this chapter, we study the groves of connected Green's functions in gauge theories, employing the gauge flips, as defined in section 4.3. We shall argue that the formalism of gauge flips and groves is mainly useful in spontaneously broken gauge theories. To this end, we briefly discuss the situation in QCD, as an example of an unbroken gauge theory. After that, we turn to our main goal, the classification of groves of connected Green's functions in the (minimal) Standard Model, the external lines of which correspond to physical particles.

It will then prove extremely useful to express the possible actions of gauge flips in terms of more intuitive, higher level graphical transformations of Feynman diagrams, such as shifting a certain line along other lines of a diagram, breaking up a loop or joining two loops into a single one. These operations, called *gauge motions* will enable us to determine the structure of SM forests for very general SM forests. We then turn to a specific example, which we discuss in much detail. Finally, we compare the theoretical results thus obtained with the results of an investigation by means of a computer program implementing the decomposition of the forest by gauge flips as we have described it.

6.1 Flips in Gauge Theories

In the previous chapter we have investigated the forest $F(E, L)$ of connected Feynman diagrams in unflavored ϕ-theory. Flips were interpreted as higher level graphical operations on Feynman diagrams, through which the connectedness of the complete forest $F(E, L)$ as well as various subsets could be proven. While the connectedness of these subsets is of considerable practical interest, it has no physical significance. In particular, amplitudes in unflavored ϕ-theory are not constrained by any symmetries. Consequently, there are no relations among Feynman diagrams induced by a gauge symmetry.

The situation is different in gauge theories. As we have demonstrated at length in the first part of this work, the STIs in gauge theories induce relations among diagrams. In particular, in chapter 4 we proved that the groves of a connected Green's function G, i. e. the minimal gauge invariant subsets of G, can be constructed by applying gauge flips to diagrams of G.

Now, if we forget about the flavors pertaining to the lines of a diagram d in G, we can treat d as a diagram in unflavored ϕ-theory, because the renormalizable interactions of a gauge theory are covered by the interaction degrees of ϕ-theory. The gauge flips in d are then just a subset of all possible flips of d. Consequently,

under gauge flips the forest $\mathcal{F}(G)$ of G will fall into disjoint subsets, which are just the groves of G.

Since gauge flips have already been defined in 4.3—more specifically, in (4.53), (4.56), and (4.58)—we are now in principle in a position to analyze the structure of the groves in a general gauge theory. However, it turns out that, in order to obtain useful results, we have to be sufficiently explicit about the field content of the gauge theory. Therefore, we will discuss the QCD and the SM, as paradigms for an unbroken and broken gauge theory, respectively, in detail. The generalization of our results to other gauge theories should then be obvious.

6.2 Gauge Flips in QCD

Gauge flips develop their full power only in spontaneously broken gauge theories. To appreciate why this is the case, consider QCD as an example of an unbroken gauge theory. We have already mentioned in the introduction that the most efficient ways to calculate QCD amplitudes actually abandon the definition of the amplitude in terms of a sum of all possible Feynman diagrams.[1] Nevertheless, let us see what gauge flips have to say.

The elementary gauge flips of four-gluon subdiagrams are given by the transformations among the set of diagrams contributing to the four-gluon connected Green's function at tree level:

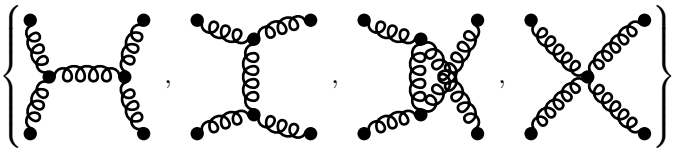

(6.1)

Essentially, this set of diagrams is identical to the set $F(4)$ of diagrams in unflavored ϕ-theory. This means that a pure gluon forest at tree level is no different from the unflavored forest $F(E)$. In particular, the forest of pure gluon connected Green's function at tree level always consists of a single grove. The same applies in higher orders, if we consider QCD without quarks, because the diagrams with ghost loops cannot produce separate groves. Thus, in an unbroken pure Yang-Mills theory, the forest can never be partitioned in more than a single grove.

If quarks are taken into account, the situation changes because then diagrams with a fixed number of quark loops are gauge invariant by themselves. This can be demonstrated using gauge flips, because a gauge flip never changes the number of fermion loops, as is apparent from the set of four-point diagrams with a single quark line, defining the relevant elementary gauge flips:

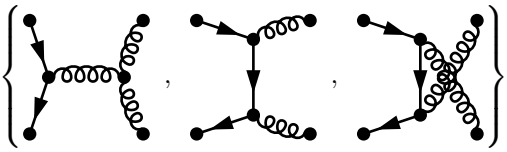

(6.2)

Thus, the formalism of gauge flip confirms the known fact [25] that the STIs in gauge theories apply separately to diagrams with a fixed number of fermion loops.

However, gauge flips were invented in order to search for a finer partitioning than the partitioning according to the number of fermion loops. On the other hand, as we have argued above, the usual treatment of QCD diagrams implies that, concerning flips, they behave effectively like unflavored diagrams. In other words, the group structure of QCD is completely ignored by the QCD gauge flips in (6.1) and (6.2).

To illustrate this, we consider the four-quark connected Green's function at one-loop level. Assuming, for simplicity, that the flavors of the quarks are different, the diagrams without a quark loop form a single grove:

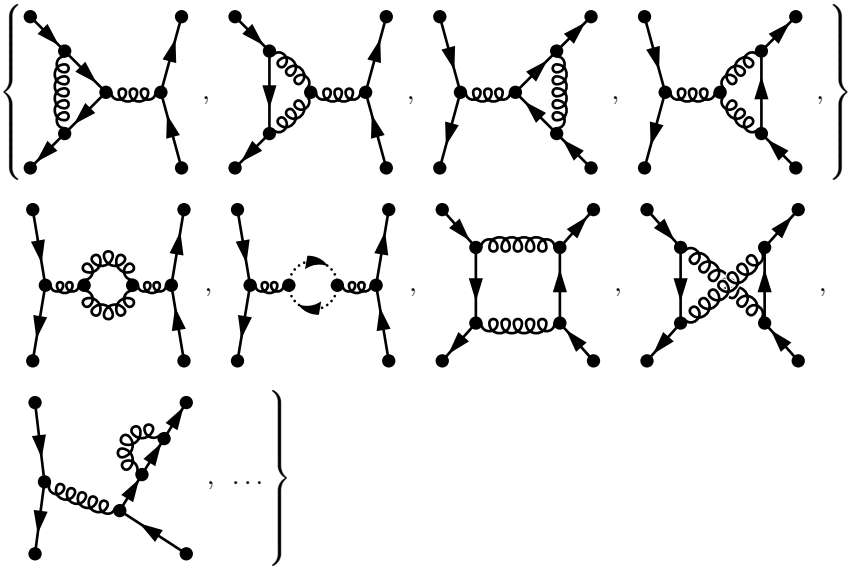

(6.3)

We have omitted all but one of the four diagrams with a quark self energy in an external leg.

Without any specific information on the colors of gluon and quarks, we cannot exclude a single diagram of this set. On the other hand, the structure constants f^{abc} of the color gauge group $SU(3)$ *do* vanish for many choices of color indices. For instance, in the usual Gell-Man basis, the structure constants f^{abc} are identically zero if both a and b are equal to 3 or 8, because the Gell-Man matrices λ^3 and λ^8 mutually commute. Thus, if we choose the two gluons in the last two diagrams of (6.3) to correspond to these generators, the diagrams with the triple gluon vertex will be absent. This, in turn, implies that the following subsets of the above grove are in fact groves themselves:

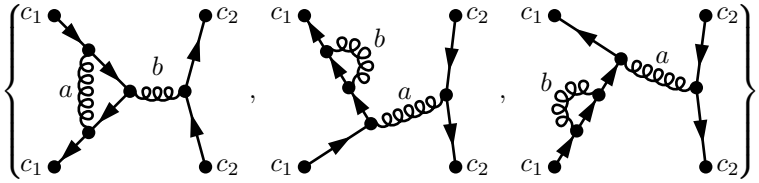

(6.4)

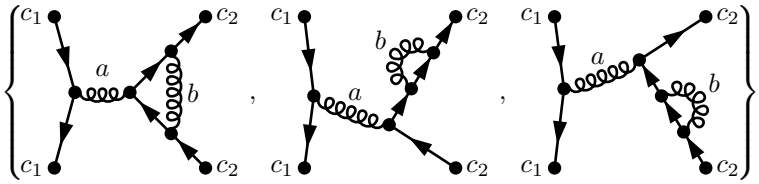

(6.5)

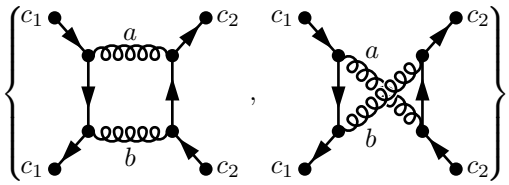

(6.6)

Here, the color indices a and b of the gluons take on the values 3 or 8. Of course, these diagrams are identically zero if either of a or b is 3 and one of the quark colors c_1 or c_2 has the value "blue", because λ^3 yield zero on the "blue" component of the quark color multiplet. Note, however, that for other combinations of gluon colors, like 1 and 2, 4 and 5, or 6 and 7, the diagrams in (6.3) will all be present and form a single grove.

The origin of this additional structure in the QCD forests is caused by the introduction of an arbitrary but fixed basis in color space. This was done here by choosing the representation of Gell-Man for the generators of $SU(3)$. As a matter of principle, there is nothing wrong with such an approach. On the other hand, Green's functions with colored external states are unphysical due to confinement in QCD. Therefore, in all practical applications, color sums will have to be performed. It is then *much* more convenient not to use an explicit basis, because, at least if amplitudes are defined through Feynman diagrams, the color structure can always be separated from the Lorentz and kinematical structure. Color sums can then be performed by group theory techniques, which is generally more efficient than using the brute force method of summing over a fixed basis. But without specifying an explicit color value for the two intermediate gluons, the forest has no structure but the one induced by the number of fermion loops. Thus, the real reason why gauge flips are not very useful for QCD is that in QCD the gauge symmetry is *unbroken*, such that every choice of basis in color space is necessarily an arbitrary one.

To turn the argument on its head, this means that gauge flips will be useful if physics chooses a direction in the representation space of the gauge group. This happens precisely in gauge theories with spontaneous symmetry breaking, where the choice of ground state fixes a direction in group space, at least for the broken generators of the gauge group. We will discuss this in detail in the next section.

6.3 Gauge Flips and Groves in the Standard Model

To determine the structure of Standard Model (SM) forests, we must list the possible gauge flips in some detail, taking into account the real field content of the SM. In order not to get lost in notation, we use a collective notation for the SM fields where this is appropriate. For instance, we shall distinguish quarks and leptons only if QCD couplings are considered. Also, we shall use a single symbol for the photon as well as the Z^0 boson (together with its associated

Goldstone boson). To be specific, the following notation is employed for the fields of the SM:[1]

$$W_\mu^\pm, \phi^\pm \quad \rightarrow \quad \text{} \tag{6.7a}$$

$$A_\mu, Z_\mu^0, \phi^0 \quad \rightarrow \quad \text{} \tag{6.7b}$$

$$H \quad \rightarrow \quad \text{} \tag{6.7c}$$

$$\ell, \nu_\ell, q \quad \rightarrow \quad \text{} \tag{6.7d}$$

$$G_\mu^a \quad \rightarrow \quad \text{ 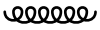 } \tag{6.7e}$$

Ghosts can be ignored for the determination of groves.

It is important to note here, that we consider only fermions in the *dublet* representation of $SU(2)$, that is, the usual quarks and leptons. If other representations are of interest, as e. g. in supersymmetric extensions of the SM, the set of gauge flips involving fermions, discussed in the next section, and hence the structure of the forest, will change. We will indicate the places where modifications would be necessary.

Also, we consider fermions generically as *massive*. This means that fermions generally are coupled to the H boson and the Goldstone bosons. Later, we shall investigate the changes brought about by considering fermions as massless in detail. We shall, however, indicate briefly the places where a vanishing fermion mass would make a difference.

Sometimes, we have to distinguish clearly between photon and Z^0. In this case, the latter shall be represented by a zigzag line:

$$Z_\mu^0, \phi^0 \quad \rightarrow \quad \text{  } \tag{6.8}$$

Note that we shall refer to the bosons of the electroweak (EW) sector of the SM, i. e. H, A_μ, Z_μ^0, W_μ, and the associated Goldstone bosons, collectively as *EW bosons*, or even just as bosons, if no confusion is possible. Gluons, on the other hand, shall always be referred to as such.

6.3.1 Gauge Flips

Neglecting the flips of ghost subdiagrams in (4.58), the gauge flips in the SM are given by the transformations among the four-point subdiagrams with at least one external gauge boson as well as the five-point subdiagrams with at least one external gauge boson and three H bosons. The SM gauge flips have been derived in the context of tree level diagrams in [5]. We list them here for reference purposes. On one hand, there are the four-point subdiagrams with only bosonic external lines:

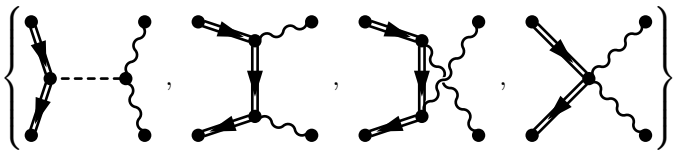 (6.9a)

[1] We denote the field corresponding to the photon as A_μ. However, we shall refer to the photon as a particle as γ.

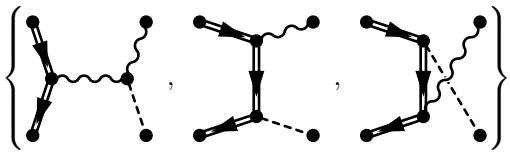

(6.9b)

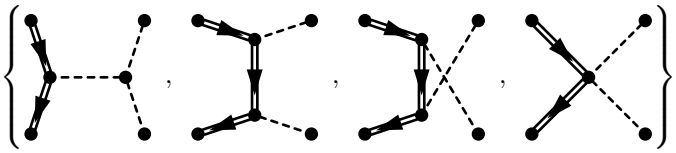

(6.9c)

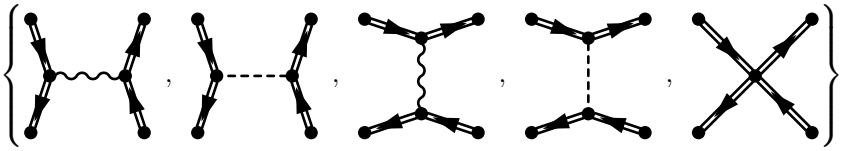

(6.9d)

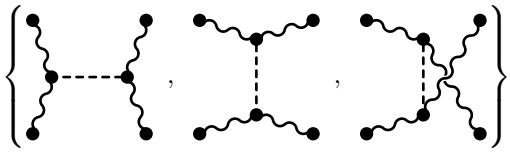

(6.9e)

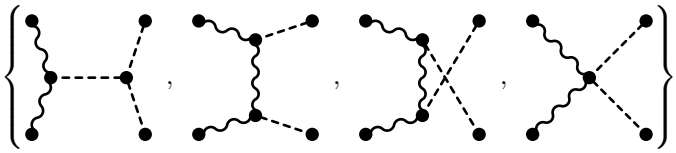

(6.9f)

If QCD corrections are taken into account, we have to include in addition the flips among the four-gluon subdiagrams (6.1).

On the other hand, there are four-point subdiagrams with two external fermion lines:

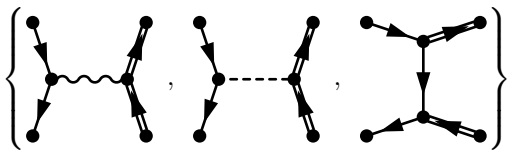

(6.10a)

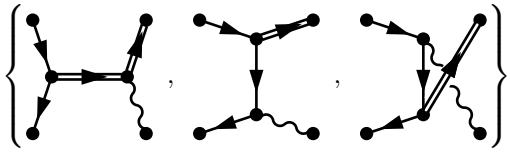

(6.10b)

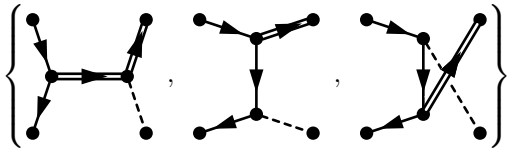

(6.10c)

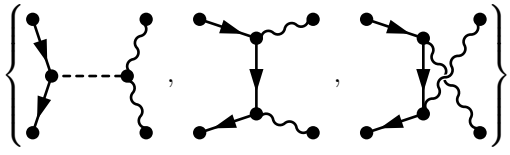

(6.10d)

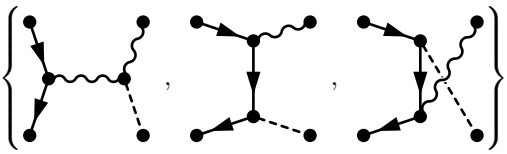

(6.10e)

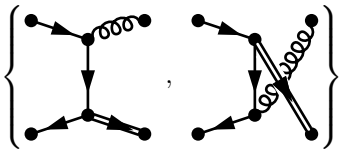

(6.10f)

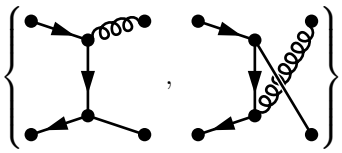

(6.10g)

Note that, in the last subset, we have chosen a plain line to represent any neutral EW boson. Here, we have to add the quark-gluon subdiagrams from (6.2) to account for QCD corrections.

This set of gauge flips is the correct one for *massive* fermions in the *dublet* representation of $SU(2)$. For massless fermions, the subdiagrams with couplings of the H boson to the fermion line are absent. We do not consider fermions in representations of $SU(2)$ other than the dublet representation in this work. However, we would like to mention that, for fermions in other representations of $SU(2)$, additional gauge flips appear of four-point subdiagrams with two W bosons of *like* charge. Such diagrams simply cannot exist for fermions in the dublet representation.[2]

Finally, there are the following gauge flips of five-point subdiagrams:

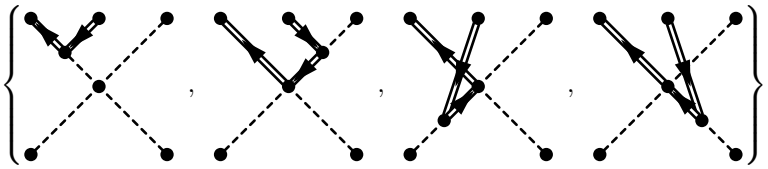

(6.11)

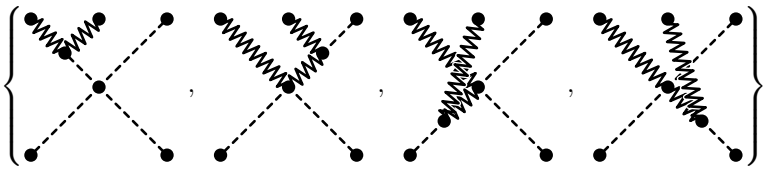

(6.12)

Using a collective notation for SM fields comes at the price that we are not guaranteed the existence of the displayed subdiagrams for all allowed choices of external lines. For instance, neutrinos will not couple to the photon. More importantly, for massless fermions no coupling to the H boson exists. Massless fermions will be discussed in detail later. However, we note that in the SM every fermion couples to the Z^0 boson, which is a simple consequence of the $SU(2)$ part in the SM gauge group $SU(2) \times U(1)$. This fact will be put to use later in the determination of the groves of SM connected Green's functions.

[2]For a discussion of the structure of the forest in and $SU(2)$ gauge theory with fermions in arbitrary irreducible representations of $SU(2)$, see [6].

In [6], such an analysis has been performed for tree level amplitudes with all external lines corresponding to fermions, ignoring the contributions of the Higgs boson.[3] In the remainder of this section, we shall now generalize this analysis to the case of SM forests consisting of diagrams with a non-vanishing number of loops.

6.3.2 Gauge Motions

As in the case of the unflavored forest, it is useful to abstract the action of single gauge flips into higher level graphical operations. We shall denote them as *gauge motions*, because they can be interpreted as motions of lines in SM Feynman diagrams caused by sequences of gauge flips. Since the structure of the forest is determined solely by the diagrams without quartic vertices, we ignore the elementary contractions and expansions, i. e. flips producing or eliminating a quartic vertex.

In this section, we need a sufficiently precise terminology for parts of an SM Feynman diagram, to avoid misunderstandings. In particular, we shall refer to tree level propagators of the field φ as *φ-lines*. A chain of successive φ-lines will be denoted as a *φ-thread*. For fermions, this definition needs some qualification, because the fermion flavor can change along a chain of fermion lines. Therefore, we take a fermion thread to denote any chain of successive fermion lines.

Elimination of Internal Higgs Lines

To begin with, we shall demonstrate that internal H-lines coupled to a gauge boson thread can be eliminated by gauge flips, except if the H-line couples to two Z^0-threads. (Of course, H bosons in the external state can never change their identity.)

The statement follows by inspection of the gauge flips involving a four-point subdiagram with an intermediate H-line. Some intermediate H-lines can be trivially eliminated by replacing them with a Z^0-line. The corresponding flips are given by (6.9d) and (6.10a). In all other cases we need to perform a flip changing the topology of the subdiagram. As an example, consider the relevant flip in (6.9a):

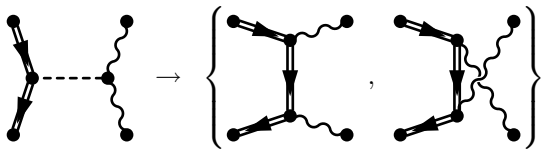

(6.13)

Similar flips can be performed in (6.9c), (6.9f), and (6.10d).

The only exception is provided by the flips of four-point subdiagrams with four external Z^0-lines in (6.9e). Observe, however, that in this case all three subdiagrams without quartic vertex are allowed.

[3] Actually, the gauge theory considered in [6] was an $SU(2)$ toy theory. If Higgs boson contributions are ignored, the structure of the groves is, however, essentially the same as in the SM. If the toy $SU(2)$ is broken by a dublett Higgs, this statement applies also to the full forest, including Higgs contributions.

Parallel Motions

The second higher level operation we consider, is the motion of neutral bosons and gluons along threads. In this respect, we first note that H-lines can be moved freely past other H-lines along Z^0 or W-threads. This is a simple consequence of the flips permuting two external H-lines in (6.9c) and (6.9f). In the latter case, the relevant flip is given explicitely by

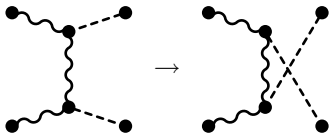

(6.14)

We say that H-lines can be moved *parallel* to Z^0 and W-threads and denote this as $H \parallel Z^0$ and $H \parallel W$, respectively.

In an analogous way, according to the relevant flips in (6.9a), (6.10b), (6.10d), (6.10e), and (6.10g), Z^0-lines can be moved parallel to W and fermion threads, i. e. we have $Z^0 \parallel W$ and $Z^0 \parallel f$, where f represents a general SM fermion. We display two example flips:

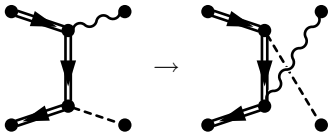

(6.15)

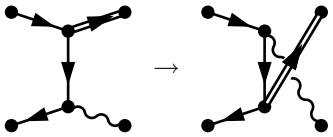

(6.16)

The same motions are possible for photon lines, with the one exception that a photon may not be moved across a neutrino line. Keeping this exception in mind, we thus get $\gamma \parallel W$ and $\gamma \parallel f$.

In addition, we have the parallel motions $G \parallel q$ of gluons along quark threads, following from (6.10g) and (6.10f).

Perpendicular Motions

Parallel motions of neutral bosons along a thread ℓ will necessary terminate when ℓ ends. If ℓ happens to end at a second thread ℓ' (which, of course, implies that ℓ is a boson line), it will often be possible to move the neutral boson from ℓ onto ℓ'.

For instance, Z^0-lines can be moved from fermion threads onto W threads and *vice versa*, as the following flip in (6.10b) shows:

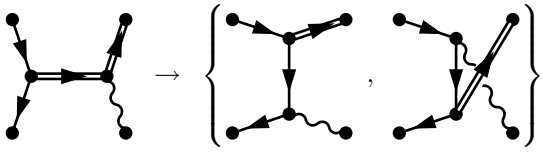

(6.17)

We say that Z^0-lines can be moved *perpendicular* from fermion threads onto W-threads, and *vice versa*, denoting this as $Z^0 \perp fW$. Again, the same applies

for photon lines, i. e. there is a perpendicular motion $\gamma \perp fW$. Note that there is no restriction for photon lines if the photon is moved from the fermion thread onto the W-thread. For if the last line of the fermion thread was a neutrino line, the photon would not have been there in the first place.

For H-lines, there are three perpendicular motions. Instead of displaying the relevant flips explicitely, we will refer to the respective subsets. Thus, (6.10c) implies $H \perp fW$, (6.10e) implies $H \perp fZ^0$, and (6.9b) implies $H \perp Z^0W$.

Observe that we have chosen to define the perpendicular motions of H-lines involving fermions as motions from the fermion thread onto the gauge boson thread. The reverse motions, from a gauge boson thread onto a fermion thread, are possible only for a massive fermion thread. As we shall later see, the lack of this gauge motion for massless fermions leads to additional structure of the SM forests with massless fermions.

Finally, for gluons we have the perpendicular motion $G \perp qG$, which follows from (6.2). Note that the interpretation is slightly different in this case. In particular, it does not actully make sense to speak of a gluon *thread*, because color can flow into all three directions at a triple gluon vertex. However, it is certainly true that a gluon coupled to quark thread can always be moved onto a neighboring gluon *line*. We shall understand $G \perp qG$ in this way.

Crossover Motions

There are yet more intricate motions of neutral bosons. In particular, while a Z^0-line certainly cannot move parallel to a Z^0-thread, it can use a Z^0-line to switch from a W-thread to another W-thread or a fermion thread. For the case of two W-threads, the relevant flips come from (6.9d) and (6.9a):

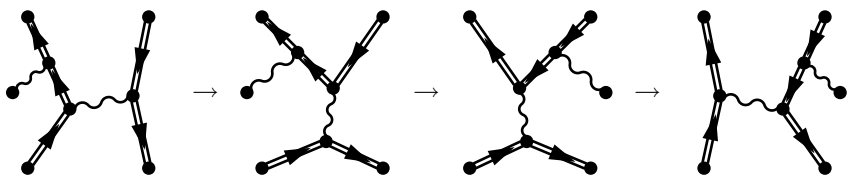

(6.18)

We say that the Z^0-line is moved *crossover* from W-thread to W-thread, using a Z^0-line as a *bridge*, and denote this as $Z^0 \times WZ^0W$.

For the case of one fermion thread and one W-thread we need (6.10a) and the perpendicular motion $Z^0 \perp fW$:

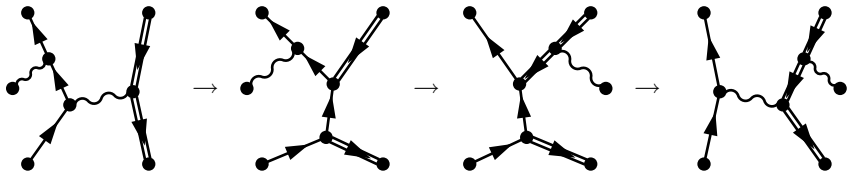

(6.19)

Thus, we have $Z^0 \times fZ^0W$. Again, for photons the identical motions $\gamma \times WZ^0W$ and $Z^0 \times fZ^0W$ are possible.

Finally, using (6.9f), we can show that H has the crossover motion $H \times Z^0HZ^0$. That is, a H-line can use another H-line as a bridge from Z^0-thread

to Z^0-thread:

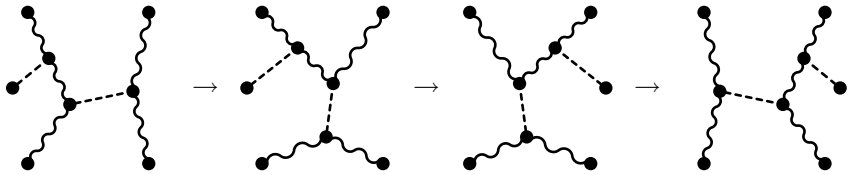

(6.20)

Note that $H \times WZ^0W$ and $H \times fZ^0W$ as well as $H \times fZ^0f$, $Z^0 \times fWf$, and $G \times qGq$, although valid motions with the effect of a crossover motion, are actually sequences of perpendicular motions. In contrast, the real crossover motions displayed above cannot be represented as sequences of perpendicular motions only.

Crossing Threads

The last two operations we shall need in order to discuss the structure of SM forests are concerned with the crossing of threads. Actually, we have seen such an operation at work in the discussion of crossover motions. To see this, take a look back at (6.18). In the first diagram, we recognize two W-threads, connected by a Z^0-line. The flip to the second diagram then breaks up both W-threads and reconnects them in a different way. In particular, if we take the arrows to indicate a direction along the threads, the tail of the first thread is joined onto the head of the second thread, and *vice versa*. We say that the two W-threads have been *crossed*.

To appreciate the significance of thread crossing, suppose the diagrams in (6.18) were contributions to the amplitude (or, rather, connected Green's function) for the process $W^+W^- \to W^+W^-Z^0$. In that case, beginning and end of the W threads are distinguished by the momenta of the external W bosons. Thread crossing then realizes the two possible ways of connecting the external W-lines into threads. As we shall see below, this generalizes to the case of more than two W-threads.

Thread crossing is also possible for two Z^0-threads connected by an H-line, which follows readily from (6.9e). In fact, since a Z^0-thread has no intrinsic direction, the broken up threads can be reconnected in all possible ways.

Absorbing Closed Threads

Thread crossing can be used to absorb a closed W-thread or Z^0-thread, i. e. a W-loop or Z^0-loop, into another W-thread or Z^0-thread, respectively. We list this case separately, because it is very important for the structure of the SM forests.

As an example, consider the case of a closed W-thread:

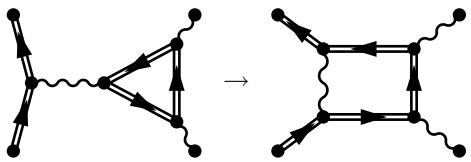

(6.21)

In an analogous way, closed Z^0-threads can be absorbed into into Z^0-threads. Note that the absorbing thread can be either an open thread or a closed thread.

The possibility of absorbing closed threads clearly shows that the number of W-loops and Z^0-loops is *not* invariant under gauge flips. Of course, the total number of loops remains fixed.

Elimination of H^4 Vertices

This gauge motion answers the question under which conditions a H^4 vertex can be expanded by a gauge flip. This is important, because the expansion of a H^4 vertex as a *four-point* subdiagram into a subdiagram with two H^3 vertices is *not* a gauge flip. Consequently, diagrams with different numbers of H^4 vertices would be candidates for separate invariant subsets, unless the five-point gauge flips can be used to perform this transformation indirectly.

This is, however, the case, as is apparent from (6.11) and (6.12). For definiteness, we consider the former five-point subdiagrams with two W bosons. We first use a five-point flip to replace the H^4 vertex by a $W^+W^-H^2$ vertex:

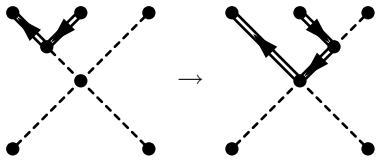

(6.22)

The $W^+W^-H^2$ vertex can then be expanded by a gauge flip of a four-point subdiagram:

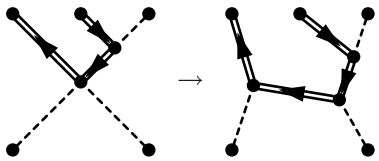

(6.23)

In the same way, the H^4 vertex can be expanded if the W-thread is replaced by a Z^0-thread. Thus, if a H^4 vertex is coupled to a W-thread or Z^0-thread, the three H-lines not connected to the thread can be absorbed onto the thread by a gauge motion.

Summary of Gauge Motions

Let us summarize the set of valid gauge motions, i. e. the possible transformations of Feynman diagrams achievable by sequences of gauge flips:

1. Elimination of *internal* H-lines, *except* for H-lines connecting two Z^0-threads.
2. The parallel motions $H \parallel Z^0$, $H \parallel W$, $Z^0 \parallel W$, $Z^0 \parallel f$, $\gamma \parallel W$, $\gamma \parallel f \neq \nu$, $G \parallel q$.
3. The perpendicular motions $Z^0 \perp fW$, $\gamma \perp fW$, $H \perp fW$, $H \perp fZ^0$, $H \perp Z^0W$, $G \perp qG$.
4. The crossover motions $Z^0 \times WZ^0W$, $Z^0 \times fZ^0W$, $\gamma \times WZ^0W$, $\gamma \times fZ^0W$, $H \times Z^0HZ^0$.

5. Thread crossing of two W-threads or two Z^0-threads.

6. Absorption of closed W-threads and Z^0-threads.

7. Elimination of H^4 vertices coupled to W-threads or Z^0-threads.

6.3.3 Pure Boson Forests

In this section, we shall analyze the structure of SM forests without fermions. Connected Green's functions without any fermionic contributions are of limited direct physical interest, because the initial and final states of high energy scattering processes usually contain many fermions. However, knowledge of the structure of the pure boson forests will prove indispensable for unraveling the structure of general forests.

Pure gluon forests have been discussed in 6.2. On the other hand, a pure boson forest involving EW bosons can never contain gluons, because color $SU(3)$ commutes with $SU(2) \times U(1)$, and hence gluons do not couple to EW bosons. Thus, we can ignore gluons in this section.

In the following, we leave the number L of loops of the diagrams in the forests implicit. A general SM forest is then characterized completely by the *external state* $\mathcal{E}$, i. e. the number and nature of the external lines. Given a particular external state $\mathcal{E}$, we shall denote the corresponding forest as $F(\mathcal{E})$. Note that we characterize all external lines by particle labels corresponding to *outgoing* particles. In the SM, this implies that the sum over the electromagnetic charges of the external particles vanishes.

We shall distinguish pure boson forests according to the number N_W of external W lines. Owing to charge conservation, this number must be a multiple of two. As we are going to demonstrate shortly, the number of neutral external boson lines is irrelevant for the determination of the structure of the forest. Therefore, we denote a purely bosonic external state with N_W external W-lines as $\mathcal{B}(N_W)$.

Diagrams With a Single Open W-Thread

We begin our discussion with the forest $F(\mathcal{B}(2))$ corresponding to external states containing exactly one W^+ and one W^- boson, and in addition an arbitrary number of neutral bosons. Because all interactions in the SM conserve the electromagnetic charge, diagrams in $F(\mathcal{B}(2))$ contain precisely one open W-thread, starting and terminating at two external vertices. We will now demonstrate that this W-thread is sufficient to make $F(\mathcal{B}(2))$ connected under gauge flips. That is, $F(\mathcal{B}(2))$ always consists of a single grove.

To prove this, we adopt a strategy similar to the one we used when we proved the connectedness of subsets of the forest in unflavored ϕ-theory. In particular, we first restrict our attention to the subset $F_3(\mathcal{B}(2))$ of diagrams without a quartic vertex. Next, we shall designate a subset T_3 of $F_3(\mathcal{B}(2))$, connected under gauge flips, with a canonical topology. Connectedness of $F_3(\mathcal{B}(2))$ then follows if we can show that every diagram in $F_3(\mathcal{B}(2))$ can be transformed into a diagram in T_3 by means of gauge motions.

To be specific, we choose the diagrams in T_3 to have the following topology:

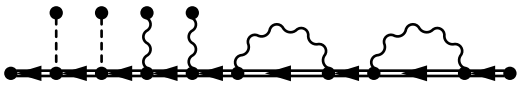

(6.24)

Of course, the numbers of self-energy loops and external lines are not restricted to the values displayed in this example. Rather, the number of self-energy loops should equal L, while the numbers of neutral external bosons are arbitrary.

It should be obvious that all diagrams with this topology are connected by gauge motions. Indeed, the external lines can be permuted arbitrarily through the parallel motions $H \parallel W$, $Z^0 \parallel W$, and $\gamma \parallel W$. Therefore, T_3 is connected.

Now consider an arbitrary diagram d in $F_3(\mathcal{B}(2))$:

$d \;=$ 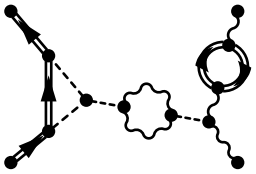

(6.25)

We first replace each internal photon line by a Z^0-line (which just means that we interpret any internal wavy line as a Z^0-line) and eliminate as much internal H-lines in d as possible:

$d \;\rightarrow$ 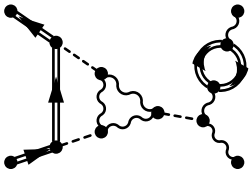

$\rightarrow$ 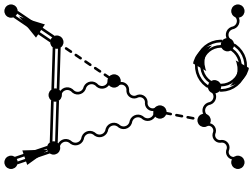 $\rightarrow$ 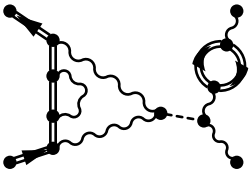

(6.26)

The only internal H-lines left must then necessarily connect two Z^0-threads. Some of these Z^0-threads may be closed ones, which we absorb into an open thread.[4] We would now like to eliminate the remaining internal H-lines, which by now interconnect open Z^0-threads. These Z^0-threads must be coupled to a W-thread with at least one end. Since H-lines can be moved parallel to Z^0-threads and perpendicular from Z^0-threads onto W-threads, we can move all remaining H-lines onto W-threads:

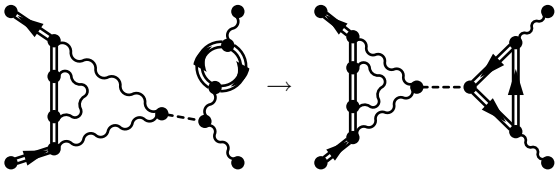

(6.27)

[4]Note that there must be at least one open Z^0-thread, for else any closed Z^0-loops would have to be connected to the W-thread through a H-line. But in this case, the closed Z^0-thread would have been broken up already in the elimination of the connecting H-line. (Cf. (6.13))

The H-lines can now be eliminated again using the gauge flip (6.13). At this point, d has been transformed, using gauge motions, into a diagram d' without internal H-lines:

$d' \;\rightarrow$ 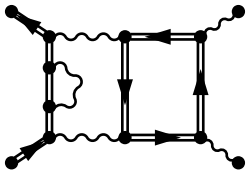 (6.28)

d' must then necessarily consist of one open and an unspecified number of closed W-threads, interconnected by Z^0-*lines*. That is, there can be no Z^0-thread consisting of more than a single Z^0-line. But then all closed W-threads can be absorbed into the single open W-thread by means of thread crossing:

$d' \;\rightarrow$ 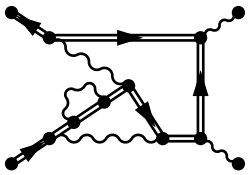 (6.29)

The resulting diagram is easily transformed into a diagram of the form (6.24) by parallel motions along the W-thread. Therefore, $F_3(\mathcal{B}(2))$ is connected under gauge flips.

For this to imply that the complete forest $F(\mathcal{B}(2))$, including diagrams with quartic vertices, is connected under gauge flips, we yet have to demonstrate that every diagram in $F(\mathcal{B}(2))$ can be transformed into a diagram in $F_3(\mathcal{B}(2))$ using gauge flips. This is readily seen to be true for diagrams without a H^4 vertex, because all other quartic vertices involve gauge bosons, and hence their expansion is always a gauge flip. Thus, the only potential obstacle is provided by diagrams with H^4 vertices. However, according to the gauge motion 7, these can be absorbed into the W-thread, thereby replacing the H^4 vertex by two cubic vertices. This means that every diagram in $F(\mathcal{B}(2))$ can be transformed into a diagram in $F_3(\mathcal{B}(2))$ using gauge motions, as was to be shown.

Diagrams With Several Open W-Threads

We now consider the forests $F(\mathcal{B}(N_W))$ for $N_W > 2$, which means that there are several open W-threads present. We claim that these forests are also connected under gauge flips.

The treatment of this case is very similar to the case of a single open W-thread. Indeed, given a diagram in $F_3(\mathcal{B}(N_W))$, we can eliminate all internal H-lines and closed Z^0-threads exactly as before. We then have a diagram with $N_W/2$ open W-threads and any number of closed W-threads, interconnected by Z^0-lines. The closed W-threads are absorbed into open ones, no matter which. This leaves us with a diagram consisting of just $N_W/2$ W-threads,

interconnected by Z^0-lines:

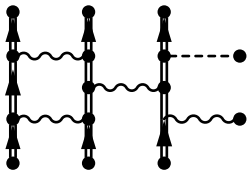

(6.30)

Evidently, through crossover motions we can transform this diagram into the form:

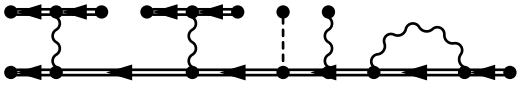

(6.31)

Let T_3 be the subset of $F_3(\mathcal{B}(N_W))$ containing only diagrams of the above topology. Our proof is complete if we can show that T_3 is connected under gauge flips. Now remember that the various external W-lines actually carry momentum labels. Therefore, we need to demonstrate that we can perform arbitrary permutations of the momenta of the W^+-lines *or* the W^--lines using gauge flips. For definiteness, we choose to permute the W-lines with the outgoing arrow.

To permute two external W-lines with momenta p_1 and p_2, we have to make sure that the following flip can be performed:

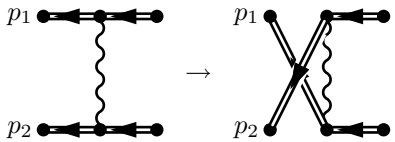

(6.32)

Clearly, we can arrange for this flip for any pair of external W-lines by using parallel motions and crossover motions. Therefore, $F_3(\mathcal{B}(N_W))$ is connected under gauge flips. The connectedness of $F(\mathcal{B}(N_W))$ then follows by the same arguments as used in the discussion of $F(\mathcal{B}(2))$.

Diagrams without an Open W-Thread

We have seen that pure boson forests of diagrams with a nonzero number of open W-threads always consist of a single grove. For diagrams without an open W-thread, the situation is different. This can readily be seen by recalling that we used an open W-thread to absorb all closed W-threads. If there is no open W-thread, we can eliminate at most all but one closed W-thread. This is because, while several W-threads can be merged and joined, the last W-thread, open or closed, cannot be destroyed. Nor can a W-thread be created by a gauge flip in a diagram where no W-thread was present before. Therefore, a pure boson forest $F(\mathcal{B}(0))$ of diagrams without external W lines may consist of more than one grove.

Independent of the precise nature of the neutral bosons in the external state, there is always a subset of diagrams with at least one closed W-thread, except at tree level. Therefore, let us assume that the number L of loops is nonzero. Omitting diagrams with a quartic vertex, we obtain the subset C_3. We can make use of the results for the forests with a nonzero number of open W-threads in the following way. Given a diagram d in C_3, pick one of the closed W-threads. By

cutting a W-line, we obtain a diagram d' with a single open W-thread. But these are connected. Therefore, C_3 is connected, too. As before the connectedness of all diagrams in $F(\mathcal{B}(0))$ with at least one W-thread (including those with quartic vertices), follows from this result.

Next, consider the case where the external state contains a nonzero (even) number N_{Z} of Z^0 bosons. The subset of $F(\mathcal{B}(0))$ of diagrams without any W-thread then consists of diagrams with $N_{\mathrm{Z}}/2$ open and an arbitrary number of closed Z^0-threads. Denote by N_3 the restriction of this subset to diagrams without quartic vertices. Note that diagrams in N_3 cannot contain a photon line, because photons do not couple to neutral bosons. On the other hand, N_3 is non-empty even at tree level. We claim that N_3 is connected under gauge flips. To see this, choose an arbitrary diagram d in N_3. We first eliminate as many internal H-lines as possible. Afterwards, we absorb all closed Z^0-threads into an open Z^0-thread. This leaves us with a diagram d' consisting of open Z^0-threads, interconnected by H-lines:

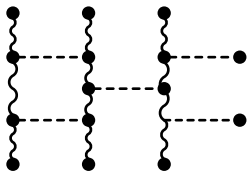

(6.33)

Since H-lines can be moved parallel along Z^0-threads and crossover from one Z^0-thread onto another, all diagrams in N_3 can be transformed into the following topology:

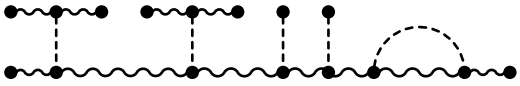

(6.34)

By an argument similar to the one given below (6.31), arbitrary permutations of external Z^0-lines can be performed by crossing Z^0-threads. Therefore, diagrams of the form (6.34) are connected, hence N_3 is connected, which in turn implies that, for nonzero N_{Z}, all diagrams in $F_3(\mathcal{B}(0))$ without a W-thread are connected. Again, this implies that the subset of diagrams without a W-thread of the complete forest $F(\mathcal{B}(0))$ is connected, because all quartic vertices can be replaced by two cubic vertices through gauge motions, where H^4 vertices are absorbed into some Z^0-thread.

This leaves us with an external state consisting of H bosons only. The subset of diagrams with at least one (closed) W-thread is connected by the same arguments as before. Next, consider the subset of diagrams without W-thread, but with at least one (closed) Z^0-thread (which, of course, requires a nonzero number of loops). By arguments similar to the case of diagrams with one or more closed W-threads, this subset is connected under gauge flips. The remaining diagrams contain neither a W-thread nor a Z^0-thread, which, in the present context of pure boson forest, means that they contain H bosons only. Every such diagram is trivially gauge invariant, because it does not depend on unphysical degrees of freedom in any way.

Summary of the Structure of Pure Boson Forests

We collect the results about the pure boson forests $F(\mathcal{B}(N_W))$ with N_W open W-threads in a theorem. To make our notation more concise, we shall refer to a diagram with at least one W-thread as a *charged diagram*, and to a diagram without a W-thread as a *neutral diagram*. Correspondingly, the terms *charged grove* and *neutral grove* are used to denote a grove containing only charged and only neutral diagrams, respectively.[5] The theorem about the pure boson forest can then be stated as follows:

Theorem 6.1

1. *A pure boson forest with external W bosons consists of a single grove.*
2. *A pure boson forest with external photons consists of a single grove.*
3. *A pure boson forest with an external state consisting solely of neutral bosons, at least one of which is a Z^0 boson, decomposes into*
   (a) *a grove containing all charged diagrams;*
   (b) *a grove containing all neutral diagrams.*
4. *A pure boson forest with an external state consisting solely of H bosons decomposes into*
   (a) *a grove containing all charged diagrams;*
   (b) *a grove containing all neutral diagrams with at least a single Z^0-loop;*
   (c) *a separate grove for each diagram without gauge boson lines.*

6.3.4 General SM Forests

In this section, we investigate the structure of SM forests with *massive* fermions. Massless fermions will be discussed later on an explicit example.

As mentioned before, the STIs in gauge theories apply separately to diagrams with a fixed number of fermion loops.[25] In the present context, this can easily be seen by inspection of the gauge flips involving fermion lines, (6.10) and (6.2). Indeed, none of these flips can create or destroy a fermion loop. It is then clear that the groves of a general SM forest respect this structure. This can also be seen from the fact that, in principle, arbitrarily many fermion dublets can be added to the SM Lagrangian without violating gauge invariance. Therefore, if we increase the number of fermion loops by one, can always imagine that the additional fermion loop belongs to a new, distinct flavor. Consequently, the diagrams with an additional fermion loop must be separately gauge invariant.

Let us denote by $F(\mathcal{E}, \lambda)$ the subset of a general SM forest with external state $\mathcal{E}$ and λ fermion loops. We will refer to $F(\mathcal{E}, \lambda)$ as a *subforest*. The total number L of loops is left implicit. (Of course, $\lambda \leq L$.) More specifically, we denote by $\mathcal{E}(N_f)$ an external state containing N_f fermion lines, where, owing to fermion number conservation, N_f must be a multiple of two.

Like for the pure boson forest discussed in the last section, a subset S of $F(\mathcal{E}, \lambda)$ is connected under gauge flips if and only if the subset S_3 of diagrams

[5] This terminology for groves is justified, because, as we shall see, a grove can never contain both charged and neutral diagrams.

in S without a quartic vertex is connected. Therefore, we shall infer the decomposition of $F(\mathcal{E}, \lambda)$ from the subset of diagrams without a quartic vertex. To keep our notation compact, we shall not, however, introduce an extra notation for this subset. It should then be implicitely understood that only diagrams without a quartic vertex are to be considered.

In order to put the results of the last section to use in the investigation of SM forests with fermions, we shall proceed according to the following general strategy. We will try to move as many boson lines as possible perpendicular from the fermion threads onto boson threads. Clearly, if *all* boson lines except a single one can be stripped off the fermion lines, the remaining gauge motions are just those of pure boson forests, for which the above results can be applied.

Note that, since diagrams without gauge bosons (including Goldstone bosons) are trivially gauge invariant, every such diagram forms a separate grove. We will mention these trivial groves briefly when they can occur. Our main focus is, however, on diagrams with at least one gauge boson line, where the cancellation of unphysical degrees of freedom is essential to ensure the consistency of the theory.

Diagrams With a Single Open Fermion Thread

We begin by analyzing $F(\mathcal{E}(2), 0)$, i. e. the subforest of diagrams with a single open fermion thread and no closed fermion thread. Of course, $\mathcal{E}(2)$ can contain an arbitrary number of SM bosons. However, as long as the precise nature of the additional external bosons does not matter, we will leave this part of the external state implicit.

For simplicity, we will consider external states $\mathcal{E}(2)$ without gluons at first. To begin with, we want to show that, in a charged diagram, all boson lines but one can be stripped off the fermion thread. To this end, we focus on the bosons coupled to the fermion thread. Assuming that at least one W-thread is coupled to the fermion line, the structure of the fermion thread looks as follows:

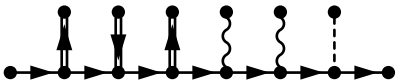

(6.35)

Of course, the number of boson lines is arbitrary, except that, ignoring neutral bosons, W^+ and W^--lines must be alternating, with at most one excess W^+ or W^--line. The reason is that we have restricted ourselves to fermions in the dublet representation of $SU(2)$. In other representations, more general distributions of the W-lines would be possible.

Note that some of the displayed boson lines may couple to the same vertex, or may even coincide. Also, photons cannot always be brought into the displayed order, because neutrino lines may inhibit their parallel motion along the fermion thread. For the moment, we treat photons and Z^0 bosons on the same footing. This will be justified below.

Now, we first move all neutral bosons onto a single W-thread:

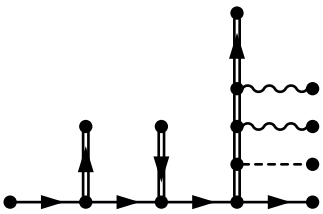

(6.36)

If, unlike in the present example, there is only a single W-thread coupled to the fermion thread, we have accomplished our goal. Else, we join the remaining W-threads in pairs, using the gauge flip (6.10a):

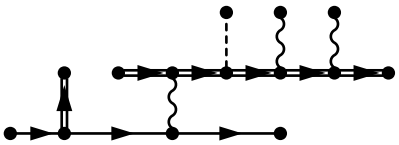

(6.37)

Note that we have chosen to join the W-thread with the attached neutral bosons, because this works also if no additional W-thread is coupled to the fermion thread. At this point, at most a single W-thread is coupled directly to the fermion thread. In addition, there are one or more W-threads coupled to the fermion thread by a single Z^0-line. If, as in the present example, there is a single W-thread coupled to the fermion thread left, we move all Z^0-lines onto this thread by means of the perpendicular motion $Z^0 \perp fW$:

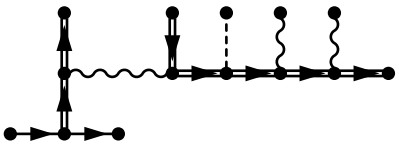

(6.38)

On the other hand, if there is no W-thread coupled to the fermion line, we can employ the crossover motion $Z^0 \times fZ^0W$ to move all but one Z^0-line onto some W-thread:

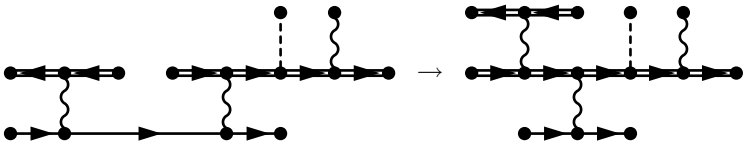

(6.39)

Thus, if at least one W-thread is coupled directly to the fermion thread, all but one boson can be stripped of the fermion thread by gauge motions.

The same is true, if the diagram d contains a W-thread, which is not coupled directly to the fermion thread. To see this, recall that any diagram in a pure boson forest with at least one W-thread can be brought into the form (6.24). Now, if we remove the fermion thread in d, the diagram will be partitioned into

several disconnected pure boson subdiagrams:

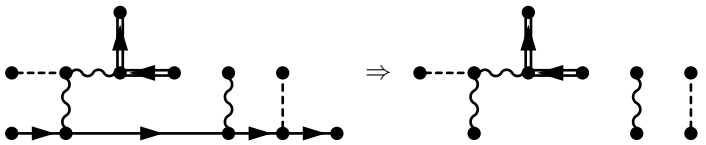

(6.40)

One of these subdiagrams must contain the W-thread, and therefore can be transformed into the form (6.24):

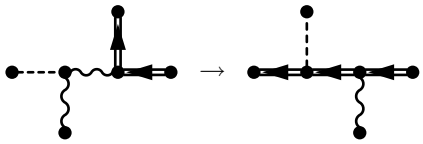

(6.41)

Evidently, this means that, if we reintroduce the fermion thread again, the W-thread is connected to the fermion thread by a single Z^0-line:

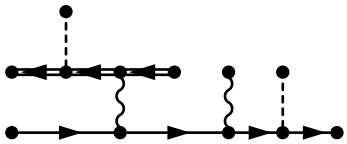

(6.42)

This Z^0-line can be used as a bridge to move all other neutral bosons from the fermion thread onto the W-thread:

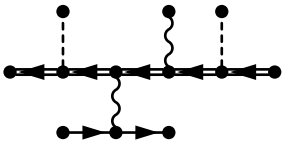

(6.43)

We conclude that the presence of a single W-thread in a diagram of $F(\mathcal{E}(2), 0)$ is sufficient to strip off all but one boson from the fermion thread.

If we now remove the fermion thread, we obtain a diagram in the pure boson forest $F(\mathcal{B}(N_W))$, where N_W is determined by the number of external W bosons present in the original external state $\mathcal{E}(2)$ and, in addition, by the flavors f_1 and f_2 of the two external fermions. In particular, if the sum of the eletromagnetic charges of f_1 and f_2 is nonzero, the stripping of the fermion thread will leave a W boson as last boson, as in (6.38). On the other hand, if the sum of charges is zero, the last boson will be a Z^0 boson, as in (6.43). We say that the fermion pair (f_1, f_2) is *charged* or *neutral*, respectively.

For a given original external state $\mathcal{E}(2)$, then, the external state $\mathcal{B}(N_W)$ obtained by removing the fermion thread is uniquely determined. Therefore, $F(\mathcal{E}(2), 0)$ is connected if $F(\mathcal{B}(N_W))$ is. According to theorem 6.1, this is true for $N_W > 0$. For $N_W = 0$, $F(\mathcal{B}(0))$ decomposes into the two groves of diagrams with and without W-threads. Therefore, the charged diagrams in $F(\mathcal{E}(2), 0)$ are always connected.

At this point, a word must be said about photons and neutrinos. In the foregoing discussion, we have implicitely assumed that neutral gauge bosons can

be moved arbitrarily parallel to the fermion thread. Obviously, for photons this is impossible if the fermion thread contains neutrino lines. We must make sure that this cannot invalidate our arguments. Now, if the fermion thread is actually a pure neutrino thread, a photon could not have been coupled to the fermion thread in the first place. On the other hand, if the fermion thread contains neutrino lines as well as charged lepton lines, there must be W-lines coupled to the fermion thread whenever a charged lepton line meets with a neutrino line. Since the photons on the fermion thread must be coupled to charged lepton lines, this implies that photons can always be moved perpendicular from the fermion thread onto some W-thread.

We turn now to the discussion of neutral diagrams in $F(\mathcal{E}(2), 0)$. In this case, to avoid ambiguities, it is advantageous to distinguish clearly between photons and Z^0 bosons. Therefore, we shall now use a zigzag line to represent the latter, as indicated in (6.8).

The treatment of photons is actually very simple: Since photons do not interact with neutral bosons, they can at most be moved parallel along the fermion thread. In fact, because neutral current interactions cannot change flavor in the SM, photons either cannot couple to the fermion thread at all, if it is a neutrino thread, or else can be moved arbitrarily parallel to the fermion thread. Also, recall that, for the determination of groves, we replace *internal* photon lines by Z^0-lines anyway.

Let us, then, consider a diagram in $F(\mathcal{E}(2), 0)$, containing, apart from the fermion thread, only Z^0-lines and H-lines. (Remember that we assume that at least one Z^0-line is present.) We can take over essentially all results from the foregoing discussion of diagrams with W-threads. For, if we substitute Z^0 for W and H for Z^0, then all motions required to remove W and Z^0-lines from the fermion thread are now valid motions to remove Z^0-lines and H-lines from the fermion thread. Thus, if there is an odd number of Z^0-threads coupled to the fermion thread (plus an arbitrary number of H-lines), the diagram can be brought into the form corresponding to (6.38):

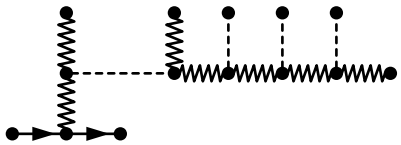

(6.44)

On the other hand, a diagram with an even number of Z^0-threads coupled to the fermion thread can be transformed into the equivalent of the second diagram in (6.39):

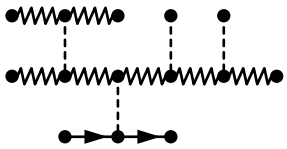

(6.45)

We emphasize again that this is only possible for massive fermions, because else the H-line cannot be coupled to the fermion thread.

In either case, by removing the fermion thread, we get a diagram with at least one Z^0-thread in the pure boson forest $F(\mathcal{B}(0)$. Observe that the external state $\mathcal{B}(0)$ is uniquely determined by the number of Z^0-lines coupled to the

fermion thread in the original diagram: for an odd number, the last boson is a Z^0 boson, as in (6.44); for an even number, the last boson is a H boson, as in (6.45).

However, we emphasize that, in contrast to the case of diagrams with a W-thread, the external state $\mathcal{B}(0)$ is *not* uniquely determined by the fermion flavors f and $\bar{f}$ in the external state $\mathcal{E}(2)$. For both Z^0 bosons and H bosons are neutral and hence can be coupled to a neutral fermion thread in arbitrary numbers. On the other hand, the external state $\mathcal{B}(0)$ *is* uniquely determined by the *bosons* in $\mathcal{E}(2)$. To see this, observe that the Z^0-H interactions conserve the Z^0-number. Therefore, if $\mathcal{E}(2)$ contains an odd number of Z^0 bosons, the fermion thread must contain an odd number of couplings to Z^0 bosons. These observations will be very important for the structure of a subset of of diagrams with more than one fermion thread.

In any event, the neutral pure boson diagrams in $F(\mathcal{B}(0))$ form a grove, according to theorem 6.1. Hence, the neutral diagrams in $F(\mathcal{E}(2), 0)$ are connected under gauge flips, too. Thus, for an SM subforest with a single open fermion thread and no closed fermion thread, we get essentially the same decomposition as for the pure boson forests, if the external state $\mathcal{E}(2)$ does not contain gluons.

Finally, we have to consider gluons in the external state $\mathcal{E}(2)$, which requires the fermion thread to be a quark thread. Because gluons can be moved arbitrarily parallel to a quark thread, we can clearly arrange the boson and gluon lines coupled to the fermion thread so that the gluons are to the right of all bosons:

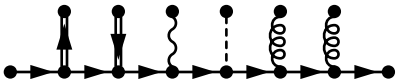

(6.46)

The gluons can then successively be moved perpendicular onto a single gluon line, while the EW bosons are treated as discussed above. If the quark thread is removed, we obtain a uniquely determined SM pure boson forest plus a pure gluon forest. Both forests are separately connected under gauge flips according to theorem 6.1 and the discussion QCD in section 6.2. Consequently, the structure of the forest $F(\mathcal{E}(2), 0)$ is determined by the gauge flips of EW bosons alone.

We summarize our results in the next theorem:

Theorem 6.2 *Consider the subforest $F(\mathcal{E}(2), 0)$ of diagrams with two external fermions and without a closed fermion loop.*

1. *If the fermion pair in the external state $\mathcal{E}(2)$ is* charged*, or if $\mathcal{E}(2)$ contains W bosons, $F(\mathcal{E}(2), 0)$ forms a single grove.*

2. *If the fermion pair in the external state $\mathcal{E}(2)$ is* neutral*, and if all bosons in $\mathcal{E}(2)$ are neutral, $F(\mathcal{E}(2), 0)$ decomposes into*

   (a) *a grove containing all charged diagrams;*

   (b) *a grove containing all neutral diagrams.*

Diagrams With a Single Closed Fermion Thread

Having discussed diagrams with a single open fermion thread, it is natural to consider diagrams with a single closed fermion thread next, i. e. the subforest

$F(\mathcal{E}(0), 1)$. An external state $\mathcal{E}(0)$ without fermions is actually equal to a pure boson external state $\mathcal{B}$. Thus, we are now taking into account the contributions of diagrams with a single fermion loop to the pure boson forest $F(\mathcal{B})$.

Evidently, the treatment of diagrams with a closed fermion thread is quite similar to the treatment of diagrams with an open fermion thread. Indeed, we made essentially no use of the fact that the fermion thread was open in the discussion of $F(\mathcal{E}(2), 0)$, except that a charged fermion thread must be open. On the other hand, for a neutral open fermion thread, nothing prevents us from connecting the end of the thread to the start, thus forming a closed thread.

Observe, that when all but one boson are stripped of a closed neutral fermion thread, the resulting diagram contains a one-loop tadpole diagram contributing to the one-point function of some neutral boson:

(6.47)

Such a tadpole diagram is zero by Lorentz invariance for the neutral gauge bosons, i. e. photon and Z^0, because the corresponding integral would, if nonzero, define a preferred four-momentum:

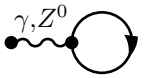

$= 0$ (6.48)

However, the Goldstone boson and H tadpole diagrams are generally nonzero for massive fermions. In fact they are proportional to the fermion masses. Therefore, we can really take over all arguments from the case of a closed fermion thread and obtain the following result:

Theorem 6.3 *Consider the subforest $F(\mathcal{E}(0), 1)$ of diagrams without external fermions and with a single closed fermion loop. $F(\mathcal{E}(0), 1)$ decomposes into*

1. *a grove containing all charged diagrams;*
2. *a grove containing all neutral diagrams.*

General SM Diagrams

We are now in a position to study general SM forests, i. e. diagrams with an arbitrary number of fermion threads, open or closed. As we have seen above, closed fermion threads can be treated in the same way as open ones. Therefore, it suffices to consider diagrams with a fixed number of fermion threads. Since no gauge flip can change the number of fermion threads, this is automatically compatible with gauge invariance.

Denote by $F(\mathcal{E}, \tau)$ a forest of diagrams with τ fermion threads and an external state $\mathcal{E}$, which is only subject to the constraint that it must not contain more than 2τ fermions. The τ fermion threads can be assumed to belong mutually distinct fermion *dublets*. For, if some fermion threads belong to identical dublets, the complete forest will decompose into invariant subsets related to each other by permutations of fermion threads and crossing symmetry.

For instance, take $F(\mathcal{E}, 3)$ to be the forest of diagrams without fermion loop for the SM process $e^+e^- \to e^+e^-\mu^+\mu^-$ at one-loop level. For every diagram

d_1 contributing to this process, there is a second diagram d_2 related to d_1 by a permutation of external electron lines, i. e. by crossing symmetry. *A priori* both d_1 and d_2 might belong to a single grove of the forest for this process. However, the e^+-e^- pair in the final state could have been replaced by a quark-antiquark pair without violating gauge invariance, in which case no permutation of external lines would be possible. Consequently, d_1 and d_2 must belong to different groves S_1 and S_2, related to each other by crossing symmetry.

Given that all fermion threads belong to distinct fermion dublets, our strategy for determining the structure of the subforest $F(\tau)$ will be as follows: Leaving QCD couplings aside, we first consider external states $\mathcal{E}$ without photons. For such external states, we can remove all but one boson from every fermion thread. This should be clear, because we just have to treat each fermion thread in turn like we did above. Removing afterwards the trivial fermion threads will give us a diagram from a pure boson forest $F(\mathcal{B})$ with a bosonic external state $\mathcal{B}$. The structure of $F(\tau)$ then follows from the structure of the pure boson forest, which, according to theorem 6.1, is characterized by the bosonic external state $\mathcal{B}$. Once we have derived the structure of the forest for an external state $\mathcal{E}$ without photons, the effects of adding the latter gauge bosons can easily be determined.

Consider, then, an external state $\mathcal{E}$ without photons. If $\mathcal{E}$ contains W bosons or charged external fermion pairs, the last boson kept at each fermion thread is uniquely determined, if we demand that the last boson at all neutral fermion threads be a Z^0 (or ϕ^0, for closed fermion threads). This is true because these diagrams contain open W-threads, to which all neutral bosons can eventually be attached. But a H-line coupled to a W-thread can always be eliminated in favor of a Z^0-line or ϕ^0-line. Consequently, the external state $\mathcal{B}$ of the pure boson forest obtained by removing the stripped fermion threads is uniquely determined and contains external W bosons. According to theorem 6.1, $F(\mathcal{B})$ is connected in this case. Therefore, $F(\mathcal{E},\tau)$ is connected, too. The same is true if photons are added to the original external state $\mathcal{E}$, because these can always be moved onto some W-thread. Thus, adding external photons just changes the purely bosonic external state $\mathcal{B}$.

If no W bosons or charged fermion pairs are present in the original external state $\mathcal{E}$, the forest $F(\mathcal{E},\tau)$ decomposes into the invariant subsets containing charged and neutral diagrams, respectively. The subset of charged diagrams is, in fact, a grove, which follows again from the uniqueness of the purely bosonic external state $\mathcal{B}$ obtained by first stripping and then removing all fermion threads. Theorem 6.1 then ensures the connectedness of the charged diagrams. Again, photons can be added to $\mathcal{E}$ without invalidating this result, because they may be attached to a W-thread.

Thus, independent of the external state $\mathcal{E}$, the charged diagrams in $F(\mathcal{E},\tau)$ always form a single grove.

We turn now to the discussion of neutral diagrams. Of course, for these to exist, the external state $\mathcal{E}$ must not contain charged bosons or fermion pairs. This will be implicitely understood in the sequel. Because, even with these constraints, there are still charged diagrams in $F(\mathcal{E},\tau)$, we denote the subset of neutral diagrams as $F_0(\mathcal{E},\tau)$.

Let $\mathcal{E}$ again denote an external state without photons. For each diagram in $F_0(\mathcal{E},\tau)$, we can remove all but one boson from open fermion threads. Once we have done this, removing the open fermion threads gives us a purely bosonic

external state $\mathcal{B}$ containing H and Z^0 bosons only. This time, however, $\mathcal{B}$ is *not* uniquely determined. To see this, observe that, since all fermion threads in diagrams of $F_0(\mathcal{E},\tau)$ are neutral, the last boson at each fermion thread must be either a H or a Z^0 (or ϕ^0). However, in a neutral diagram there is no way to replace a H-line by a Z^0-line.

Indeed, in a neutral diagram, an internal H-line must either connect two fermion threads or else be coupled to at least one HZ^0Z^0 or HHH-vertex. In the latter case, the absence of a HHZ^0 or a $Z^0Z^0Z^0$-vertex in the SM forbids the replacement of a H-line. In the former case, a replacement would in principle be possible. It is, however, not a gauge motion, because the exchange of H-line and Z^0-line in a four-point subdiagram with four fermion lines is *not* a gauge flip:

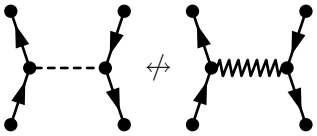

(6.49)

Therefore, different ways of choosing the last boson at each fermion thread, corresponding to different pure boson external states $\mathcal{B}$ obtained by stripping and removing the fermion threads, lead to separate groves. Thus, in order to determine the groves of $F_0(\mathcal{E},\tau)$, we must determine all possible pure boson external states $\mathcal{B}$.

For instance, consider $F_0(\mathcal{E},3)$ for an external state $\mathcal{E}$ containing three distinct neutral fermion pairs at the one-loop order. A specific example is provided by the SM process $e^+e^- \to e^+e^-\mu^+\mu^-$ described above. In this case, we have to take into account all pure boson external states $\mathcal{B}$ consisting of three neutral bosons, each either a Z^0 or a H. Because the Z^0-H interactions conserve the Z^0 number, $\mathcal{B}$ must contain either zero or two Z^0 bosons. For the latter possibility, there are three choices, characterized by specifying the fermion threads to which the Z^0-lines are attached. We illustrate this by displaying one representative diagram for each choice of external state:

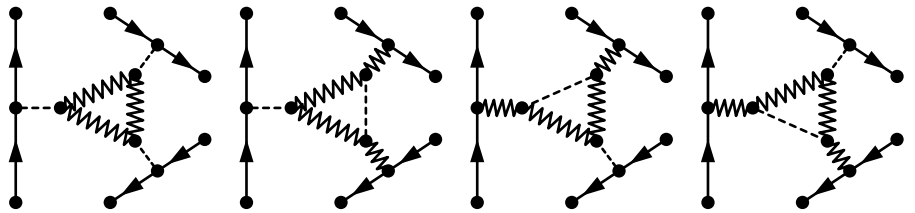

(6.50)

Evidently, the four choices of external state $\mathcal{B}$ are independent of the number of loops, as long as we do not introduce a fermion loop (which would be equivalent to changing τ). This is true because, according to 6.1, the neutral pure boson groves are uniquely determined by the external state $\mathcal{B}$ for any number of loops.

It is also easy to extend the original external state $\mathcal{E}$ by adding H bosons or *pairs* of Z^0 bosons, because these can always be attached to one of the Z^0-threads already present in the pure boson part of the diagram. The groves would then still be characterized by the four choices of last boson at the three fermion threads. On the other hand, if we wanted to add just a single Z^0 boson to the external state $\mathcal{E}$, we would have to choose an odd number of fermion threads for which the last boson is a Z^0.

In any event, the foregoing discussion shows that in $F_0(\mathcal{E},\tau)$ there are generally several independent choices of last boson at the τ fermion threads. Each choice leads to a different pure boson external state $\mathcal{B}$ and hence to a separate grove. Alternatively, because the number modulo two of Z^0 bosons at a fermion thread is determined uniquely by the choice of last boson, we can characterize the groves of $F_0(\mathcal{E},\tau)$ by these numbers. This will be illustrated further when we discuss an explicit example later.

We summarize what we have learned about the subforest $F_0(\mathcal{E},\tau)$ of neutral diagrams without external photons in a lemma:

Lemma 6.1 *The forest $F_0(\mathcal{E},\tau)$ of neutral diagrams with τ fermion threads decomposes into one grove for every independent choice of last boson at the τ fermion threads. If the number of external Z^0 bosons is even or odd, these choices correspond to all possible ways of selecting an even or odd number of fermion threads, respectively, for which the last boson is a Z^0.*

Adding external photons will in general lead to a further decomposition of $F_0(\mathcal{E},\tau)$. To see this, observe that, while photons can be moved parallel to a fermion thread, it is impossible to remove a photon from a fermion thread in a diagram containing only neutral bosons through gauge motions, simply because there is no charged boson to which the photon could be attached. This means that we cannot transfer photons from one fermion thread to another by gauge flips.

Therefore, if photons are added to the external state $\mathcal{E}$, the groves described in the lemma will decompose further into one grove for every independent way of distributing the photons over the fermion threads.

As a simple example, consider the process $e^+e^- \to \mu^+\mu^-\gamma$ at tree level. Ignoring the photon, there are two choices of last boson at the fermion threads, corresponding to Z^0-exchange or H-exchange. For both choices, we can attach the photon to the electron line or the muon line. Consequently, the forest for this process decomposes into four groves:

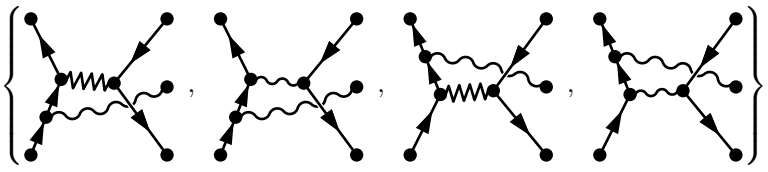

(6.51)

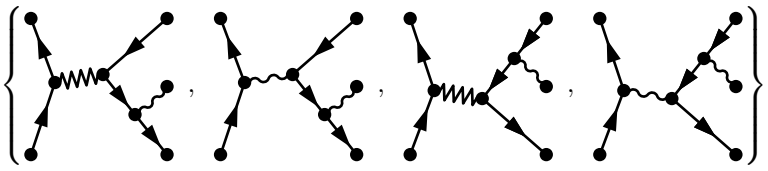

(6.52)

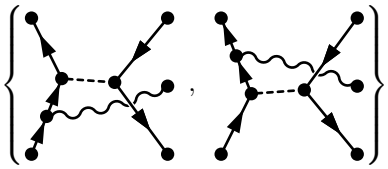

(6.53)

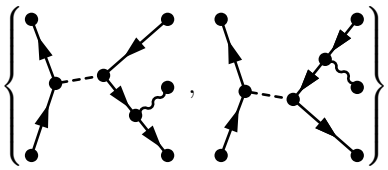

(6.54)

We emphasize that, if we replace the external photon by a Z^0 boson, the forest consists of just *two* groves, corresponding to choosing the last boson at the electron line as a Z^0 or H boson:

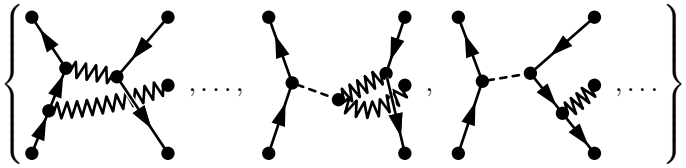

(6.55)

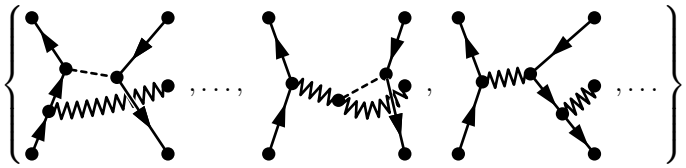

(6.56)

Here, the omission dots represent the diagrams obtained from the preceding one by replacing the intermediate Z^0-line by a photon line and permuting the external Z^0-line along the fermion thread.[6]

We have now nearly completed the decomposition of the subforest $F(\mathcal{E}, \tau)$ (neglecting QCD contributions). The only missing piece in the puzzle concerns the counting of fermion loops. To this end, let λ denote the number of *closed* fermion threads, i. e. fermion loops. Recall that we proposed above to distinguish fermion threads according to *dublets*, not dublet *components*. For closed fermion threads in neutral diagrams, (to which only neutral bosons are coupled) this gives us in general a choice between two possible dublet components (unless photons and neutrinos are involved). Therefore, if fermion threads are distinguished according to dublets, we shall generally have 2^λ copies of every *neutral* grove, identical except for the exchange of dublet components in some of the closed fermion threads.

On the other hand, the closed fermion threads in charged diagrams will always link both components of a dublet. This is so because we can always use gauge motions to couple the fermion thread to some W-thread by a single neutral boson and then use the gauge flip (6.10a) to break up the W-thread and couple both open ends to the closed fermion thread:

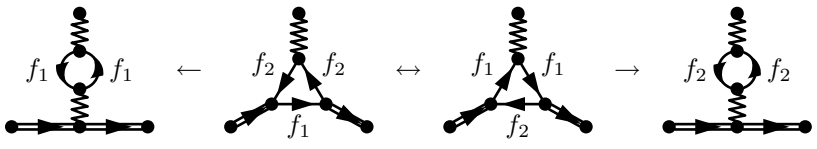

(6.57)

[6] It should be noted that, if the fermion-Higgs couplings are neglected, i. e. if fermions are treated as massless, there will be two identical groves (up to the exchange of external photon and Z^0) in both cases. However, we defer the treatment of massless fermions to a separate section.

Evidently, in the presence of a charged thread, the contributions of the two dublet components in neutral closed fermions are linked by gauge flips.

We summarize the structure of the subforest $F(\mathcal{E},\tau)$ in the following theorem:

Theorem 6.4 *Consider the subforest $F(\mathcal{E},\tau)$ of diagrams with λ closed fermion loops and $\tau-\lambda$ external fermion lines, all belonging to mutually distinct dublets.*

1. *All charged diagrams in $F(\mathcal{E},\tau)$ form a single grove.*
2. *The neutral diagrams in $F(\mathcal{E},\tau)$ decompose further into groves characterized by*
   (a) *a choice of last boson between Z^0 and H for each of the τ fermion thread according to lemma 6.1;*
   (b) *a choice of distributing the external photons in $\mathcal{E}$ over the τ fermion threads;*
   (c) *one of 2^λ choices of dublet component in the λ closed fermion threads.*

This completes our analysis of general SM forests without QCD contributions. We shall not give a detailed analysis of QCD contributions. Apart from the simplest cases, the combinatorics quickly becomes too complicated to provide a useful yet complete general description of SM forests in the presence of QCD couplings. Rather, we shall comment briefly on the principal criteria, which govern the decomposition into groves in this case. In the next section, we will then demonstrate in detail the decomposition of a forest with QCD contributions on a concrete example.

For the analysis of QCD contributions, it is important to note that, in perturbation theory, the SM diagrams of a fixed order in the strong coupling constant α_s must be gauge invariant by themselves *for a fixed number L of loops.* A second crucial observation is that, by using QCD gauge flips, all gluon self-couplings can eventually be eliminated in favor of quark-gluon couplings. That is, every grove of diagrams with QCD couplings contains a diagram d in which all gluon lines start and end at a quark thread. In d, the replacement of an internal gluon by a neutral EW boson, Z^0 say, always leads to a valid diagram of order α_s^{n-1}, if d was of order α_s^n. Conversely, then, by replacing a neutral SM boson line starting and ending at a quark thread in an arbitrary SM diagram of order α_s^{n-1}, we obtain a valid diagram of order α_s^n.

For simplicity, we restrict ourselves now to groves without external gluons. In this case, the groves of diagrams with QCD couplings can then in principle be found in the following way: We first determine the groves $S_i^{(0)}$ of diagrams without QCD couplings, as described in the above theorem. To determine the groves of diagrams of order α_s, we choose a grove $S_i^{(0)}$ and select the subset T of diagrams with internal neutral EW boson lines connecting with both ends to a quark thread. Obtain a new set T' by replacing one such neutral boson line in every diagram of T in all possible ways. T' then contains representatives of groves of order α_s. The crucial point now is that, *by applying QCD gauge flips to T' in all possible ways, we necessarily get a union of groves $S_k^{(1)}$ of order α_s.* This process can be continued to higher orders in α_s, until there are no more neutral bosons that could be replaced by a gluon. All this will be demonstrated in the next section.

While the procedure just described gives us a way to construct the groves of diagrams with QCD couplings, it does not actually characterize these groves. We will now make some general remarks about the characterization of groves with QCD couplings. Suppose, then, that we want to classify the groves of order α_s. A diagram of order α_s contains a single gluon, which can either connect two different quark threads or couple to a single quark thread. The groves are then distinguished at least by the choices of two or one quark thread, respectively. In most cases, there will be further choices associated with the couplings of EW bosons to the quark threads. We shall demonstrate this explicitely for a sufficiently simple, yet nontrivial, example in the next section.

In a similar way, one can in principle characterize the groves of higher orders in α_s. However, the combinatorics required for devising a general scheme becomes forbiddingly complicated. On the other hand, the formalism of flips is ideally suited for an implementation in a computer program. We have implemented the algorithm for the construction of groves of the SM. The results will be presented later. However, in order to make a connection with our theoretical discussion, we shall demonstrate the decomposition of the forest into groves on an explicit example, which we shall then analyze by means of our computer program.

6.3.5 Structure of SM Forests: An Explicit Example

We have now all the information at hand which is needed to decompose a general SM forest into its groves. Instead of describing the general procedure, which would soon become very awkward, we shall discuss a specific example illustrating the essential steps. Our arguments will also be applicable in the general case. For simplicity, we specialize to the one-loop case, i. e. $L = 1$.

Consider, then, the connected Green's function G for the process $e^+e^- \to u\bar{u}d\bar{d}$. The complete forest of all one-loop diagrams contributing to G, including QCD contributions, will be denoted as F. The invariant subsets of diagrams of order α_s^0, α_s^1, and α_s^2 are referred to as $F^{(0)}$, $F^{(1)}$, and $F^{(2)}$, respectively.

Purely Electroweak Contributions

We shall first treat the forest $F^{(0)}$ of diagrams without QCD couplings, taking account of QCD contributions later. There are two ways of associating the external fermions to fermion threads, corresponding to the groupings $(u, \bar{u})$ and $(d, \bar{d})$ or $(u, \bar{d})$ and $(d, \bar{u})$, respectively. In other words, the forest of one-loop diagrams of G decomposes into two invariant subsets $F^{(0)}\big(\mathcal{E}_n\big)$ and $F^{(0)}\big(\mathcal{E}_c\big)$, characterized by the external states

$$\mathcal{E}_n = \big\{(e^+, e^-), (u, \bar{u}), (d, \bar{d})\big\} \tag{6.58}$$

$$\mathcal{E}_c = \big\{(e^+, e^-), (u, \bar{d}), (d, \bar{u})\big\} \ . \tag{6.59}$$

$F^{(0)}\big(\mathcal{E}_n\big)$ and $F^{(0)}\big(\mathcal{E}_c\big)$ can be further decomposed according to the number λ of fermion loops, which can be 0 or 1. For $\lambda = 0$, we denote the subsets as $F^{(0)}\big(\mathcal{E}_n, 0\big)$ and $F^{(0)}\big(\mathcal{E}_c, 0\big)$, respectively. For $\lambda = 1$, we characterize the fermion loop by the fermion dublet, f, in the case of $\mathcal{E}_c$, or by the dublet component, f_k, in the case of $\mathcal{E}_n$, writing, respectively, $F^{(0)}\big(\mathcal{E}_n, f_k\big)$ or $F^{(0)}\big(\mathcal{E}_c, f\big)$.

Before going into the details of the decomposition, we have to say that it would be too much to display the complete groves. However, since groves are

equivalence classes of diagrams under gauge flips, we can display a *representative* for each grove, using brackets to denote the respective equivalence class. Thus, if d is a diagram in a grove S, we write $S = [d]$. In the next section, we will then report the sizes of these groves as we have obtained them by means of our computer program.

We begin with the decomposition of $F^{(0)}(\mathcal{E}_c)$. All diagrams in this subset are charged, because the external state $\mathcal{E}_c$ contains charged fermion threads. According to theorem 6.4, the charged diagrams without fermion $F^{(0)}(\mathcal{E}_c, 0)$ loop form a single grove:

$$F^{(0)}(\mathcal{E}_c, 0) \quad = \quad \left[\right. \tag{6.60}$$

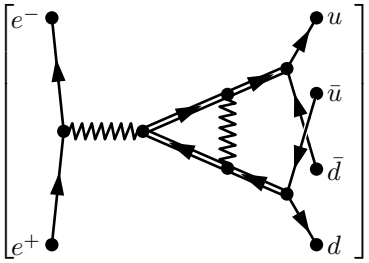

$\left. \right]$

Note that this diagrams is the same as (1.3), which we choose to illustrate the action of gauge flips in the introduction. Therefore, any of the diagrams in chapter 1 could have been used as a representative for this grove.

The diagrams with a single fermion loop form one grove $F^{(0)}(\mathcal{E}_c, f)$ for each fermion *dublet* f:

$$F^{(0)}(\mathcal{E}_c, f) \quad = \quad \left[\right. \tag{6.61}$$

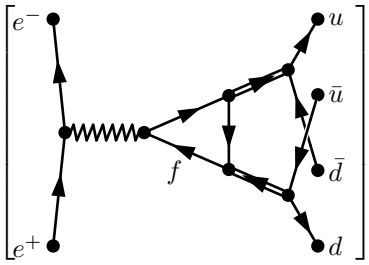

$\left. \right]$

The subset $F^{(0)}(\mathcal{E}_n, 0)$ contains, according to theorem (6.4), a charged grove $F^{(0)}_+(\mathcal{E}_n, 0)$:

$$F^{(0)}_+(\mathcal{E}_n, 0) \quad = \quad \left[\right. \tag{6.62}$$

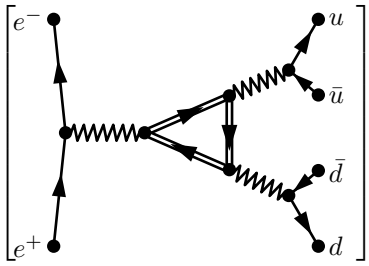

$\left. \right]$

We have now exhausted all charged diagrams. Indeed, a diagram in $F^{(0)}(\mathcal{E}_n, f_k)$ cannot contain a W-thread, because in a diagram with a neutral external state the W-thread must be part of a loop. However, the only loop in $F^{(0)}(\mathcal{E}_n, f_k)$ is a closed fermion thread, hence there is no room for a W-thread.

The invariant subset $F_0^{(0)}\big(\mathcal{E}_n, 0\big)$ of neutral diagrams in $F^{(0)}\big(\mathcal{E}_n, 0\big)$ decomposes, according to theorem 6.4, into neutral groves according to the number (modulo two) of Z^0 bosons coupled to each fermion thread. We have illustrated these choices for the case at hand as an example in (6.50). Thus, there are four groves, which we characterize by specifying the flavors of the fermion threads to which an odd number of Z^0 bosons is coupled. We display three of these:

$$F_0^{(0)}\big(\mathcal{E}_n, 0; 0\big) \;=\; \Big[\quad \Big] \tag{6.63}$$

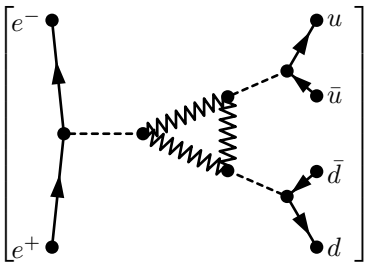

$$F_0^{(0)}\big(\mathcal{E}_n, 0; u, d\big) \;=\; \Big[\quad \Big] \tag{6.64}$$

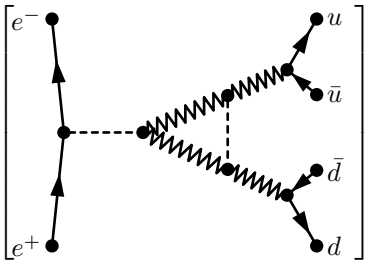

$$F_0^{(0)}(\mathcal{E}_n, 0; e, u) \;=\; \Big[\quad \Big] \tag{6.65}$$

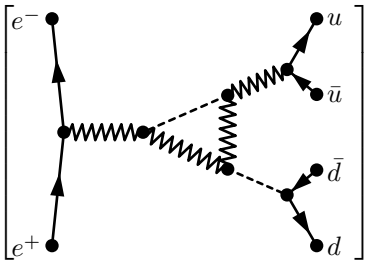

The representative for the remaining grove $F_0^{(0)}\big(\mathcal{E}_n, 0; e, d\big)$ is obtained by permuting u and d in an obvious way.

In a similar manner, the neutral groves in $F^{(0)}\big(\mathcal{E}_n, f_k\big)$ decompose into neutral groves, which can again be characterized by specifying the flavor of the fermion threads to which have an odd number of couplings to Z^0 bosons. First, there is the grove $F^{(0)}\big(\mathcal{E}_n, f_k; e, u, d, (f_k)\big)$ corresponding to an odd number of Z^0 couplings at every fermion thread:

$$F^{(0)}\big(\mathcal{E}_n, f_k; e, u, d, (f_k)\big) \;=\; \Big[\quad \Big] \tag{6.66}$$

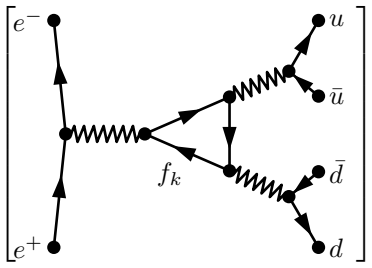

Here, the fermion propagating in the loop has been put into extra parentheses to distinguish it from the external fermions.

Then, we can choose an odd number of Z^0 couplings at just two fermion threads, which may be either two external fermion threads or one external thread and the loop. We display one choice for both cases (the notation should be evident by now):

$$F^{(0)}\big(\mathcal{E}_n, f_k; u, d\big) \;=\; \Big[\qquad (6.67)$$

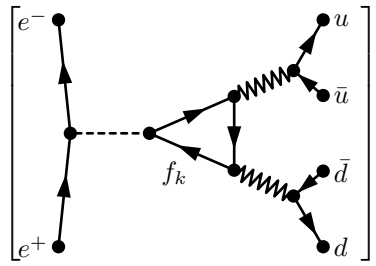

$$F^{(0)}\big(\mathcal{E}_n, f_k; e, (f_k)\big) \;=\; \Big[\qquad (6.68)$$

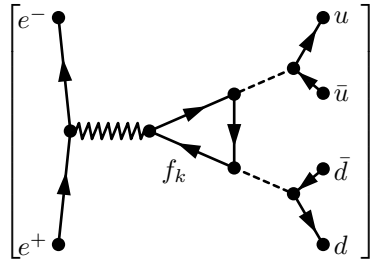

The other four choices lead to the groves $F^{(0)}\big(\mathcal{E}_n, f_k; e, u\big)$ and $F^{(0)}\big(\mathcal{E}_n, f_k; e, d\big)$ on one hand as well as $F^{(0)}\big(\mathcal{E}_n, f_k; u, (f_k)\big)$ and $F^{(0)}\big(\mathcal{E}_n, f_k; d, (f_k)\big)$ on the other hand.

This completes the decomposition of the forest for the Green's function G. Let us briefly summarize the groves, neglecting trivial groves of diagrams without gauge bosons, and restricting ourselves to a simplified version of the SM with just one generation of fermions, i. e. the leptons e and ν as well as the quarks u and d. There is no loss of generality in this restriction, because, as we have argued above, the groves of the complete SM can be obtained from the one-generation SM by merely exchanging flavors in the fermion loops.

First, we have the groves without fermion loop, which are the two charged groves $F^{(0)}\big(\mathcal{E}_c, 0\big)$ and $F_+^{(0)}\big(\mathcal{E}_n, 0\big)$ as well as the neutral groves $F_0^{(0)}\big(\mathcal{E}_n, 0; 0\big)$ plus three groves $F_0^{(0)}\big(\mathcal{E}_n, 0; t_1, t_2\big)$, where t_1 and t_2 refer to the open fermion threads. Thus, there are six groves without fermion loop. The groves with fermion loop are given by two copies of the charged grove $F^{(0)}\big(\mathcal{E}_c, f\big)$, one each for the two dublets, and four copies each of $F^{(0)}\big(\mathcal{E}_n, f_k; e, n, d, (f_k)\big)$, of the three choices $F^{(0)}\big(\mathcal{E}_n, f_k; t_1, t_2\big)$, and of the three choices $F^{(0)}\big(\mathcal{E}_n, f_k; t, (f_k)\big)$ (where t again refers to the three open fermion threads), one for each of the four dublet *components*. All in all, this makes up for 36 nontrivial groves.

Of course, the forest of G, as we have discussed it, is not really equal to the set of diagrams from which G would be computed in practice. For, at the moment we include Higgs couplings to *all* SM fermions, whereas, for practical purposes, the couplings of light fermions to the Higgs can often be ignored. We will discuss the implications of treating fermions as massless below. Here, we just make two general remarks. First, the structure of the charged groves is not affected by treating fermions as massless. This is intuitively clear, because internal H-lines can always be eliminated in a diagram with W-thread. Second,

treating fermions as massless will usually lead to a further decomposition of some neutral groves for massive fermions, although other neutral groves may be completely absent. Also, we have to say something about QCD contributions. We will take up these issues below.

Before we do that, however, we want to briefly comment on the impact on the structure of the forest brought about by adding an external photon. That is, we consider now the process $e^+e^- \to u\bar{u}d\bar{d}\gamma$. The corresponding external states external states $\mathcal{E}'_n$ and $\mathcal{E}'_c$ are then given by including the extra photon in $\mathcal{E}_n$ and $\mathcal{E}_c$, respectively:

$$\mathcal{E}'_n = \big\{(e^+, e^-), (u, \bar{u}), (d, \bar{d}), \gamma\big\} \tag{6.69}$$

$$\mathcal{E}'_c = \big\{(e^+, e^-), (u, \bar{d}), (d, \bar{u}), \gamma\big\} \ . \tag{6.70}$$

According to theorem 6.4, the structure of charged groves is unaffected by the additional photon. For instance, the grove $F^{(0)}\big(\mathcal{E}'_c, 0\big)$ is obtained by adding the photon in all diagrams of $F^{(0)}\big(\mathcal{E}_c, 0\big)$ in all possible places.

On the other hand, adding the photon to a neutral grove will lead to several separate groves, one for each choice of fermion thread to which the photon can be attached. We illustrate this for the neutral grove $F^{(0)}\big(\mathcal{E}'_n, f_k; u, d\big)$, characterizing the four groves by the flavor of the fermion thread to which the photon is attached:

$$F^{(0)}\big(\mathcal{E}'_n, f_k; u, d; e\big) \ = \ \Big[\tag{6.71}$$

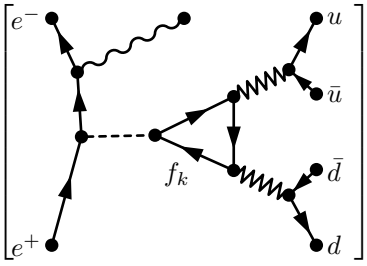

$$F^{(0)}\big(\mathcal{E}'_n, f_k; u, d; u\big) \ = \ \Big[\tag{6.72}$$

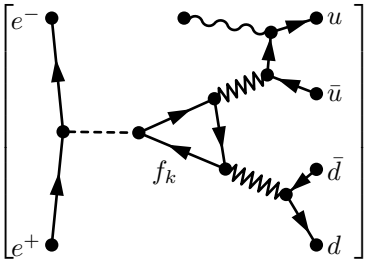

$$F^{(0)}\big(\mathcal{E}'_n, f_k; u, d; d\big) \ = \ \Big[\tag{6.73}$$

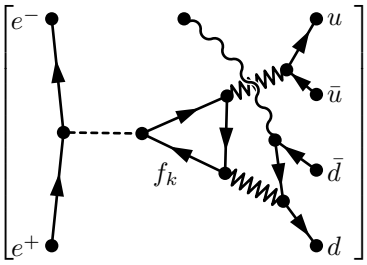

$$F^{(0)}\big(\mathcal{E}'_n, f_k; u, d; (f_k)\big) \;=\; \Big[$$

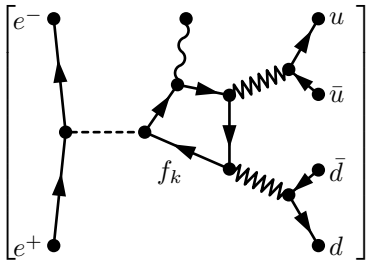

$$\Big] \tag{6.74}$$

Of course, the last grove does not exist if f_k corresponds to a neutrino. Other neutral groves are handled in an analogous way.

QCD Contributions

According to the general remarks about QCD contributions made above, the one-loop contributions of order α_s to the Green's function G for the process $e^+e^- \to u\bar{u}d\bar{d}$ form an invariant subset $F^{(1)}$ of the complete one-loop forest F. We are now going to demonstrate how $F^{(1)}$ can be decomposed into groves, given the decomposition of the diagrams $F^{(0)}$ of order α_s^0.

We argued above that representatives for groves of $F^{(1)}$ can be generated from diagrams in groves of $F^{(0)}$ by replacing neutral EW lines connecting quark threads through gluons. Therefore, we shall now successively scan the groves of $F^{(0)}$ for diagrams containing such lines.

We begin with $F^{(0)}\big(\mathcal{E}_c, 0\big)$. Using gauge motions, it is easily seen that this grove contains a candidate:

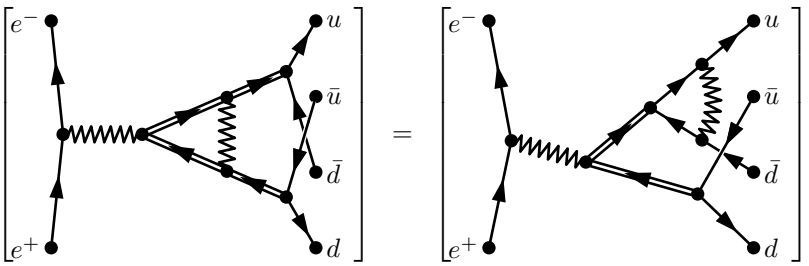

(6.75)

Replacing the Z^0-line connecting the u-thread to itself, we obtain a representative for the grove $F^{(1)}\big(\mathcal{E}_c, 0|u\big)$, where the u refers to the gluon attached to the u-thread:

$$F^{(1)}\big(\mathcal{E}_c, 0|u\big) \;=\; \Big[$$

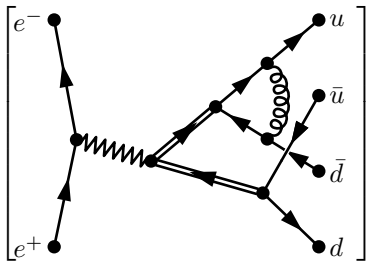

$$\Big] \tag{6.76}$$

Of course, the gluon could also have been attached to the d-thread, yielding a second grove $F^{(1)}\big(\mathcal{E}_c, 0|d\big)$ (which we are not going to display).

This does not yet exhaust the groves obtained from $F^{(0)}\big(\mathcal{E}_c, 0\big)$, because there is also a representative with a Z^0-line connecting both quark threads:

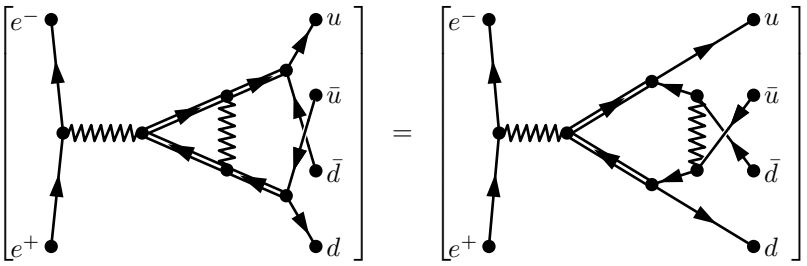

(6.77)

Replacing the Z^0-line here gives us a third grove $F^{(1)}\big(\mathcal{E}_c, 0|u, d\big)$:

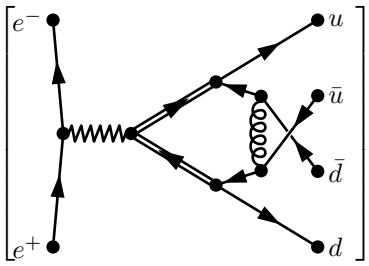

(6.78)

Since the general principle should by now be clear, we shall no longer display the original representatives and candidates. Rather, we display the representative from $F^{(1)}$ directly. The candidate can be inferred from this representative in an obvious way by replacing the gluon with a Z^0 or H-line.

Two further charged groves can be constructed from $F_+^{(0)}\big(\mathcal{E}_n, 0\big)$. We display the first one:

$$F_+^{(1)}\big(\mathcal{E}_n, 0|u\big) \;=\;$$

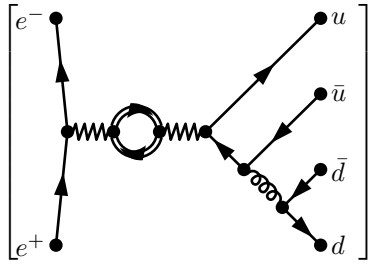

(6.79)

The second grove, $F_+^{(1)}\big(\mathcal{E}_n, 0|d\big)$ is obtained in an obvious way by attaching the Z^0-line to the d-thread instead of the u-thread. This exhausts the list of charged groves, because in $F^{(0)}\big(\mathcal{E}_c, f\big)$ there are no candidate diagrams.

Let us, then, turn to neutral diagrams. There, we can replace a Z^0-line between quark threads by a gluon line, which can be part of the loop or not. In the former case, we obtain three groves from each of $F_0^{(0)}\big(\mathcal{E}_n, 0; t_1, t_2\big)$. For

$t_1, t_2 = u, d$, the first two are given by:

$$F_0^{(1)}\big(\mathcal{E}_n, 0; u, d|u, d\big) \;=\; \Big[$$

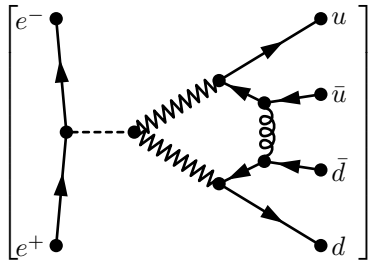

$$\Big] \tag{6.80}$$

$$F_0^{(1)}\big(\mathcal{E}_n, 0; u, d|u\big) \;=\; \Big[$$

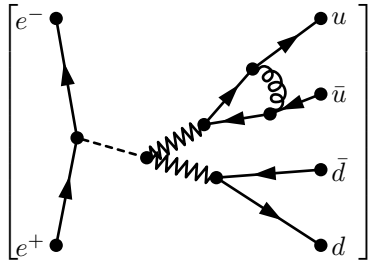

$$\Big] \tag{6.81}$$

The third grove, $F_0^{(1)}\big(\mathcal{E}_n, 0; u, d|d\big)$, is obtained by connecting the gluon to the d-thread instead of the u-thread in the second diagram.

Evidently, the single H-line can be attached to the u or d-thread as well, which will give us the six further groves $F_0^{(1)}\big(\mathcal{E}_n, 0; e, q|u\big)$, $F_0^{(1)}\big(\mathcal{E}_n, 0; e, q|d\big)$, and $F_0^{(1)}\big(\mathcal{E}_n, 0; e, q|u, d\big)$, for q equal to u or d.

Then, there are a number of groves with the gluon not part of the loop:

$$F^{(1)}\big(\mathcal{E}_n, 0; e, u|u, d\big) = \Big[$$

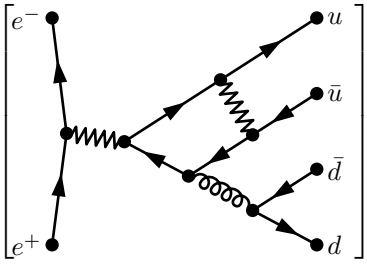

$$\Big] \tag{6.82}$$

$$F^{(1)}\big(\mathcal{E}_n, 0; u|u, d\big) = \Big[$$

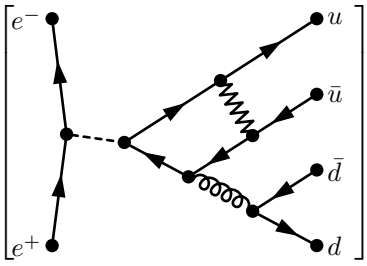

$$\Big] \tag{6.83}$$

Note that replacing the Z^0-line in the loop of the first diagram by a H-line does not lead to a new grove, because we may only specify the number modulo two of Z^0-lines attached to a fermion thread, which remains unchanged under this replacement.

Finally, there are neutral groves with a fermion loop. From the grove $F^{(0)}\big(\mathcal{E}_n, f_k; e, u, d, (f_k)\big)$, we obtain a number of groves, of which we display

some explicitely:

$$F^{(1)}\big(\mathcal{E}_n, f_k; e, (f_k)|u, d\big) \;=\; \Big[\quad (6.84)$$

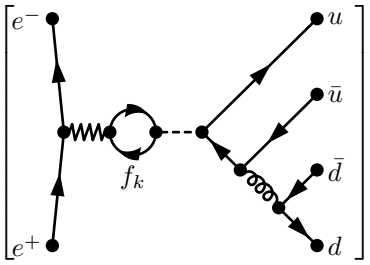

$$F^{(1)}\big(\mathcal{E}_n, q_k; e, (q_k), u, d|u, q_k\big) \;=\; \Big[\quad (6.85)$$

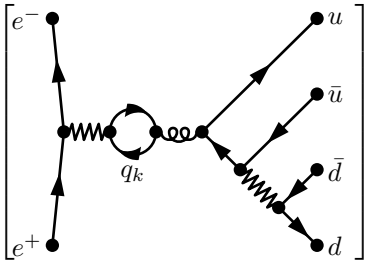

$$F^{(1)}\big(\mathcal{E}_n, q_k; e, d|u, q_k\big) \;=\; \Big[\quad (6.86)$$

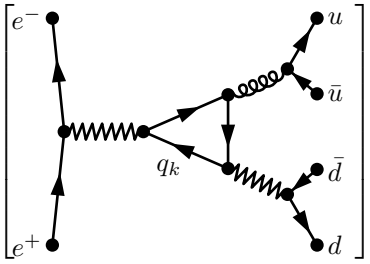

Here, q_k refers to the component of a quark multiplet. The further groves obtained from $F^{(0)}\big(\mathcal{E}_n, f_k; e, u, d, (f_k)\big)$ correspond to permuting u and d-thread in the above diagrams. Observe that some of these groves can also be obtained from other groves of $F^{(0)}$. For instance, the grove $F^{(1)}(\mathcal{E}_n, q_k; e, d|u, q_k)$ can also be obtained from $F^{(0)}(\mathcal{E}_n, h_k; e, d)$, by replacing a H-line with a gluon. This does not contradict our general remark that a grove in $F^{(0)}$ is turned into a union of groves in $F^{(1)}$ when all possible replacements and QCD gauge flips are performed, because we did not claim that the groves in $F^{(1)}$ would be different for different original groves in $F^{(0)}$.

The remaining neutral groves in $F^{(1)}$ are similar in structure to the three ones displayed last, with Z^0-lines replaced by H-lines, and *vice versa*, in all possible ways. This completes the construction of the groves of $F^{(1)}$. Looking back at the representatives for these groves, it is apparent that these can indeed be characterized by specifying the quark threads to which the gluon is attached, and, in addition, to which fermion threads the EW bosons are coupled. We have used this fact in an intuitive way to denote the groves in $F^{(1)}$.

We shall not analyze the subset $F^{(2)}$ of order α_s^2 in the same detail. The construction of the groves can be performed in an analogous way. Instead, we just display example representatives for all occuring structures (without introducing

a notation for the groves):

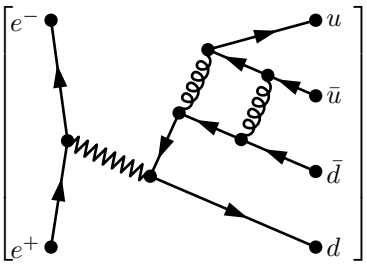

(6.87)

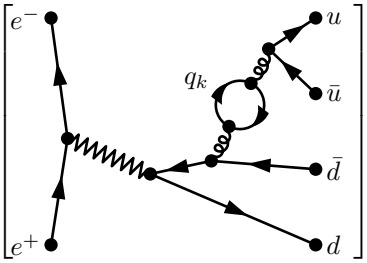

(6.88)

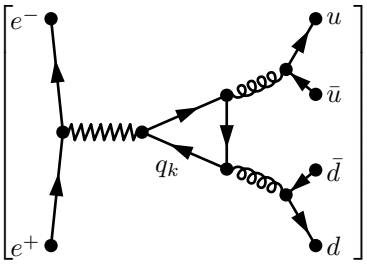

(6.89)

Observe that there can be no charged diagrams in $F^{(2)}$. Again, it is apparent that, in principle, the groves of $F^{(2)}$ can be characterized by specifying to which quark thread the Z^0 boson and the two gluons are coupled, respectively.

Massless Fermions

In this subsection, we turn our attention to a consideration of massless fermions. Upto now, we have implicitely assumed that all fermions are massive, which means that all fermions couple to the Higgs boson. Without this assumption, our arguments fail because it is no longer possible to strip neutral bosons from fermion threads arbitrarily. Formally, this can be seen by observing that, without the couplings of the H boson to fermions, the gauge motion $H \perp fZ^0$ is forbidden, and we can no longer strip Z^0 bosons off a fermion thread as in (6.45). It is therefore reasonable to expect that, for massless fermions, new groves will appear.

We can restrict our attention to neutral diagrams, because in a charged diagram, a W-thread can always be used to remove all neutral bosons from a fermion thread by gauge motions which do not involve H-lines. On the other hand, as we have argued, for neutral diagrams H-lines are essential if we want to strip neutral bosons from a fermion thread. Now consider an arbitrary neutral grove S in a forest containing only massive fermions. If we make one of the fermions, f say, massless, it may happen that some diagrams in S become disconnected under gauge flips, if the diagrams with couplings of f to the H boson

are removed. In this case, the grove S corresponding to a massive fermion f is partitioned into smaller groves corresponding to a massless fermion f.

For a general classification of groves for massless fermions, one could use the following observation: Due to the absence of fermion-Higgs couplings, the number of Z^0 bosons coupled to a massless fermion thread is invariant under gauge flips. Since the same statement applies, in neutral diagrams, to photons, we could in principle classify the groves of forests containing massless fermion threads according to the number of Z^0 bosons and photons coupled to the massless fermion threads. However, even for the relatively simple diagrams in the present example, the number of choices is so large that such a classification is no longer useful.

Therefore, rather than giving a general classification of groves for diagrams with massless fermions, we shall demonstrate the appearance of new groves on an explicit example. This will suffice to understand the origin of the additional structure of the forest.

For definiteness, we consider the forest for the process $e^+e^- \to Z^0Z^0$ at the one-loop order. If the e is taken as massive, i. e. if a e-H coupling is included, there is a neutral grove S_0 including the following diagrams, linked by a sequence of gauge flips:

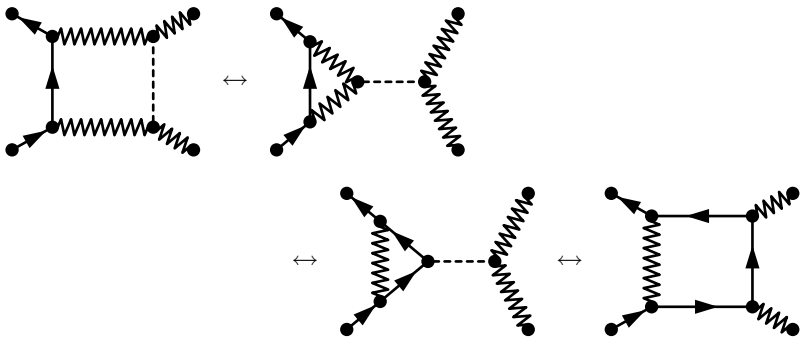

(6.90)

If we now make the e massless, the third diagram does no longer exist. In this simple example, it is not hard to convince oneself that this diagram is really essential for the first and last diagram to be connected by gauge flips. Therefore, the original grove S_0 must decompose into at least two groves. In fact, it turns out that S_0 decomposes into four groves, the two additional groves containing diagrams of the form

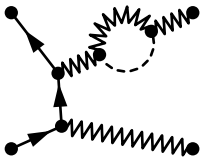

. (6.91)

No gauge flip can transform this diagram with an external leg correction into an amputated diagram, because this would require the perpendicular motion $H \perp eZ^0$ of the H boson onto the e-thread.

Now observe that, from the displayed diagrams, we can easily obtain contributions to the forest for $e^+e^- \to u\bar{u}d\bar{d}$, by coupling the external Z^0 bosons to an external u-thread and d-thread, respectively. Comparison with (6.64) shows, that the diagrams so obtained are all contained in the neutral grove

$F_0^{(0)}\big(\mathcal{E}_n, 0; u, d\big)$, if the e, as well as u and d, is taken as massive. Consequently, for a massless e, the neutral grove $F_0^{(0)}\big(\mathcal{E}_n, 0; u, d\big)$ should decompose into four groves. This is, in fact, confirmed by constructing the groves of $e^+e^- \to u\bar{u}d\bar{d}$ by means of a computer program (cf. 6.2). In a similar manner, additional groves would arise if the u and/or d were taken as massless, too.

If we look at the representatives for the groves corresponding to the first and last diagram in (6.90), which are given, respectively, by

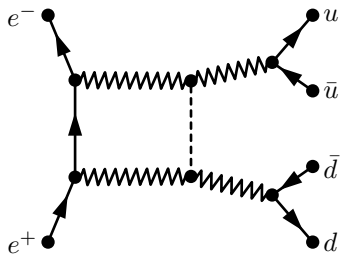

(6.92)

and

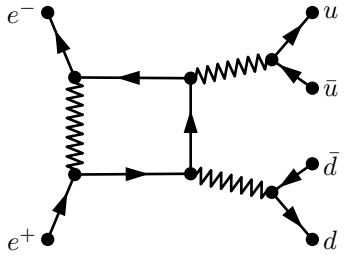

, (6.93)

we see that these are, indeed, characterized by different numbers of couplings of Z^0 bosons to the e-thread. Thus, this information can be used to classify forests with massless fermions.

6.3.6 Generalization

From the example above, it should be clear that the classification of more general forests, with more external fermions and/or more than one loop, can be discussed in principle along the same line of reasoning used above. At the same time, however, the foregoing example demonstrate that the combinatorial complexity of this classification becomes forbiddingly complicated very soon. Therefore, in practice the construction of groves can sensibly done only by a computer program implementing the algorithm which we have described in 4.3.1 and 4.4.4.

We have written such a computer program and used it to reexamine the above example. Since the groves can be uniquely identified by the representatives we have displayed above, we have in principle full control over the groves, even though most of them are too large to be diplayed explicitely in this work. We shall present a summary of the results obtained by means of this program in the next section.

6.3.7 Results

In order to put our theoretical considerations to practical use, we have implemented the algorithm for the construction of groves of general SM forests.

$e^+e^- \to u\bar{u}d\bar{d}$ $(L=1)$	$m_f \neq 0$	$m_\nu = 0$	$m_e = 0$	$m_q = 0$
$O(\alpha_s^0)$				
Number of Diagrams	58382	54272	18713	4233
Gauge Groves	36	36	45	57
Pure Higgs Groves	601	520	0	0
$O(\alpha_s^1)$				
Number of Diagrams	6712	6404	2584	1188
Gauge Groves	122	122	80	58
Pure Higgs Groves	147	133	0	0
$O(\alpha_s^2)$				
Number of Diagrams	352	352	176	176
Gauge Groves	8	8	8	8
Pure Higgs Groves	8	8	0	0

Table 6.1: Total number of diagrams (omitting diagrams with ghost loops) and number of groves for the one-loop corrections to $e^+e^- \to u\bar{u}d\bar{d}$ in a one-generation SM, according to the number of fermions treated as massless. Details are explained in the text.

In this section, we will present the results obtained for the one-loop forest of the process $e^+e^- \to u\bar{u}d\bar{d}$, which we have discussed in much detail in the last section.

For the sake of simplicity, we have again restricted the SM to one fermion generation. Furthermore, we have omitted diagrams with ghosts. As we have shown in chapter 4, the number of groves is unaffected by this restriction. Of course, if numerical calculations of matrix elements should be performed, the diagrams with ghost loops would have to be included. This can, however, easily be done once the groves of diagrams without ghosts have been constructed.

In the following, we consider different ways of choosing SM fermions as massless. If all fermions, including ν, are considered as massive, we refer to this choice of fermion masses as "$m_f \neq 0$". If neutrinos are considered massless, we denote this as $m_\nu = 0$. If the electron e is also taken as massless, we write $m_e = 0$. Finally, if quark masses are set to zero as well, we denote this as "$m_q = 0$".

In the table 6.1, we first report the total number of diagrams as well as the number of groves for the pure electroweak diagrams, the diagrams including QCD corrections of order α_s, and the diagrams including QCD corrections of order α_s^2, respectively. In all cases, we refer to the non-trivial groves of diagrams with *SM bosons* as "gauge groves", while the remaining groves are denoted as "pure Higgs groves". For diagrams with QCD couplings, the latter term is meant to *include* diagrams containing gluons, because we are not particularly interested in diagrams without SM bosons.

Note that, for the $O(\alpha_s^2)$ corrections, the equality of the cases $m_f \neq 0$ and $m_\nu = 0$ on one hand and of $m_e = 0$ and $m_q = 0$ on the other hand, is a simple consequence of the fact that with two gluons in the diagram there is just no

room for a ν-thread or for couplings of H to u and d.

In table 6.1 we find the confirmation of our counting of gauge groves for the $m_f \neq 0$ case, where we recognize the 36 non-trivial gauge groves.

In table 6.2 we then present a detailed analysis of the decomposition of the groves pertaining to the purely electroweak corrections, when more and more fermions are taken as massless. The table contains an entry for each grove of $F^{(0)}$, for which we have displayed a representative in (6.61) through (6.67). When the groves contain a fermion loop with a generic fermion f_k, we make a separate entry corresponding to f_k equal to ν, e, and u, respectively, because these will behave differently under the various choices of massless fermions. Of course, the names of the groves in the first column corrrespond to choosing all fermions as massive. The numbers listed are the sizes of the respective groves. The decomposition of groves is indicated by a subdivision of the rows.

Table 6.2 confirms a number of statements we made in the above discussion. First, it shows that the charged groves never decompose into several groves, no matter how many fermions are taken as massless. The reason is that the W-threads present in charged diagrams can always be used to strip the fermion threads to the minimal possible length. The neutral groves, on the other hand, feature a rich structure, especially if all fermions are taken as massless.

Next, we find the confirmation for our claim at the end of the previous section, that the neutral grove $F_0^{(0)}\big(\mathcal{E}_n, 0; u, d\big)$ would decompose into four groves if the electron e is taken as massless. Indeed, the corresponding decomposition is apparent from the second row of the neutral groves.

From table 6.2 we can also learn something about the relative weight (regarding size) of charged and neutral groves. It is immediately apparent that the charged groves are generally large. This was to be anticipated, because the charged W-threads are very effective in connecting diagrams.

Interestingly, the size of the largest neutral groves is almost of the same order as that of the charged groves, as long as all fermions are massive. The reason is that, as we have seen in the discussion of the neutral diagrams around (6.45), the H-Z^0 flips are nearly as effective as the W-Z^0 flips in connecting diagrams, as long as the H boson couples to the fermion threads. On the other hand, the last column demonstrates that the situation changes dramatically if all fermions are massless. In this case, we end up with two huge charged groves without fermion loops, containing almost two third of the total 3624 diagrams listed in table 6.1.

From a practical point of view, this result means that the combinatorial complexity in defining the amplitude for the process $e^+e^- \to u\bar{u}d\bar{d}$ at one-loop *via* a sum of Feynman diagrams is reduced by a factor of three by decomposing the forest into groves.

Grove	$m_f \neq 0$	$m_\nu = 0$	$m_e = 0$	$m_q = 0$
Charged Groves				
$F^{(0)}\left(\mathcal{E}_c, 0\right)$	14218	14074	5986	1349
$F^{(0)}\left(\mathcal{E}_c, \ell\right)$	2430	1334	81	42
$F^{(0)}\left(\mathcal{E}_c, q\right)$	2516	2500	1020	58
$F^{(0)}_{+}\left(\mathcal{E}_n, 0\right)$	12022	11772	4735	1317
Neutral Groves				
$F^{(0)}_{0}\left(\mathcal{E}_n, 0; 0\right)$	1330	1330	186	64
$F^{(0)}_{0}\left(\mathcal{E}_n, 0; u, d\right)$	4526	4526	233	48
				48
				3
			208	48
				28
			208	48
				28
			96	96
$F^{(0)}_{0}\left(\mathcal{E}_n, 0; e, u\right)$	4526	4526	1677	96
				48
				48
				28
				28
				3
			108	48
			54	48
$F^{(0)}\left(\mathcal{E}_n, \nu; e, u, d, (\nu)\right)$	470	2	2	2
$F^{(0)}\left(\mathcal{E}_n, u; e, u, d, u\right)$	556	556	242	16
$F^{(0)}\left(\mathcal{E}_n, \nu; u, d\right)$	436	10	5	4
		10	4	4
$F^{(0)}\left(\mathcal{E}_n, e; u, d\right)$	534	534	16	16
			16	16
$F^{(0)}\left(\mathcal{E}_n, u; u, d\right)$	534	534	48	16
			48	16
$F^{(0)}\left(\mathcal{E}_n, \nu; e, (\nu)\right)$	269	0	0	0
$F^{(0)}\left(\mathcal{E}_n, e; e, (e)\right)$	292	292	0	0
$F^{(0)}\left(\mathcal{E}_n, u; e, (u)\right)$	292	292	147	0

Table 6.2: Decomposition of the groves for $e^+e^- \to u\bar{u}d\bar{d}$ at one-loop in a one-generation SM, according to the number of fermions treated as massless. The table contains an entry for each of the purely electroweak groves displayed explicitely in 6.3.5. Details are explained in the text.

—7—
Summary

The experimental accuracy of planned high energy physics experiments at future particle colliders requires equally accurate theoretical predictions for the measured observables like cross sections, branching ratios, decay widths etc. In order to achieve the required precision, radiative corrections have to be included.

Now, in the Standard model, scattering amplitudes and decay matrix elements are usually computed from a perturbative expansion defined in terms of Feynman diagrams. The inclusion of radiative corrections to these quantities implies that Feynman diagrams with loops have to be taken into account. This is a difficult problem, mainly for two reasons: On one hand, the number of Feynman diagrams contributing to a particular Standard Model process grows very rapidly with the number of loops and the number of external particles. On the other hand, the Standard Model being a gauge theory, care must be taken not to violate gauge invariance.

The resulting complexity of Standard Model calculations makes the use of automatization indispensable. However, even with the computing power of modern computers the construction of fully automated tools remains a challenging task. For numerical reasons, one would therefore like to subdivide the calculation of the scattering amplitude into smaller pieces, which independently of each other give sensible, i. e. gauge invariant, results. It is therefore of interest whether a partitioning of the full set of diagrams contributing to a scattering amplitude or decay matrix element into separately gauge invariant pieces can be found.

For the lowest order scattering amplitude, i. e. the set of tree level diagrams, an algorithm for the construction of minimal gauge invariant subsets has been described in [4] and formally proven in [5]. The algorithm uses a set of graphical operations on Feynman diagrams, called *gauge flips*, to decompose the full set of Feynman diagrams into the minimal gauge invariant subsets.

In the present work, we have extended this algorithm to Feynman diagrams with loops. To this end, we have studied the Slavnov-Taylor-Identities of connected Green's functions in a general gauge theory. We have shown how the STI for the expansion of a connected Green's function at n-loop order follows from the STIs for the tree level vertices of the theory. We have then used the gained insight to show that the *gauge flips* of [4] can indeed be used to construct minimal gauge invariant subsets also for diagrams with loops.

We emphasize that, although diagrammatical proofs for the STIs in gauge theories have been given before [26][27], they make statements only about the full set of diagrams defining the expansion of the Green's function under consid-

eration. Therefore, our proof of the STIs for *subsets* of the full set of Feynman diagrams is original.

We have then used the formalism of gauge flips to derive rules for a classifcation of the minimal gauge invariant subsets of general connected Green's functions in the Standard Model. Using these rules, we have studied the minimal gauge invariant subsets of a specific Standard Model process. The theoretical results so obtained were then confirmed and further illustrated by reexamining the diagrams for this process by means of a computer program for the construction of the minimal gauge invariant subsets for Feynman diagrams with loops, which we have designed and implemented on the basis of the theoretical considerations in this work.

The explicit results we obtained show that the decomposition of the full set of diagrams into minimal gauge invariant subsets leads to a moderate reduction of the combinatorial complexity.

—A—
BRST Feynman Rules

In this appendix, we collect the Feynman rules for insertions of the operators $s\varphi$, where s is the generator of BRST transformations and φ a generic field of the gauge theory. $s\varphi$ is split into an inhomogeneous part and a homogeneous part according to (2.26):

$$s\varphi = \varrho_\varphi[c] + c^a \Delta^a \varphi \ . \tag{A.1}$$

The inhomogeneous part, $\varrho_\varphi[c]$ is, in fact, nonzero only for gauge bosons or Goldstone bosons.

The Feynman rules for the homogeneous part can be read off from the BRST transformation laws (2.18) and (2.60). We shall refer to them as *BRST vertices*.

In order to define the Feynman rules for the inhomogeneous parts, we must carefully distinguish between connected Green's functions and 1PI Green's functions, because identical symbols are used for different expressions. We have pointed out in section 2.5, why this is indeed useful. Anyway, we shall emphasize the distinction clearly below.

A.1 Unbroken Gauge Theories

We use the conventions of section 2.1 to denote fields and generators of the gauge group. The fields are represented with the following line styles:

$$W^a_\mu \quad \rightarrow \quad \sim\sim\sim \tag{A.2}$$

$$\Phi_j \quad \rightarrow \quad ——— \tag{A.3}$$

$$\{\psi_j, \bar{\psi}_j\} \quad \rightarrow \quad \bar{\psi} \longrightarrow \psi \tag{A.4}$$

$$\{c^a, \bar{c}^a\} \quad \rightarrow \quad \bar{c} \cdots\!\blacktriangleright\cdots c \tag{A.5}$$

A.1.1 BRST Vertices

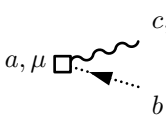

$$= -g f^{abc} \delta^\nu_\mu \tag{A.6}$$

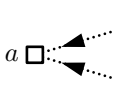

$$= -g f^{abc} \tag{A.7}$$

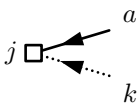

$$= \mathrm{i}g t^a_{jk} \tag{A.8}$$

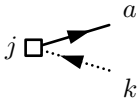

$$= -\mathrm{i}g t^a_{kj} \tag{A.9}$$

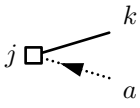

$$= -g X^a_{jk} \tag{A.10}$$

A.1.2 Inhomogeneous Parts

First, we list the Feynman rules for *connected* Green's functions, which are distinguished by the dot at the end of the line. Note that the momentum is directed from left to right.

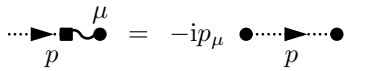

(A.11)

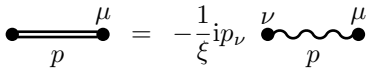

(A.12)

Now, we specify the Feynman rules for *1PI* Green's functions. Again, the momentum points from left to right.

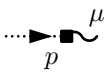

$$= \frac{1}{\xi}\mathrm{i}p_\mu \tag{A.13}$$

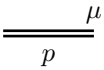

$$= -\mathrm{i}p_\mu \tag{A.14}$$

A.2 Spontaneously Broken Gauge Theories

For spontaneously broken gauge theories, we use the conventions of section 2.2.2. In particular, to denote the generators of the gauge group, we use the letters a, b, c for arbitrary generators, α, β, γ for broken generators, and q, r, s for unbroken generators.

The scalar multiplet Φ is decomposed into Goldstone bosons ϕ and Higgs bosons H according to:

$$\Phi = \begin{pmatrix} \phi \\ v + H \end{pmatrix} \tag{A.15}$$

In this basis, the generators X^a in the scalar sector are parametrized as follows:

$$X^a = \begin{pmatrix} t^a & u^a \\ -(u^a)^T & T^a \end{pmatrix} \tag{A.16}$$

Of course, $u^q = 0$ for unbroken generators.

Gauge bosons and Goldstone bosons are combined into a five-dimensional gauge field as in (2.64):

$$A^a_r = \left(W^a_\mu, \phi^a\right) \tag{A.17}$$

In Feynman rules, gauge bosons and Goldstone bosons will then be distinguished by the five-dimensional index, which is a Lorentz index (μ or ν) for gauge bosons, and 4 for Goldstone bosons.

The following line styles are used to represent the fields of a spontaneously broken gauge theory:

$$A_r^a \quad \rightarrow \quad \sim\sim\sim \tag{A.18}$$

$$H_j \quad \rightarrow \quad - - - - - - \tag{A.19}$$

$$\{\psi_j, \bar{\psi}_j\} \quad \rightarrow \quad \bar{\psi} \longrightarrow \psi \tag{A.20}$$

$$\{c^a, \bar{c}^a\} \quad \rightarrow \quad \bar{c} \cdots\cdots\blacktriangleright \cdots\cdots c \tag{A.21}$$

A.2.1 BRST Vertices

Note that, for all particles but scalars, the BRST Feynman rules for the homogeneous parts are identical to the rules in an unbroken theory. Therefore we list only the rules for scalars:

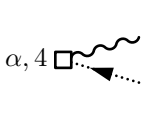

$$= -gt^{\beta}_{\alpha\gamma} \tag{A.22}$$

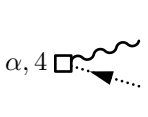

$$= -gt^{\beta}_{\alpha\gamma} \tag{A.23}$$

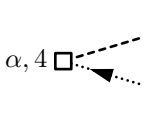

$$= -gu^{\beta}_{\alpha j} \tag{A.24}$$

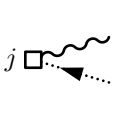

$$= gu^{\alpha}_{j\beta} \tag{A.25}$$

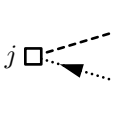

$$= -gT^{\alpha}_{jk} \tag{A.26}$$

A.2.2 Inhomogeneous Parts

To define the Feynman rules for the inhomogeneous parts in the BRST transformation laws of gauge bosons and Goldstone bosons, we make use of the five-dimensional contraction operators $\Theta(p)$ and $\bar{\Theta}(p)$, defined in (2.93) and (2.94):

$$\Theta_r(p) = \left(-\mathrm{i}p_\mu, -M\right) \tag{A.27}$$

$$\bar{\Theta}_r(p) = \left(\frac{1}{\xi}\mathrm{i}p_\mu, M\right) \quad . \tag{A.28}$$

These formulae can be taken over for massless gauge bosons by setting $M = 0$.

First, we list the Feynman rules for *connected* Green's functions, which are distinguished by the dot at the end of the line. Note that the momentum is directed from left to right.

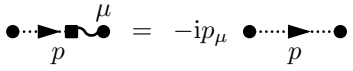

(A.29)

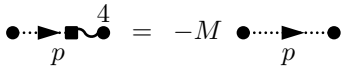

(A.30)

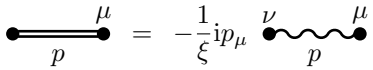

(A.31)

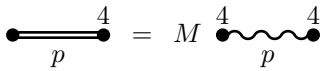

(A.32)

Now, we specify the Feynman rules for *1PI* Green's functions. Again, the momentum points from left to right.

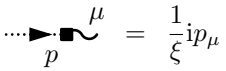

(A.33)

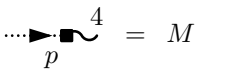

(A.34)

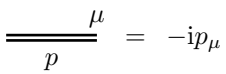

(A.35)

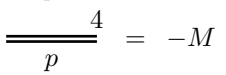

(A.36)

—B—
Tree Level STIs

In this appendix we collect all tree level STIs used in the proof of the STI for connected Green's functions in chapter 4.

B.1 Propagator and Inverse Propagator STIs

(B.1)

(B.2)

Note in particular the minus sign.

B.2 Vertex STIs

B.2.1 Cubic Vertices

In the STIs for cubic vertices, the lines with a cross at the end denote a tree level inverse propagator. (Cf. (3.6))

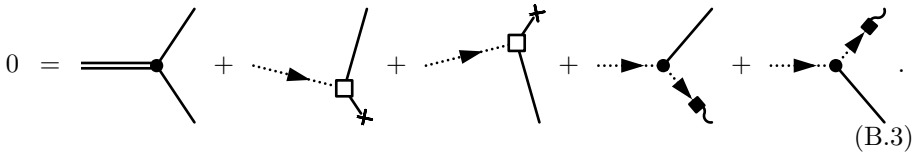

(B.3)

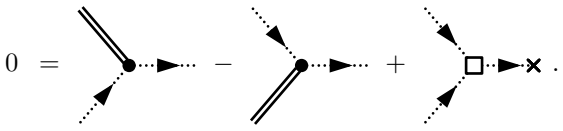

(B.4)

For use inside larger diagrams, the STIs (B.3) and (B.4) are often inconvenient due to the occurrence of the inverse propagators. Therefore, we list separately the STIs obtained from (B.3) and (B.4) by multiplying with three propagators. Note the sign changes.

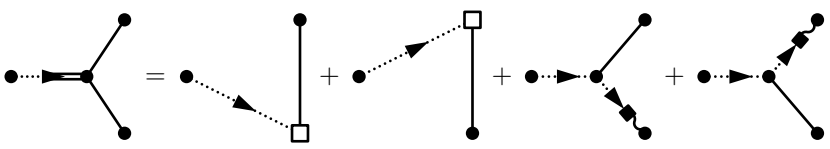

(B.5)

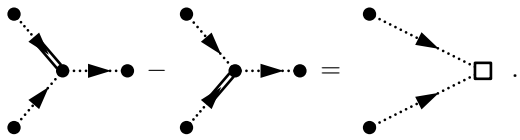

(B.6)

B.2.2 Quartic Vertices

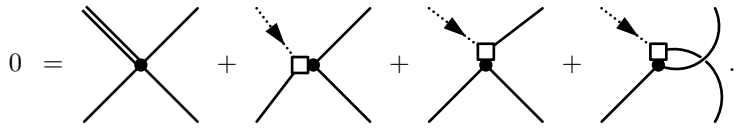

(B.7)

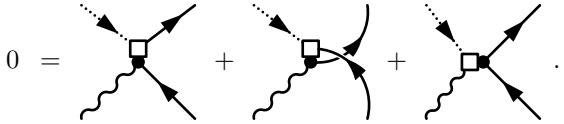

(B.8)

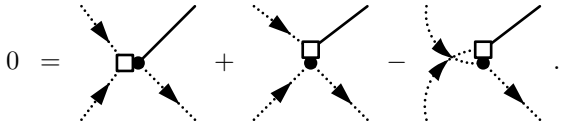

(B.9)

B.2.3 Five-Point Vertices

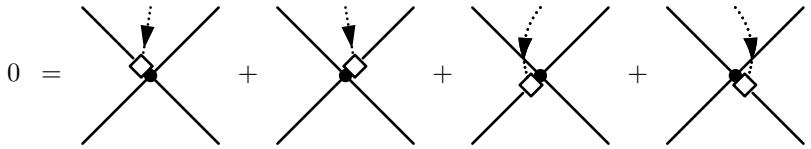

(B.10)

—C—
Automated Grove Construction

In this appendix we sketch our implementation of a computer program for the automated construction of groves in gauge theories, specifically the Standard Model.

C.1 Implementation

C.1.1 Representing Feynman Diagrams

In order to manipulate Feynman diagrams with a computer, we must first choose a representation of Feynman diagrams as a data structure in computer memory. This can be done by indicating which pairs of vertices are connected by propagators. To this end, we must be able to reference the vertices of the Feynman diagram. The simplest way to do this is to attach an internal index to each vertex (an integer, say) and then refer to a vertex by its index.

The particular representation we have chosen can be described as a map, specifying, for each vertex, to which neighbors it is connected, and the corresponding flavors. Consider the following simple example:

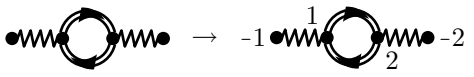

$$\rightarrow \begin{pmatrix} -1 & \rightarrow & \begin{pmatrix} 1 & \rightarrow & \{Z^0\} \end{pmatrix} \\ -2 & \rightarrow & \begin{pmatrix} 2 & \rightarrow & \{Z^0\} \end{pmatrix} \\ 1 & \rightarrow & \begin{pmatrix} -1 & \rightarrow & \{Z^0\} \\ 2 & \rightarrow & \{W^+, W^-\} \end{pmatrix} \\ 2 & \rightarrow & \begin{pmatrix} -1 & \rightarrow & \{Z^0\} \\ 2 & \rightarrow & \{W^+, W^-\} \end{pmatrix} \end{pmatrix} \tag{C.1}$$

At the left, the Feynman diagram is displayed in the usual way, without any indices at the vertices. By introducing indices to reference vertices, we get to the next drawing. Observe that the ends of external lines have also been given an index. In fact, in our representation the introduction of external vertices is necessary for the representation of external lines. Of course, these external vertices are mere artifacts of the representation and have no physical meaning. We have chosen positive and negative indices for internal and external vertices, respectively, because this allows for an easy distinction between both in our computer program.

The indexed Feynman diagram is easily translated into the displayed map. For instance, one should read the first entry as stating that "vertex -1 is connected to vertex 1 by a Z^0-line". Observe that the notation for the map is still an abstract representation. There may be many different ways to implement such a map as a data structure. However, it turns out that, in order to deal with comparisons efficiently (cf. the next section), the chosen data structure should satisfy the constraint that identical maps correspond to identical data structures.

C.1.2 Comparing Feynman Diagrams

The algorithm for the construction of groves instructs us to repeatedly add all gauge flipped diagrams to a given set of diagrams, starting from a single diagram, until no more new diagrams are created. In order to implement this algorithm, we have to be able to test the representations of Feynman diagrams in computer memory for equality, or else we will not be able to assert whether or not a diagram has already been produced.

We have already argued that our representation of Feynman diagrams with loops introduces indices to identify the vertices of the diagram. However, these indices are unrelated to the physical meaning of Feynman diagrams. Therefore, two representations of Feynman diagrams that differ only by a permutation of the vertex indices actually denote the *same* Feynman diagram. On the other hand, different permutations of indices will usually lead to different data structures (unless the permutation corresponds to an automorphism of the Feynman diagram). This means that we cannot *naively* compare representations, i. e. data structures in computer memory, in order to test two Feynman diagrams for equality.

We *can*, however, compare representations if we find a prescription to produce a *unique* indexation for every possible Feynman diagram. In graph theory, this strategy is formalized by considering permutations of indices as an equivalence relation on the set of representations of Feynman diagrams. A Feynman diagram corresponds then actually to an equivalence class of representations. A unique prescription to pick a representative from an equivalence class is said to be a *canonical label*. Accordingly, the corresponding representative is called a *canonical representative*. Given a canonical label, two Feynman diagrams can be compared by comparing the data structures of their canonical representatives.

We have based our canonical label algorithm on the algorithm `nauty`,[28] by adapting it to the peculiarities of Feynman diagrams with loops. Due to the nature of the `nauty` algorithm, we are able to produce not only canonical representatives of Feynman diagrams, where external lines are assumed to carry distinct momenta, but also *topologies* of Feynman diagrams, by ignoring the momenta of some or all external lines. Recall that, for forests with external fermions, the groves can be characterized by permutations of identical fermions. Our canonical label algorithm allows for a simple way to produce just one of all possible permutations.

C.1.3 Constructing Groves

Given an implementation of flips for canonically labeled Feynman diagrams, the construction of groves is performed precisely as described in the main part of

this work, by partitioning the forest.

At present, we use an external program, `qgraf`,[29] for the production of the forest. The groves can then be constructed by a simple depth-first-search.

On the other hand, since the unflavored forest is connected according to the results of chapter 5, it is also possible to construct the groves incrementally, starting from a single diagram. In particular, once the grove corresponding to the first diagram has been completed, we try to obtain a new diagram by performing unflavored non-gauge flips. If we find one, it can be used to construct a new grove, and we can repeat the procedure. If no more new diagram is found, the forest must be complete.

This strategy is, however, not very well suited for theories with many different fermion flavors, like the SM. The reason is that, in order for the forest to be connected, we must ignore the fermion flavors completely. But this will generally lead to the production of redundant diagrams, because the unflavored diagrams generated may not be compatible with the flavors of the actual external state.

C.2 Usage

We have actually written two implementations of the algorithm for grove construction: The first one, `mangroves`, deals with general gauge theories, while the second one, `smgroves`, is tailored to the special properties of the Standard Model. It is the latter implementation that we have used to produce the results of section 6.3.7 and that we shall describe here.

The program `smgroves` is run from the command line. To illustrate the possible options, we display the output of the command `smgroves -help`:[1]

```
Usage: smgroves [options] -l #loops flavor_1 ... flavor_n
  -sm:no_fermions         SM without fermions.
  -sm:one_dublet          SM with a single quark dublet.
  -sm:one_generation      SM with one lepton and one quark.
  -sm:massive_neutrinos   SM with all fermions massive.
  -sm:massless_neutrinos  SM with massless neutrinos.
  -sm:massless_leptons    SM with massless leptons.
  -sm:massless_fermions   SM with massless fermions.
  -sm:with_ghosts         Include ghost diagrams.
  -sm:with_QCD            Include QCD contributions.
  -qcd n                  Select of order n in alpha_s.
  -onshell                Select amputated diagrams.
  -onepi                  Select 1PI diagrams.
  -notadpoles             Omit diagrams with tadpoles.
  -topl                   Produce topologies, not diagrams.
  -help                   Display this list of options
  --help                  Display this list of options
```

As can be seen, `smgroves` must be given the number of loops and the set of external flavors. Further options can be used to control the particle and coupling content of the SM.

A typical invocation of `smgroves` is given by:

[1] There are actually more options, most of them for controlling the output of `smgroves`, which are not listed here.

```
smgroves \
  -sm:one_generation -sm:massive_fermions \
  -sm:with_QCD -qcd 2 -l 1 ep em u ubar d dbar
```

In fact, the groves of the $O(\alpha_s^1)$ contributions to the $m_f \neq 0$ case in the example of section 6.3.7 have been generated with precisely this command. The output of `smgroves` for this run has been used to produce the $O(\alpha_s^1)$ entry in table 6.1.

In addition to the program `smgroves`, we have written a helper program `smanalyze` to determine the inclusion of groves for different choices of massless fermions. This program has been used to produce the numbers in table 6.2.

Bibliography

[1] L. Dixon, in *QCD and beyond*, edited by D. E. Soper (World Scientific, Singapore, 1996), p. 539, hep-ph/9601359.

[2] M. Moretti, T. Ohl, and J. Reuter, *O'Mega: An optimizing matrix element generator*, Technical Report No. LC-TOOL-2001-040, DESY, in *2nd ECFA/DESY Study 1998-2001* 1981-2009 (2001).

[3] F. Caravaglios and M. Moretti, Phys. Lett. **B358**, 332 (1995).

[4] E. Boos and T. Ohl, Phys. Rev. Lett. **83**, 480 (1999), hep-ph/9903357.

[5] C. Schwinn, Gauge Checks, Consistency of Approximation Schemes and Numerical Evaluation of Scattering Amplitudes, 2003, PhD thesis, TU-Darmstadt.

[6] D. Ondreka, Eichinvarianzklassen von Feynman-Diagrammen in einer Eichtheorie mit Fermionen in irreduziblen $SU(2)$-Darstellungen, 2000, Diplomarbeit, TU-Darmstadt.

[7] P. A. M. Dirac, *Lectures on Quantum Mechanics* (Yeshiva University, New York, 1964).

[8] L. D. Faddeev and V. N. Popov, Phys. Lett. **25B**, 29 (1967).

[9] C. Becchi, A. Rouet, and R. Stora, Ann. Phys. **98**, 287 (1976).

[10] I. V. Tyutin, Lebedev Institute preprint N39, 1975.

[11] N. Nakanishi, Prog. Theor. Phys. **35**, (1966).

[12] B. E. Lautrup, Mat. Phys. Medd. Kon. Dan. Vid.-Sel. Medd. **35**, (1967).

[13] T. Kugo and I. Ojima, Prog. Theor. Phys. Suppl. **66**, 1 (1979).

[14] O. Piguet, *Algebraic Renormalization: Perturbative Renormalization, Symmetries and Anomalies* (Springer, Berlin, 1995).

[15] A. A. Slavnov, Theo. Math. Phys. **10**, 99 (1972).

[16] J. C. Taylor, Nucl. Phys. **B33**, 436 (1971).

[17] B. W. Lee and J. Zinn-Justin, Phys. Rev. **D5**, 3121 (1972).

[18] B. W. Lee, in *Methods in Field Theory*, edited by R. Balian and J. Zinn-Justin (North-Holland/World-Scientific, Amsterdam, 1976), p. 77.

[19] J. Goldstone, Nouvo Cim. **19**, 154 (1961).

[20] J. Goldstone, A. Salam, and S. Weinberg, Phys. Rev. **127**, 965 (1962).

[21] G. 't Hooft, Nucl. Phys. **B35**, 167 (1971).

[22] O. Piguet and K. Sibold, Nucl. Phys. **B253**, 517 (1985); E. Kraus and K. Sibold, Nucl. Phys. B (Proc. Suppl.) **37B**, 120 (1994); O. M. D. Cima, D. H. T. Franco, and O. Piguet, Nucl. Phys. **B551**, 813 (1999).

[23] C. Schwinn, Forests and Groves: From Trees To Loops, work in preparation.

[24] M. E. Peskin and D. V. Schroeder, *An Introduction To Quantum Field Theory* (Addison-Wesley, Reading, USA, 1995), p. 842.

[25] G. 't Hooft and M. Veltman, Nucl. Phys. **B44**, 189 (1972).

[26] G. 't Hooft, Nucl. Phys. **B33**, 173 (1971).

[27] G. 't Hooft and M. Veltman, Nucl. Phys. **B50**, 318 (1972).

[28] B. D. McKay, Congressus Numerantium **30**, 45 (1981).

[29] P. Nogueira, J. Comp. Phys. **105**, 279 (1993).

Danksagung

Ich danke Herrn Prof. Manakos für die Aufnahme in seine Arbeitsgruppe und dafür, dass er es mir ermöglicht hat, diese Arbeit anzufertigen. Mein besonderer Dank gilt Herrn Dr. Thorsten Ohl, der mein Interesse am Thema der Arbeit geweckt hat, für seine guten Ratschläge, seine Geduld und sein LaTeX-Paket `FeynMF`. Großen Dank schulde ich auch meinem Kollegen Dr. Christian Schwinn für die vielen fruchtbaren und geistreichen Diskussionen über Eichtheorien und für wertvolle Hinweise auf die richtige Literatur.

Danken möchte ich auch den Mitgliedern der Arbeitsgruppen von Herrn Prof. Wambach und Herrn Prof. Roth für die gute Atmosphäre im vierten Stockwerk und für die Anschaffung der Kaffeemaschine. Bei Dominik Nickel, Dr. Axel Maas und Dr. Bernd-Jochen „BJ“ Schaefer bedanke ich mich für einige hilfreiche Diskussionen über Physik. Herzlichen Dank auch an Verena Werth, Markus Hild, Mathias Wagner und Dr. Thomas Roth für die täglichen Espresso- und Cappucino-Pausen. Bei Mathias Wagner und Thomas Roth möchte ich mich insbesondere auch für ihre Hilfe bei Computerproblemen jeglicher Art bedanken.

Nicht zuletzt möchte ich auch meiner Familie danken, am meisten und innigsten meiner Frau Felizitas für die Unterstützung, die sie mir hat zuteil werden lassen, und für die Geduld, mit der sie meine langen Arbeitszeiten in den heißen Phasen der Fertigstellung dieser Arbeit ertragen hat. Danken möchte ich auch meinen Kindern, die mich oft genug vermisst haben, für ihr Verständnis. Denen, die noch zu klein sind, um Verständnis zu haben, danke ich dafür, dass sie mich, wenn es darauf ankam, doch wieder haben schlafen lassen. Für die Betreuung der Kinder möchte ich mich auch bei meinen Eltern und Schwiegereltern bedanken.

Diese Arbeit wurde in Teilen vom Bundesministerium für Bildung und Forschung, Deutschland, unterstützt. (O5HT1RDA/6)

Lebenslauf

David Ondreka
Scheffelstraße 8
63071 Offenbach

Persönliche Daten

Geburt: 27. 8. 1973 in Hanau

Eltern: Werner Ondreka (Hausmann) und Eva-Maria Ondreka (Bibliothekarin)

Familienstand: verheiratet, fünf Kinder

Staatsangehörigkeit: deutsch

Ausbildung

1980-1984 Grundschule Buchhügel Offenbach

1984-1986 Bachschule Offenbach

1986-1993 Leibniz-Gymnasium Offenbach

1993 Abitur mit der Durchschnittsnote 1.0

1993-1994 Wehrdienst bei der Bundesmarine in Eckernförde

1994-2000 Physikstudium an der TU Darmstadt

1996 Vordiplom mit der Note „sehr gut“

seit 1998 Betreuung von Übungsgruppen im Fach Theoretische Physik

Juni 2000 Diplomprüfung. Diplomarbeit mit dem Titel „Eichinvarianzklassen von Feynman-Diagrammen in einer Eichtheorie mit Fermionen in irreduziblen $SU(2)$-Darstellungen“ in der Arbeitsgruppe von Prof. Manakos an der TU Darmstadt

Juli 2000 Beginn der Doktorarbeit auf dem Gebiet der theoretischen Elementarteilchenphysik in der Arbeitsgruppe von Prof. Manakos an der TU Darmstadt

September 2001 Teilnahme an der Herbstschule für Hochenergiephysik in Maria Laach

Eidesstattliche Erklärung

Hiermit erkläre ich an Eides statt, dass ich die vorliegende Arbeit selbständig und nur mit den angegebenen Hilfsmitteln angefertigt habe. Ich habe vorher keinen weiteren Promotionsversuch unternommen.

Darmstadt, 11. April 2005

David Ondreka